Identification and characterization of *Drosophila* lipid droplet-associated proteins

Von der Gemeinsamen Naturwissenschaftlichen Fakultät
der Technischen Universität Carolo-Wilhelmina
zu Braunschweig
zur Erlangung des Grades eines
Doktors der Naturwissenschaften
(Dr.rer.nat.)
genehmigte
D i s s e r t a t i o n

von Mathias Beller
aus Mutlangen

1. Referent:	Prof. Dr. Hans-Henning Arnold
2. Referent:	Prof. Dr. Herbert Jäckle
eingereicht am:	8.11.2004
mündliche Prüfung (Disputation) am:	28.1.2005
	Druckjahr 2005

Vorveröffentlichungen der Dissertation

Teilergebnisse aus dieser Arbeit wurden mit Genehmigung der Gemeinsamen Naturwissenschaftlichen Fakultät, vertreten durch den Mentor oder den Betreuer der Arbeit, in folgenden Beiträgen vorab veröffentlicht:

Publikationen

Grönke S.*, Beller M.*, Fellert S., Ramakrishnan H., Jäckle H. and Kühnlein R. P.: Control of fat storage by a *Drosophila* PAT domain protein. Curr. Biol. 13(7): 603-6 (2003).

* geteilte Erstautorenschaft

Tagungsbeiträge

Beller M., Grönke S., Fellert S., Jänsch L., Wehland J., Jäckle H. and Kühnlein R. P.: Fat storage is controlled by Perilipin-like lipid droplet protein LSD-2 in *Drosophila.* (Poster) 44th annual *Drosophila* Research Conference, Chicago (2003).

Beller M., Wehmhöner D., Jänsch L., Wehland J., Jäckle H. and Kühnlein R. P.: Functional subcellular proteomics of *Drosophila* lipid droplets. (Vortrag) 18th European *Drosophila* Research Conference, Göttingen (2003).

Beller M., Wehmhöner D., Jänsch L., Wehland J., Jäckle H. and Kühnlein R. P. Functional subcellular proteomics of *Drosophila* lipid droplets. (Poster) 45th annual *Drosophila* Research Conference, Washington, D.C. (2004).

Table of contents

Abbreviations

2D-PAGE	2-dimensional polyacrylamide gel electrophoresis
Adh	alcohol dehydrogenase
adp	*adipose*
ADRP	adipose differentiation related protein
AKH(R)	adipokinetic hormone (receptor)
AP	alkaline phosphatase
ATP	adenosine-5'-triphosphate
BCIP	5-bromo-4-chloro-3-indolylphoshate
bp	base pair
BSA	bovine serum albumine
C-	carboxy-
cAMP	cyclic adenosine monophosphate
CIP	calf intestine phosphatase
cDNA	complementary DNA
CoA	coenzyme A
DAG	diacylglycerol
DH	dehydrogenase
DIG	digoxygenin
DNA	deoxyribonucleic acid
dNTP	deoxyribonucleoside triphosphate
DTT	dithiothreitol
EC	enzyme commission
EDTA	ethylendiamintetraacetate
EGTA	ethylenglycol-bis-(2-aminoethylether)-N,N,N',N'-tetraacetate
EIF4A	elongation initiation factor 4A
ER	endoplasmatic reticulum
ESI	electro spray ionization
EST	expressed sequence tag
Fb	fat body
FBP1	fat body protein 1
Fig.	Figure
GFP	green fluorescent protein
GST	glutathione-S-transferase
i.e.	id est (that is)
IEF	isoelectric focusing

IPG	immobilized pH gradient
kb	kilobase
kDa	kilo Dalton
Hepes	N-(2-Hydroxyethyl)piperazine-N'-2-ethansulfonate
HSL	hormone sensitive lipase
LC	liquid chromatography
Lsd-1 / -2	*Lipid storage droplet associated protein –1 / -2*
mRNA	messenger ribonucleic acid
MALDI	matrix-assisted-laser-desorption-ionization
MS	mass spectroscopy
NBT	nitroblue tetrazolium chloride
NCBI	National Center for Biotechnology Information
N-	amino-
OreR	*Oregon R – Drosophila* wildtype strain
PAGE	polyacrylamide gel electrophoresis
PAT	protein domain named after: Perilipin, ADRP and TIP47
PBS	phosphate buffered saline
PCR	polymerase chain reaction
PFA	paraformaldehyde
pI	isoelectric point
PKA	protein kinase A
PMF	peptide mass fingerprint
rpm	rounds per minute
SDS	sodium-dodecyl-sulfate
SRP	signal recognition particle
TAG	triacylglycerol
TIP47	tail interacting protein of 47kD
TOF	time-of-flight
Tris	tris-hydroxymethyl-aminomethane
UAS	upstream activating sequence
UTR	untranslated region
w	*white*
y	*yellow*

1. Introduction

Eukaryotic cells contain subcellular organelles and compartments which serve specialized functions. At the organismic level, compartmentalization and specialization of cells are reflected in the generation of differentiated cell types and organs which need to interact through intra- and intercellular communication in order to maintain the integrity and function of the organism under constant as well as variable environmental conditions. One of the most important basic features both at the cellular and organismic level is energy homeostasis, the process of keeping the energy balance constant. Energy homeostasis requires that each cell and specialized organ can store, within limits, extra energy to be used in a regulated fashion if food becomes limiting during periods of starvation or in response to rapidly increased energy consumption. The importance of energy homeostasis regulation is best demonstrated by the fact that dysregulation of energy storage causes the increasingly severe health problem of epidemic overweight among populations of Western countries (reviewed e.g. in the focus of the Science journal in 2003: Friedman, 2003; Hill et al., 2003; Marx, 2003).

1.1 Energy homeostasis regulation

The balance between energy intake and consumption is based on the adaptation to changes in locomotor or biosynthetic activity as well as on the availability of food. Those frequent changes ask for a sophisticated adjustment and fine-tuning of the metabolism of the entire organism. This requirement is best demonstrated in insects which have phases of extremely elevated energy consumption such as flight activity (van der Horst et al., 1993): The complete energy-rich phosphate pool (ATP and phosphoarginine) of a locust flight muscle would last only one second of flight activity (Canavoso et al., 2001). However, these animals can fly for several hours (Canavoso et al., 2001). The corresponding ATP production can be realized by converting the energy stores of the animal that derived from the previously consumed food. The possibility to store energy derived from extensive food

consumption and its use in case of energy requirement is conserved in all organisms from bacteria to humans.

ATP serves as the general energy currency for the organism. It is kept only in small amounts inside cells and is generated on demand from the main energy storage forms of most animals: glycogen and neutral lipids, mainly triacylglycerol (TAG) (Flatt, 1995). Of those, glycogen is used for acute responses, and therefore mainly stored in the muscles where it is needed for an initial, fast reaction. Since glycogen is stored in its hydrated form, it cannot account for the complete energy storage because of the resulting space and weight restrictions. Thus, the main energy storage form of cells is lipid, because the corresponding amount of water free lipid is capable of storing six times more energy than hydrated glycogen.

Storage lipid is either generated from dietary lipids, which are resorbed in the midgut and transported to the storage organs, or by *de novo* synthesis from several biochemical compounds including carbohydrates (Canavoso et al., 2001). It is believed that all cells can produce and temporarily store lipids for their basic energy demands (Murphy, 2001). However, the majority of organismic lipid storage occurs in specialized tissues. In vertebrates, these are mainly the liver and the adipose tissue, whereas insects have a single lipid storage organ, the fat body.

1.2 Lipid storage in the life cycle of *Drosophila melanogaster*

Lipid storage is present during all stages of the ontogenetic development of the dipteran insect *Drosophila melanogaster* (Fig. 1-1 A). From the pre-blastoderm stage onwards lipid droplets are present (Fig. 1-1 B; Welte et al., 1998). They represent an important energy source, since embryos with a decreased TAG content die during embryogenesis (Buszczak et al., 2002; Teixeira et al., 2003). The fat body as specialized energy storage organ develops during late embryogenesis. It grows extensively during the subsequent larval stages. At the end of larval development the fat body fills a large portion of the body cavity as is shown by the fat body-specific marker expression of the green fluorescent protein (GFP) in Fig. 1-1 C.

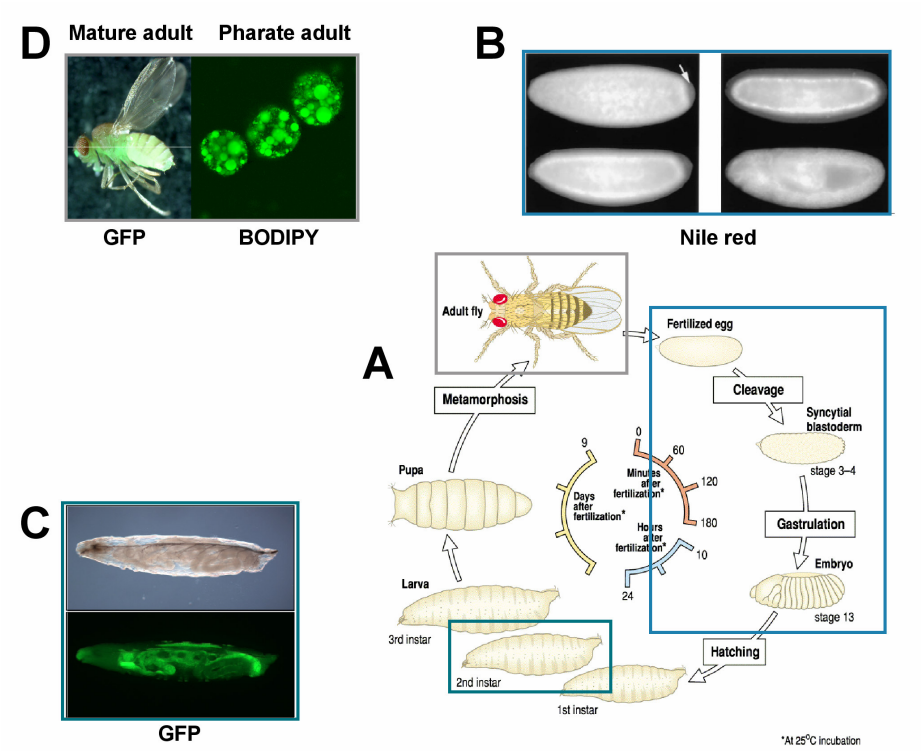

Fig. 1-1: Life cycle of *Drosophila melanogaster*

Schematic drawing of the *Drosophila* life cycle adapted from Wolpert (2001). At 25 °C, embryogenesis is completed after 24 hours with the hatching of the first instar larval stage. After two additional larval stages pupation follows. Development ends with the hatching of the mature fly after 9 days (A). Colored squares depict the developmental stages shown by photographs. (B) Embryonic lipid droplets (picture taken from: Welte et al., 1998). The arrow shows that no lipid is stored in the "pole cells", the later primordial germ cells. (C, D) *Drosophila* larva/adult. The fat body is shown by the tissue specific overexpression of the GFP marker protein (larval pictures in C taken from S. Grönke). (D) On the right, floating fat body cells of the pharate adult are shown. The lipid droplets were stained with the lipid specific dyes Nile red (Greenspan et al., 1985; B) or BODIPY (Gocze and Freeman, 1994; D).

The high amount of stored energy is necessary for the complete metamorphosis during pupation (Demerec, 1994), when most of the larval structures are transformed to form the adult fly. In the mature fly, the fat body is also present in all body parts as seen by the fat body-specific expression of the GFP marker protein (Fig. 1-1 D). In pharate adults, additional free floating fat body cells can be seen (Fig. 1-1 D). They probably represent the remains of the dissociated larval/pupal fat body and are only transiently present. About four days after hatching of the fly, these cells are vanished and functionally replaced by the mature adult fat body (Demerec, 1994). During all stages of development, lipids are stored as vesicular structures inside the cells (e.g.

Fig. 1-1 D, floating fat body cells of the pharate adult), referred to as ”lipid droplets”.

1.3 Lipid droplets–the lipid storage organelles

Lipid droplets are the lipid storage organelles of eukaryotic cells (reviewed in: Brown, 2001; Murphy, 2001; Murphy and Vance, 1999). Initially they were regarded as simple statically deposited aggregates of lipid. However, more recent findings show that lipid droplets are metabolically active organelles (Liu et al., 2004) that participate in general cellular processes and link them to other cellular organelles (Wu et al., 2000). Most recently, it has been even suggested that lipid droplets are involved in intracellular transport processes and that they are not only connected to the endoplasmatic reticulum (ER) and the cytoskeleton of cells, but also play a function in vesicular transport (Umlauf et al., 2004). In addition, lipid droplets are involved in cellular lipid uptake and its transport. In steroidogenic cells, for example, lipid droplets are transported via the cytoskeleton to the mitochondria, where lipids necessary for steroid hormone production are delivered (Servetnick et al., 1995).
Despite the fact that lipid droplets vary in size from 50 nm to 200 µm and are present in so many different organisms and cell types, the overall structure of lipid droplets is conserved (Fig. 1-2). They represent the only cellular organelles which are surrounded by a phospholipid monolayer. This monolayer membrane provides the attachment site for various proteins and shields the hydrophobic lipid-containing core (reviewed e.g. in: Murphy, 2001).

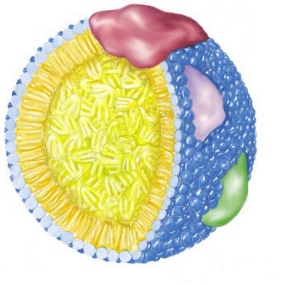

Fig. 1-2: Schematic composition of a lipid droplet
Blue: Phospholipid monolayer unique for lipid droplets. Yellow: Stored lipid, mainly TAG. Red, green and purple: associated proteins.

Details of lipid droplet cell biology are unknown. The standard model of lipid droplet biogenesis suggests that the monolayer is derived from the cytoplasm-oriented membrane leaflet of the ER, where the lipid droplets are born (Murphy and Vance, 1999). This model implies an incorporation of neutral

lipids (TAG, diacylglycerols (DAG) or sterol esters) into the ER intermembrane space. Upon filling, the outer leaflet separates from the inner layer, a process that leads to a budding-off of the droplets. Recently, an alternative model was presented which proposes that not the cytoplasm-oriented but the lumenal ER membrane-leaflet provides the surface of the nascent lipid droplet (Robenek et al., 2004). A study focusing on the lipid composition of the phospholipid monolayer indicates that lipid droplets are derived from specialized regions of the ER, since the detected large quantities of free cholesterol suggest a differentiation from the bulk ER membrane. Moreover, the fatty acid composition differs from the one characteristic for the rough ER membranes (Tauchi-Sato et al., 2002). These models favor a separation of the lipid droplets from the ER, whereas earlier studies suggested a persisting association of specialized ER membrane regions with the lipid droplet surface (Blanchette-Mackie et al., 1995).

The rather simple structure of lipid droplets is in contrast to the more recent findings implying that lipid droplets are not just static storage organelles but metabolically active compartments that can interact with several other compartments of the cell. This apparent discrepancy could be explained by a variable composition of the surface of different subsets of lipid droplets. Several attempts have been made in order to identify the proteins that are associated with lipid droplets of different organisms and cell types, including yeast (Athenstaedt et al., 1999), the mammary gland of mice (Wu et al., 2000) and four different mammalian tissue culture cell lines (Brasaemle et al., 2004; Fujimoto et al., 2004; Liu et al., 2004; Umlauf et al., 2004). The combined results reveal some 100 different proteins with little overlap between the results of the different studies (see appendix VII). This observation suggests a substantial variability of lipid droplet-associated proteins, which could either be caused by technical differences of the lipid droplet purification and protein identification procedures, or it may reflect a specific composition of the lipid droplet-proteomes of the investigated cell types. Functional data considering the lipid droplet-associated proteins is sparse. Rather profound information exists only for the plant lipid droplet-associated protein family of oleosins (reviewed e.g. in: Zweytick et al., 2000), the caveolin1 protein (e.g.: Cohen et

al., 2004; van Meer, 2001) and several mammalian members of the PAT-domain protein family.

1.4 The PAT-domain family of lipid droplet-associated proteins and mobilisation of TAG stores

Members of the evolutionary conserved PAT- (Perilipin, ADRP and TIP47) domain protein family (Lu et al., 2001; Miura et al., 2002) are associated with lipid droplets. The diagnostic PAT-domain, of unknown function, comprises 90 to 100 amino acids in the N-terminal region of these proteins (Lu et al., 2001). TIP47 (tail interacting protein of 47kD) is a cargo selector protein and interacts with the mannose-6-phosphate receptor (Diaz and Pfeffer, 1998). Its lipid droplet-association was initially disputed (Barbero et al., 2001; Wolins et al., 2001). More recent findings, however, support its lipid droplet-association (e.g.: Umlauf et al., 2004). In addition TIP47 was shown to be involved in the regulation of fatty acid uptake and incorporation into lipid droplets (A. Bulankina, personal communication). The recently solved crystal structure of TIP47 shows striking similarities to the N-terminal part of the vertebrate ApolipoproteinE. Since this protein is known to interact with the LDL-receptor in the presence of phospholipids, this observation supports the putative lipid binding function of TIP47 and provides a possible link to lipid uptake and transport processes (Hickenbottom et al., 2004). The second member of the family, ADRP (adipose differentiation related protein), is a resident of the lipid droplet surface in many different mammalian cell types (Brasaemle et al., 1997b). It is involved in surfactant production in lung epithelia by regulating lipid transport and uptake (Schultz et al., 2002), functions also demonstrated in tissue culture cells (Gao and Serrero, 1999; Imamura et al., 2002). The third functionally characterized PAT-domain protein, Perilipin, is expressed in a restricted pattern, i.e. in steroidogenic cells and differentiated adipocytes (Greenberg et al., 1991). It plays an important role in lipid mobilization control. In both, vertebrates and invertebrates, this control is hormone-regulated (reviewed in: Gibbons et al., 2000). In mammals, the antagonistic action of adrenalin and insulin has been demonstrated to regulate lipid storage and mobilization. A number of co-ordinated cAMP-dependent signaling events are

initiated or inhibited, respectively, and lead to the protein kinase A (PKA)-mediated phosphorylation of the hormone sensitive lipase (HSL) (Holm, 2003), one of the primary TAG-catabolizing enzymes, and to a hyperphosphorylation of Perilipin, which is already in unstimulated adipocytes the most prominent phosphoprotein (Clifford et al., 2000; Greenberg et al., 1991; Londos et al., 1999; Souza et al., 2002). Phosphorylation of HSL leads to a targeting to the lipid droplet surface. Hyperphosphorylation of Perilipin results in its translocation to the cytosol, making the droplet accessible for HSL action (Clifford et al., 2000), and is furthermore needed for an efficient translocation of the HSL to the lipid droplet surface. This finding suggests a dual role of Perilipin in HSL-mediated TAG mobilization (Holm, 2003; Sztalryd et al., 2003; Tansey et al., 2003).

The importance of Perilipin for the regulation of organismic TAG storage can be seen in knock-out mice lacking a functional *Perilipin* gene (Martinez-Botas et al., 2000; Tansey et al., 2001). These mice show a lean phenotype with elevated metabolic levels. Additionally, the lack-of-function studies show that the obese phenotype of the leptin receptor mutant *diabetes* mouse, a well-known obesity model, can be reverted towards the wild-type phenotype (Fig. 1-3).

Fig. 1-3: Perilipin knock-out phenotype

Loss of Perilipin (*Plin* $^{-/-}$) leads to a lean phenotype as compared to the wildtype (*Plin* $^{+/+}$). A mouse carrying a mutation in the leptin receptor and the wildtype *Perilipin* gene (*Lepr*$^{db/db}$ / *Plin*$^{+/+}$) is obese, whereas the same mutation combined with the lack-of-*Perilipin* mimicks the wildtype phenotype (*Lepr*$^{db/db}$ / *Plin*$^{-/-}$). Figure taken from: Martinez-Botas et al., 2000.

As in the case of Perilipin, posttranslational modifications might be necessary for the regulation of PAT-domain-proteins or lipid droplet-associated proteins in general. For example, ADRP is posttranslationally modified through fatty acid modifications that might be of importance for the localization to the lipid droplets (Heid et al., 1996).

Like in mammals, TAG mobilization in insects is regulated by peptide hormones. Responsible for the regulation of TAG mobilization are the adipokinetic hormone (AKH) and octopamine (reviewed in: Canavoso et al., 2001). AKH release from the neuroendocrine cells of the corpora cardiaca, which is part of the ring gland complex, has been shown to result in elevated Ca^{2+} influx in the fat body and increased levels of cAMP suggestive of a signal transduction cascade following receptor binding (Arrese et al., 1999). A phosphorylatable TAG-lipase has been additionally purified from the fat body of the tobacco hornworm *Manduca sexta* (Arrese and Wells, 1994). Activation of this lipase precedes the TAG breakdown as observed in vertebrates. However, the activation of the lipase seems to be independent of phosphorylation. Octopamine, a homologue of the vertebrate noradrenaline, acts as a neurotransmitter. It regulates the release of AKH (Passier et al., 1995), and functions as a neurohormone with energy store mobilizing activity (Canavoso et al., 2001).

These few examples demonstrate that despite the evolutionary distance between vertebrates and invertebrates, there are striking similarities in the cell biology of lipid droplets and the regulation of organismic lipid storage control. DNA sequences coding for PAT-domain proteins were also identified in insect genomes (see 2-1). This observation suggests that these proteins might be in fact evolutionary conserved regulators of organismic TAG content. In order to test this hypothesis, the function of the *Drosophila* PAT-domain protein LSD-2 was investigated. In addition, I isolated and characterized the lipid droplet-associated proteome of *Drosophila* fat body cells.

The results suggest an evolutionary conserved Perilipin-like regulatory function of LSD-2 in organismic TAG storage control. The identified protein composition of the lipid droplets supports the hypothesis that these organelles represent a metabolically active compartment of the fat body cells since it harbors proteins implicated in intracellular trafficking and the components of enzymatic pathways.

2. Results

Mammalian lipid droplet-associated proteins of the PAT-domain family such as ADRP and Perilipin are involved in the regulation of lipid metabolism in tissue culture and *in vivo* and suggest that the surface of lipid droplets serves as a cellular regulatory compartment for TAG metabolism (Gao and Serrero, 1999; Imamura et al., 2002; Brasaemle et al., 2000; Martinez-Botas et al., 2000; Saha et al., 2004; Sztalryd et al., 2003; Tansey et al., 2001).
PAT-domain proteins are not only conserved in mammals but also in lower vertebrates such as the claw frog *Xenopus laevis*, or invertebrates like the slime mold *Dictyostelium discoideum* and the fruit fly *Drosophila melanogaster* (Lu et al., 2001). Overexpressed fluorescent variants of non-mammalian PAT-domain proteins localize to the surface of lipid droplets (Miura et al., 2002). I therefore asked whether the regulatory potential of PAT-domain proteins with respect to fat storage is evolutionary conserved using *Drosophila* as an experimental system to elucidate PAT-domain protein function.

2.1 The *Drosophila* genome encodes two PAT-domain proteins

Whole genome *in silico* analysis of *Drosophila* sequences, either by BLAST (Altschul et al., 1990) or FLYBASE database searches (FlyBase, 2003) for homologous sequences of PAT-domain proteins, revealed that the genome codes for only two PAT-domain proteins, termed *Lipid storage droplet associated proteins 1* and *2* (*Lsd-1* and *Lsd-2*; Lu et al., 2001). However, a phylogenetic tree based on the PAT-domain amino acid sequences of selected PAT-domain proteins of different organisms (Fig. 2-1), using the MEGALIGN software, shows that the two *Drosophila* proteins cannot be directly homologized with any one of the vertebrate protein family members. In order to establish the function of a *Drosophila* PAT-domain protein, I characterized the *Lsd-2* gene in collaboration with Sebastian Grönke (MPI für biophysikalische Chemie, Göttingen; Grönke et al., 2003).

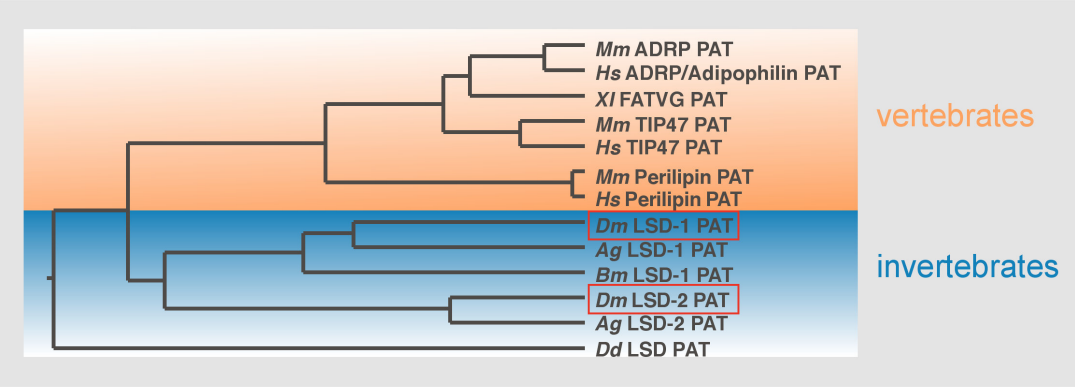

Fig. 2-1: Phylogenetic tree of PAT-domain proteins

Sequence similarity tree based on PAT-domain amino acid sequences of selected vertebrate and invertebrate PAT-domain proteins. Red boxes mark the *Drosophila* LSD-1 and LSD-2 proteins. Vertebrate representatives are shaded with the orange square, invertebrate ones with the blue square.

Abbreviations used are: *Mm Mus musculus*, *Hs Homo sapiens*, *Xl Xenopus laevis*, *Dm Drosophila melanogaster*, *Ag Anopheles gambiae*, *Bm Bombyx mori*, *Dd Dictyostelium discoideum*, ADRP adipose differentiation related protein (synonym: Adipophilin), Fatvg fat and vegetally pole expressed gene, TIP47 tail interacting protein of 47kD, LSD-1/LSD-2 Lipid storage droplet associated protein -1/-2.

2.2 Embryonic and larval *Lsd-2* mRNA expression patterns

The *Lsd-2* gene is localized on the X-Chromosome in region 13 A9-10 (FlyBase, 2003). The single 2.2 kb transcript contains four exons and codes for a protein with a predicted molecular weight of 38 kDa (Fig. 2-2 A; Rubin et al., 2000). Except for the PAT-domain, no other diagnostic protein motif could be identified in the putative LSD-2 protein sequence.

In order to visualize the spatio-temporal distribution of the *Lsd-2* transcripts, RNA *in situ* hybridizations on whole embryo preparations and larval tissue have been carried out using DIG-labeled RNA antisense probes (Goldstein and Fyrberg, 1994; see material and methods 3.2.3). Fig 2-2 B shows that *Lsd-2* transcripts can be already detected in the pre-blastoderm embryo, suggesting a maternal contribution of the mRNA. At stage 5, transcripts are restricted to the “pole cells”, the presumptive primordial germ cells (Fig. 2-2 C). Expression in those cells is present until stage 9 of development (Fig. 2-2 D), when *Lsd-2* transcripts are also transiently detectable in the amnioserosa (data not shown). At stage 14, *Lsd-2* transcripts are seen in the fat body and the midgut (Fig. 2-2 E). The spatially restricted patterns of *Lsd-2*

expression are not limited to embryogenesis but maintained during ontogenesis as can be seen in the third instar larval tissues with the most prominent expression in the fat body (Fig. 2-2 F).

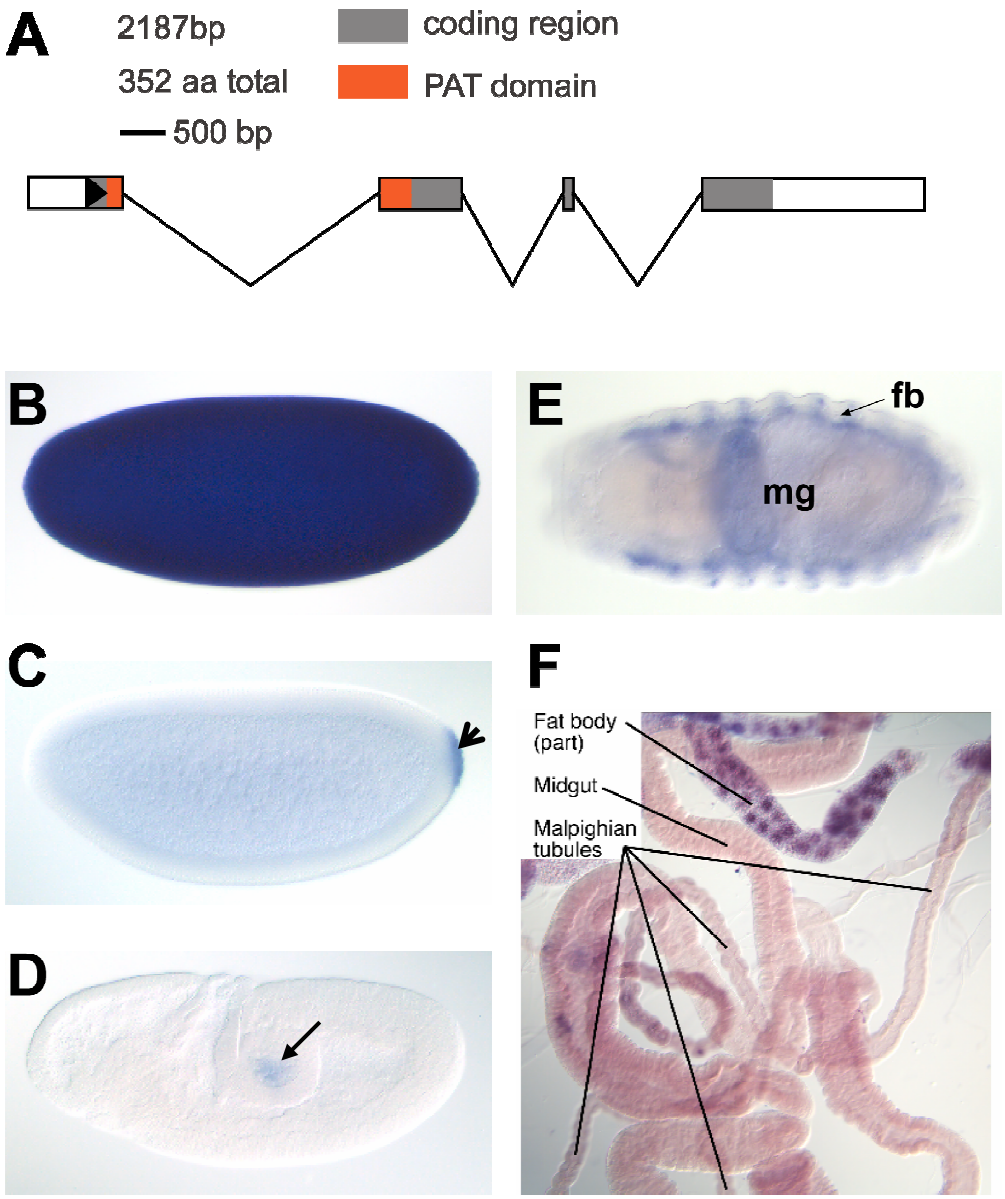

Fig. 2-2: RNA expression pattern of *Lsd-2*

(A) Intron-exon structure of the *Lsd-2* gene which is located on the X-Chromosome at cytogenetic bands 13 A9-10 (FlyBase, 2003). It is organized in four exons adding up to 2187 base pairs, encoding a protein with 352 amino acids. The grey box marks the open reading frame, in orange the PAT-domain is shown. The *Lsd-2* cDNA clone RE58939 (Rubin et al., 2000) was used to generate the DIG-labeled RNA antisense *in situ* probe as described in material and methods 3.2.3 used for the detection of *Lsd-2* expression patterns during embryonic development (B – E) and in the third instar larval stage (F) by whole mount *in situ* hybridizations (Goldstein and Fyrberg, 1994). Embryos are oriented anterior to the left and dorsal side up (B – D). E is showing a dorsal view of an embryo. F is showing the spread organs of a third instar larva.

The early presence of the transcript in the preblastoderm embryo indicates a maternal contribution of the mRNA (B). Upon cellularization (C, stage 5) the transcripts are degraded and expression is restricted to the later primordial germ cells, the pole cells (arrowhead). These transcripts are detectable until complete germ band extension (arrow in D, stage 9/10). Upon stage 14 expression in the fat body (fb) and the midgut (mg) can be detected (E). In the postembryonic stages expression is largely restricted to the fat body (F).
Classification of the embryonic stages and tissues was done according to Campos Ortega and Hartenstein (1997).

Thus, in contrast to the vertebrate PAT-domain protein encoding genes TIP47 and ADRP (Brasaemle et al., 1997b; Wolins et al., 2001), *Lsd-2* is not expressed ubiquitously but in a restricted pattern similar to Perilipin (Lu et al., 2001).

2.3 LSD-2 localizes to lipid droplets

PAT-domain proteins are the best-characterized lipid droplet-associated proteins of vertebrates. Similarly, in *Drosophila* a transgene-derived LSD-2:EGFP fusion protein was found to localize to the surface of lipid droplets in first instar larval fat body cells (Miura et al., 2002). We also found this association in fat body cells of larvae at later stages, when a corresponding fusion protein was overexpressed by a fat body specific Gal4-driver (Fb-Gal4; see material and methods 3.1.2). The fusion protein decorates intracellular vesicles of all sizes inside the fat body cells. The identity of isolated vesicles as lipid droplets was confirmed by counterstaining with a specific dye (Fig. 2-3 A).
Since proteins can be mislocalized upon overexpression, I examined the subcellular localization of the endogenous LSD-2 protein by biochemical means. For this analysis we generated a rabbit polyclonal antiserum directed against the full-length LSD-2 protein (see material and methods 3.4.1).
Fat body proteins obtained by sucrose step gradient ultracentrifugation (see material and methods 3.4.3) were separated and the antiserum was used for the detection of LSD-2 in subcellular fractions. The protein content of each fraction was used as a first quality control of the fractionation process (Fig. 2-3 B). The lipid droplet fractions of the gradient (F1, F2; Fig. 2-3 B) contained only small amounts of protein as compared to the more dense cytosolic

fractions five to eight (F5–F8) where the majority of proteins are present. In the separating mid-zone (F3, F4), again very little protein was detected.

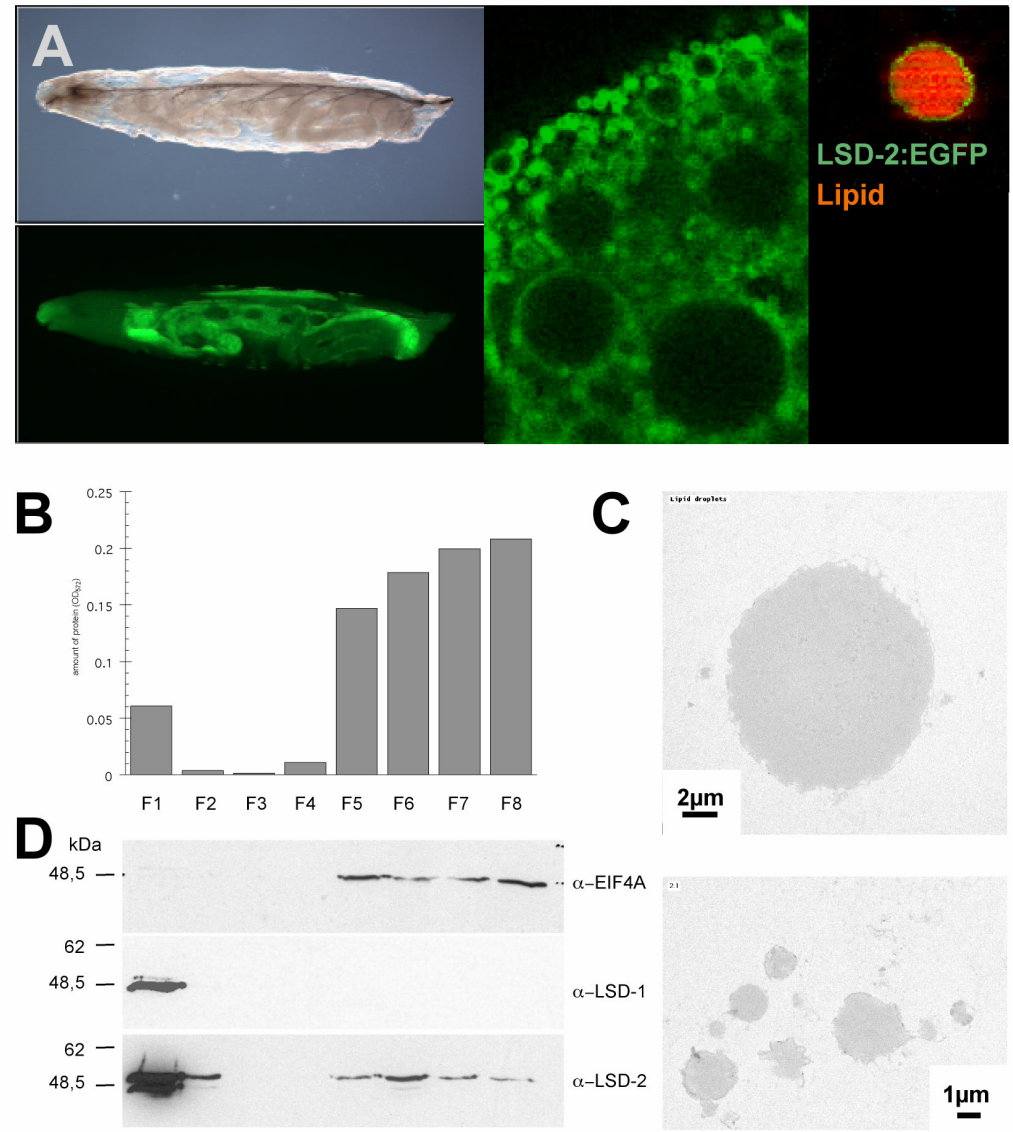

Fig. 2-3: Localization of LSD-2 to lipid droplets

The localization of LSD-2 to lipid droplets is shown both by the overexpression of a LSD-2:EGFP fusion protein (A) and by subcellular fractionation and Western blotting for the endogenous protein (D).

(A) A LSD-2:EGFP fusion protein was constructed and overexpressed in the fat body of third instar wandering larvae using the Gal4/UAS system (Brand and Perrimon, 1993). Isolated lipid droplets were counterstained with the lipid droplet specific dye Nile red (Greenspan et al., 1985). Images were taken on a Leica dissecting microscope (whole larva; pictures from S. Grönke), a confocal microscope (larval fat body; Leica TCS SP2) or a Zeiss Axiophot equipped with an openlab imaging system (isolated lipid droplet).

(B) Third instar larval fat bodies were manually dissected and the cellular extracts subjected to a subcellular fractionation using a sucrose step gradient (see material and methods 3.4.3). The protein amount of 50 µl of each fraction was measured using the standard BCA assay (material and methods 3.4.4), and the resulting OD_{572} was plotted for each fraction resulting in a protein elution profile. (C) Electron micrographs of the purified lipid droplets for detection of

putative contaminations (see material and methods 3.4.5). (D) 10 µg protein of each fraction were separated by standard SDS-PAGE and used for Western blot experiments (material and methods 3.4.8/3.4.10). The Western blot membrane was successively probed with antisera specific for the cytoplasmic marker EIF4A, the lipid droplet-specific LSD-1 protein and LSD-2. The antibody specific for LSD-2 recognizes two bands, which are most likely alternatively spliced isoforms of LSD-2 (see 2.4).

Since the enrichment and purity of the lipid droplets is of great importance for the interpretation of the subcellular protein localization data, an additional purity control using electron microscopy has been carried out (Fig. 2-3 C, see material and methods 3.4.5). The micrographs reflect the high variability in size of the lipid droplets also seen *in situ* (Fig. 2-3 C) and show only little non-vesicular membranous structures and no significant contaminations such as co-purified organelles.

Probing equal protein amounts of all sucrose gradient fractions by Western blotting, I first asked how a cytoplasmic marker (elongation initiation factor 4A - EIF4A; Hernandez et al., 2004), and the known lipid droplet-resident protein LSD-1 (R. P. Kühnlein, personal communication) are distributed. Based on their distribution, F5–F8 indeed contain the cytoplasmic protein fractions (EIF4A-signal), whereas LSD-1 is exclusively found in the uppermost lipid droplet-containing fraction F1 (Fig. 2-3 D). LSD-2 is highly enriched in the lipid droplet fractions F1 and F2 (Fig. 2-3 D) and, in much lower amounts, also present in the cytoplasmic fractions F5-F8. These results indicate that the majority of endogenous LSD-2 protein is associated with lipid droplets. They are consistent with the localization of the LSD-2:EGFP fusion protein, overexpressed in fat body cells (Fig. 2-3 A).

2.4 Generation of *Lsd-2* mutants

A direct way to characterize the function of a gene is the analysis of phenotypes associated with loss-of-function mutations. Numerous mutagenesis screens have been performed using *Drosophila*, providing a large collection of mutants. One method of randomly mutagenizing the genome is the mobilization and re-insertion of transposable P-Elements. If the insertion takes place in the coding or the regulatory region of a gene, resulting in a block of transcription or translation, loss-of-function mutations can be

obtained. If the insertion has no effect, it can subsequently be used to generate a mutant by imprecise excision of the inserted element (for review see e.g.: Ryder and Russell, 2003).

The Berkeley *Drosophila* gene disruption project (Bellen et al., 2004) provided a fly stock carrying a P-element insertion in the 5' untranslated leader of the *Lsd-2* gene (Fig. 2-4 A). This P-element insertion fly line, termed *Lsd-2[KG00149]*, carries a P{SUPor-P} insertion (Roseman et al., 1995). The P-element is marked with the *yellow* gene, therefore it causes a yellow body color if lost from the genome of otherwise *yellow* mutant flies.

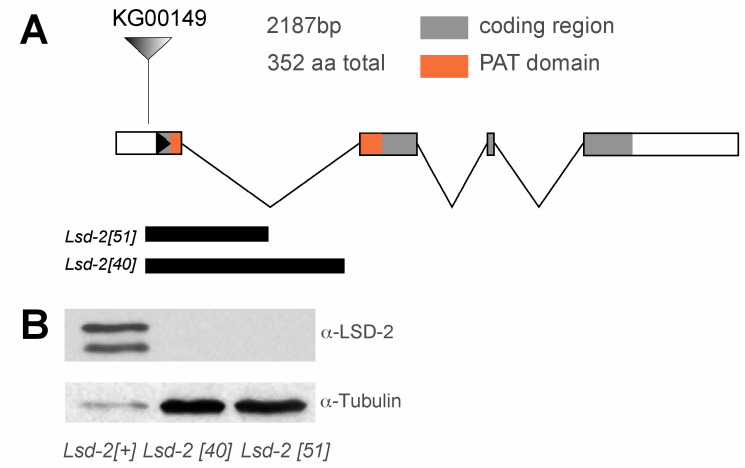

Fig. 2-4: Genomic organization of the *Lsd-2* gene and generated mutant alleles

A P-Element insertion termed *KG00149* in the first exon of the *Lsd-2* gene was obtained from the Berkeley *Drosophila* gene disruption project (A; *Lsd-2* intron-exon structure as shown in Fig. 2-2 A) (Bellen et al., 2004). By a remobilization experiment two deletion-carrying alleles were generated, termed *Lsd-2[40]* and *[51]*, both eliminating the predicted translation start carrying part of the first exon, as well as varying parts of the first intron, as shown by sequencing of the relevant genomic region (material and methods 3.1.1). (B) Western blotting experiments using the LSD-2 specific antiserum showed that both alleles are protein null mutants. Reprobing the Western blot with an antibody specific for ß-tubulin served as a loading control.

In order to generate mutants as well as a revertant control allele, a P-element remobilization experiment has been carried out according to the description in material and methods 3.1.1 (crossing scheme is shown in Fig. 3-1). Imprecise P-element excisions can be often identified by visible phenotypes or even lethality due to the loss of endogenous genomic DNA segments adjacent to the insertion site. All of the 289 P-element excision events after remobilization of *KG00149* resulted in hemizygous viable individuals with no obvious phenotype. Thus, screening for possible mutations was performed by polymerase chain reaction (PCR) to detect molecular lesions of the *Lsd-2* gene. The primer combination used for the PCR of the *Lsd-2* transcribed

region was chosen to result in a 2.2 kb amplicon with the wildtype DNA (see material and methods 3.1.1). 246 of the 289 obtained jump-out events were examined by PCR and several wildtype sized amplicons as well as some shorter ones were sequenced. DNA of a precise excision allele (*Lsd-2[+]*) and two DNA amplicons corresponding to *Lsd-2* deletion mutants (*Lsd-2[51]*, *Lsd-2[40]*) were obtained. The precise excision allele *Lsd-2[+]* contains the wildtype gene, whereas the deletion mutants *Lsd-2[51]* and *Lsd-2[40]* lack the LSD-2 encoding sequences from position –34 to +654 and –34 to +970 relative to the predicted translational start codon, respectively (Fig. 2-4 A).
In order to further characterize the two *Lsd-2* mutant alleles with respect to the presence of the LSD-2 protein, Western blotting experiments have been performed. Both deletion mutants failed to produce detectable amounts of the LSD-2 protein. Therefore, they are likely to be null mutant alleles. In the precise excision allele the protein can be clearly detected (Fig. 2-4 B). It is noteworthy that the Western blot analysis revealed two protein bands. They could represent the products of alternative spliced transcripts which include or exclude exon three, respectively (Fig. 2-4 A; S. Grönke, personal communication). Additionally, the Western blot experiments revealed that the apparent molecular weight (46 kDa) is slightly larger than the one calculated from the protein primary sequence (38 kDa, e.g.: Fig. 2-3 D and data not shown). The *Lsd-2* mutants were viable and thus the amount of organismic TAG could be measured for adult flies lacking LSD-2 activity.

2.5 *Lsd-2* mutant flies store less organismic TAG

In order to assay for a possible Perilipin-like function of *Lsd-2* in lipid storage, the effect of loss of LSD-2 activity on the organismic TAG level was investigated using an enzymatic assay that takes advantage of a lipase-mediated TAG breakdown into free fatty acids and glycerol. The concentration of the resulting glycerol was subsequently determined in a colorimetric assay and normalized against total protein content (see material and methods 3.4.2). According to this assay *Lsd-2* mutant flies contain significantly less TAG than the “normal” control flies carrying the wildtype *Lsd-2* gene (Fig. 2-5). As compared to freshly hatched *Lsd-2[+]* male individuals which carry a

functional *Lsd-2* allele (column 1), the TAG content of *Lsd-2[51]* (column 2) and *Lsd-2[40]* (column 3) mutants is reduced by 34.5 % and 28 %, respectively. For simplicity, individuals with less TAG than control flies will be called “lean”, whereas those with TAG levels higher than the control flies will be referred to as “obese”.

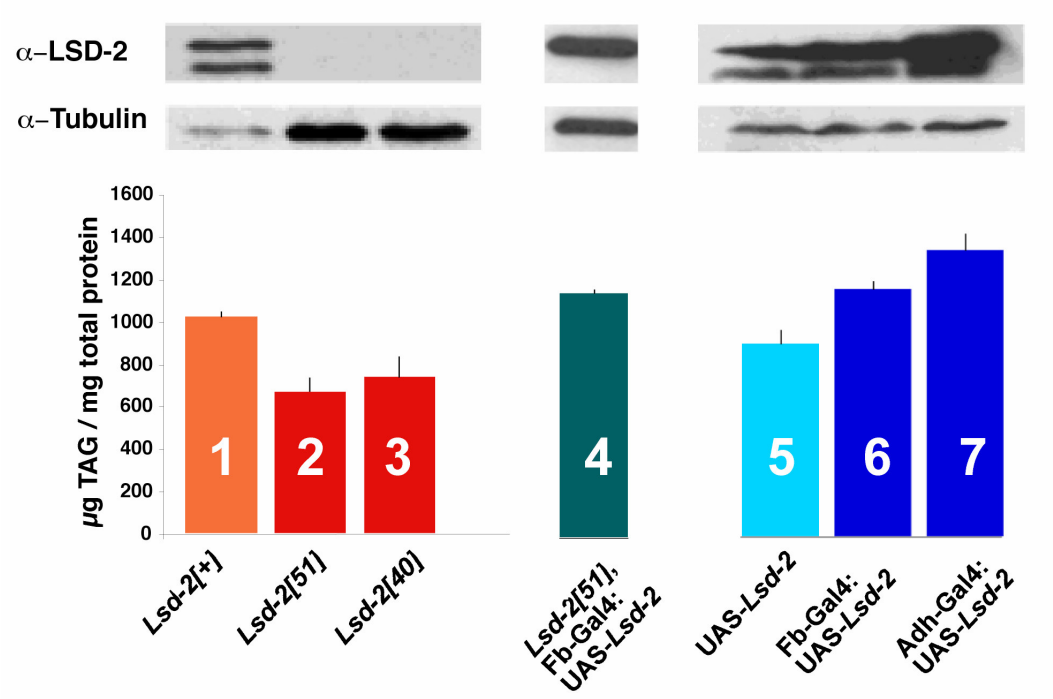

Fig. 2-5: Effect of altered LSD-2 protein amounts on the organismic TAG content

Organismic TAG content was measured in µg TAG/mg total protein by an enzyme mediated breakdown of the TAG followed by a colorimetric assay (see material and methods 3.4.2) for several genotypes with different LSD-2 protein amounts. Total protein was measured with the standard BCA assay (material and methods 3.4.4). Corresponding LSD-2 protein amount assayed by Western blot experiments is shown on the top (material and methods 3.4.10). An antibody detecting ß-tubulin was used as a loading control in the Western blot experiments.
In the LSD-2 mutant alleles *Lsd-2[51]* and *Lsd-2[40]* the TAG content is diminished resulting in a lean phenotype as compared to the precise jump out control allele *Lsd-2[+]* (columns 2 and 3 compared to column 1). This decrease is caused by the loss of *Lsd-2*, since overexpression of LSD-2 in the mutant background is able to rescue the lean phenotype (column 4).
LSD-2 is adjusting the TAG content in a dosage dependant manner since a stronger overexpression of the LSD-2 protein in the wildtype background using the Adh-Gal4 driver line (column 7) results in a higher TAG amount as compared to a moderate overexpression caused by the Fb-Gal4 driver line which is shown in column 6. The non-activated overexpression construct is not showing an increased TAG level (column 5).

In order to investigate whether the TAG content reduction in the lean mutants is caused by the loss of LSD-2 function in the fat body, a cDNA-based *Lsd-2*

transgene (UAS-*Lsd-2*) was expressed in response to the Fb-Gal4 driver in *Lsd-2* mutant individuals (material and methods 3.1.2). Transgene-derived *Lsd-2* activity in the fat body reverted the leanness of *Lsd-2[51]* mutant flies (Fig. 2-5, column 4), indicating that loss of LSD-2 activity is indeed responsible for the mutant lean phenotype due to the tissue specific loss of LSD-2 activity in fat body cells.

2.6 LSD-2 overexpression results in elevated organismic TAG levels

Loss of LSD-2 activity causes the reduction of organismic TAG storage in mutant individuals. In order to examine whether LSD-2 activity is also sufficient for modulating the TAG content of otherwise wildtype flies, the UAS-*Lsd-2* transgene was expressed in the fat body of wildtype individuals in response to different Gal4 drivers. The use of different Gal4 driver lines is usually associated with different expression levels of the UAS target gene. In fact, the *Adh*-Gal4 line (Fischer et al., 1988) and Fb-Gal4 driver caused different amounts of UAS-*Lsd-2* transgene-dependent LSD-2 protein, as shown by Western blot experiments with the LSD-2-specific antiserum (Fig. 2-5). Flies moderately overexpressing LSD-2 elevate organismal TAG storage by 28 % (FB-Gal4; column 6), whereas strong *Lsd-2* overexpression causes a TAG storage increase of 48.5 % (*Adh*-Gal4; column 7) as compared to control individuals bearing only the non-induced UAS-*Lsd-2* transgene (column 5).
These results demonstrate that, as observed for vertebrate Perilipin, LSD-2 is not only necessary to control the organismic TAG content but its activity is sufficient to alter the organismic TAG content in a dosage-dependant manner when expressed in fat body cells.

2.7 Correlation between LSD-2 protein and organismic TAG content

In order to examine whether the regulation of LSD-2 abundance can modulate the TAG content under starvation as well as in other genetically lean or obese *Drosophila* mutant individuals, their amount of LSD-2 protein was determined by quantitative Western blot analysis (material and methods 3.4.10/3.6). Protein extracts from flies were separated by SDS-PAGE and Western blots

were probed with the LSD-2 specific antiserum. After stripping, they were reprobed with antibodies directed against ß-tubulin to normalize the protein amounts loaded. Additionally, the antiserum specific for LSD-1 was used to compare the response of LSD-1 and LSD-2 in the different protein preparations.

After 24 hours of starvation, the organismic TAG content of *Drosophila* is to a large extent mobilized in order to provide the energy necessary for survival (Fig. 2-6 A). As the *Lsd-2* mutant flies show a decreased TAG level, one could assume that the starvation caused reduction of organismic TAG is correlated with a decrease of the LSD-2 protein amount. However, this is not the case (Fig. 2-6 B). In contrast to LSD-2, the LSD-1 protein amount decreases upon starvation. This reduction of LSD-1 protein amount can be reverted by re-feeding the flies, which also leads to an almost complete restoring of the TAG content to the pre-starvation level (Fig. 2-6 A, B).

Additionally to the physiological alteration of TAG level, mutant flies which are known to have altered TAG contents were assayed for corresponding alterations in the LSD protein levels. Two examples of those genetic backgrounds are the obese *brummer[1]* loss-of-function mutant and the fat body specific, UAS-mediated *brummer* overexpression resulting in a lean phenotype (Fig. 2-6 C; S. Grönke, in preparation). In the *brummer* mutant individuals, the amount of both LSD proteins is increased (Fig. 2-6 D). Furthermore, *brummer* overexpression also causes an increase of the LSD proteins (Fig. 2-6 D). These observations indicate that the organismic TAG levels are not correlated with the amount of any of the two LSD proteins. Additional measurements on individuals of five other genotypes known to alter TAG storage (data not shown) (obese genotypes: *adipose[60]*, (Häder et al., 2003); *chico[2]*, (Bohni et al., 1999) and fat body specific overexpression of *midway* (R. P. Kühnlein, unpublished) - lean genotypes: *midway[QX25]*, (Buszczak et al., 2002); fat body specific *adipokinetic hormone receptor (AKHR)* overexpression (R. P. Kühnlein, unpublished)) confirmed that LSD protein expression levels are not generally correlated with the TAG content of the individuals.

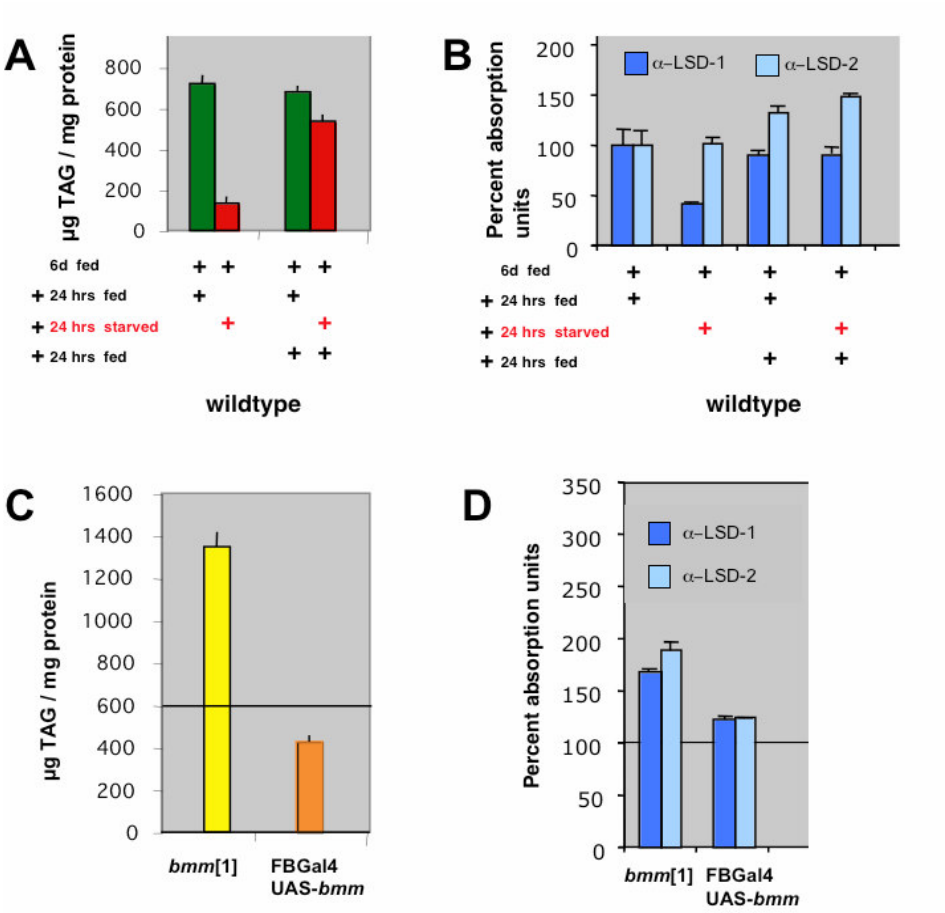

Fig. 2-6: Correlation between LSD protein amount and organismic TAG content

(A) The influence of a starvation period using a water-based diet on the organismic TAG content is shown. The TAG content decreases dramatically after 24 hours of starvations due to a breakdown of the TAG stores. Refeeding the flies for an additional 24 hours period largely restores the TAG content. (B) LSD-1 and LSD-2 protein amounts under the different feeding conditions were measured using quantitative Western blotting. ß-tubulin signal was used for normalization (see material and methods 3.4.10/3.6). (C)/(D) In addition to the exogenous alteration of TAG content, also mutants with altered TAG content were assayed for a correlation between LSD-1 and LSD-2 protein amount and the organismic TAG content. One example is the obese *brummer* mutant (*bmm[1]*) and the lean *brummer* overexpression state (C; the approximate wildtype TAG content of 600 µg TAG/mg protein is indicated). (D) shows the corresponding LSD-1 and LSD-2 protein amounts. For details see text 2.7.

The lack of such a correlation indicates that in addition to the LSD proteins, other factors or compensatory mechanisms are involved in adjusting the organismic TAG content in flies. In addition, the activity of the LSD proteins could be altered at the level of posttranslational modifications as it has been shown for the vertebrate PAT-domain protein Perilipin, the most prominent

phosphoprotein in mammalian adipocytes (see introduction 1.4 and e.g.: Brasaemle et al., 1997a; Clifford et al., 1998; Greenberg et al., 1991).

2.8 The LSD proteins are posttranslationally modified

In order to search for putative phosphorylated residues of the LSD proteins, an *in silico* analysis of the proteins primary structure was performed using the NetPhos 2.0 algorithm (Blom et al., 1999). This analysis revealed 25 putative phosphorylation sites in LSD-1 that include 15 serine, seven threonine and three tyrosine residues and 25 putative phosphorylation sites (12 serine, 10 threonine and three tyrosine residues) in the case of LSD-2 (Fig. 2-7). As posttranslational modifications are often important for protein function, an evolutionary conservation of the respective residues predicted to be posttranslationally modified supports a modification *in vivo*. Therefore, the *Anopheles gambiae* LSD-protein sequences were searched for residues being conserved in *Drosophila* with predicted phosphorylation sites in both organisms (Fig. 2-7).

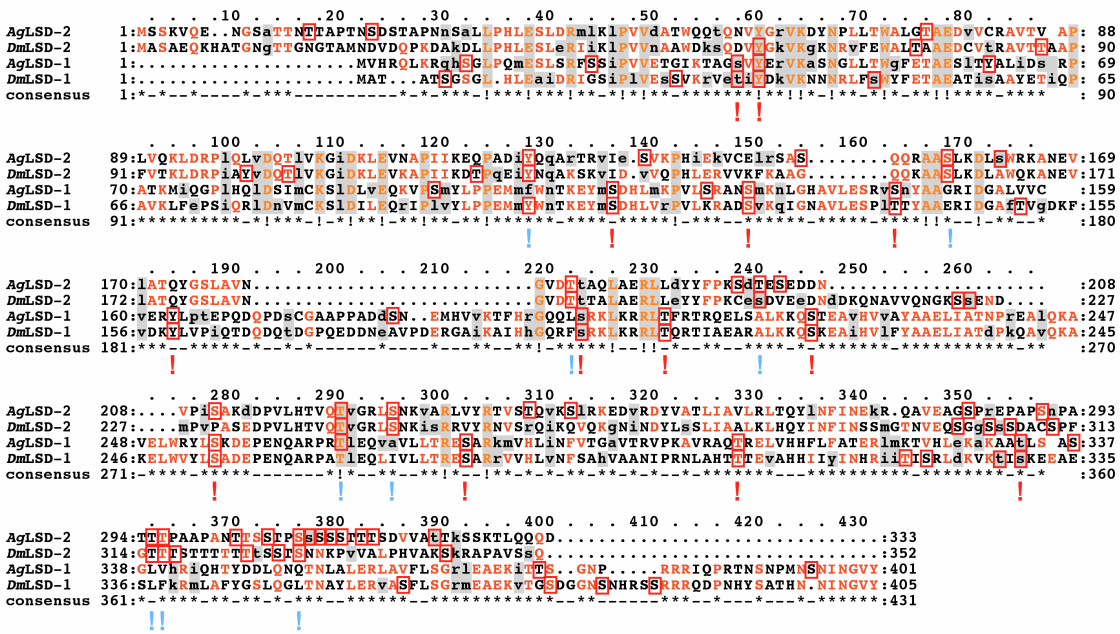

Fig. 2-7: Alignment of *Drosophila melanogaster (Dm)* and *Anopheles gambiae (Ag)* LSD proteins

Conserved residues are shown in red, similar ones in black on grey, and identical ones in orange on grey. Red squares mark the predicted phosphorylated residues. Red exclamation marks: conserved LSD-1 residues with predicted phosphorylation, blue exclamation marks: conserved LSD-2 residues with predicted phosphorylations.

For LSD-2, this analysis revealed the existence of 8 conserved residues (three serine, four threonine and one tyrosine residue plus one more serine residue which has in *Anopheles* a threonine counterpart), and ten conserved residues for LSD-1 (six serine, two threonine and two tyrosine residue plus two more threonine and one serine residue which have in *Anopheles* serine/threonine counterparts). In contrast, the *Drosophila* LSD proteins share only two conserved tyrosine residues predicted to be phosphorylated.

One method to determine posttranslational modifications of proteins is two-dimensional polyacrylamide gel electrophoresis using immobilized pH gradients (Janke et al., 2000; Resing, 2002). In the first step, proteins are separated on basis of their different isoelectric points (pI), by a technique called isoelectric focusing. The proteins migrate in an electric field along an immobilized pH gradient until they reach their “isoelectric point”. In a second step, the proteins are separated on basis of their molecular weight in a standard SDS-PAGE (2D electrophoresis reviewed e.g. in: Görg et al., 2000). As posttranslational modifications, like the charged phosphate residues, change the isoelectric point of proteins those modifications can be detected by a shift in the pI value. In case of phosphorylation, such a shift will occur towards the acidic end of the pH gradient.

Fat body proteins of third instar larvae were separated by 2D-PAGE (material and methods 3.4.7) and the presence of LSD proteins was monitored by Western blot analysis (material and methods 3.4.11). Fig. 2-8 A shows that the LSD-2 protein extracted from the fat body cells is not focused in a single spot, but forms an array of proteins with charge differences. This indicates modified states of the protein (apparent pI from approximately pH 4–8, predicted pI 8.5). After removing the LSD-2 signal and reprobing the Western blot with the antiserum directed against the LSD-1 protein (material and methods 3.4.10) it became apparent that also the LSD-1 protein is likely to be modified. In contrast to the multiple spots of LSD-2, only a single LSD-1 protein spot is detected. This spot, however, is shifted towards the acidic end of the IPG strip (Fig. 2-8 B; apparent pI appr. pH 3.5; predicted pI pH 8.6), suggesting a single protein species which is modified posttranslationally, possibly by phosphorylation. Reprobing the Western blot with an antibody specific for ß-tubulin shows that the focusing process itself was successful,

since the signal is represented by a single protein spot in the appropriate position (Fig. 2-8 C; apparent and predicted pI of tubulin is pH 4.5). These findings indicate the existence of several modified isoforms of the LSD-2 protein and a single form of LSD-1, which however is likely to be posttranslationally modified.

In order to investigate whether the modifications observed are indeed phosphorylations, fat body protein extracts were incubated with calf intestine phosphatase (CIP), which removes the phosphate moieties from serine, threonine and tyrosine residues (material and methods 3.4.11). After the treatment, the ß-tubulin spots were unaffected, whereas the LSD-1 and LSD-2 proteins were shifted towards the basic end of the gel (see Fig. 2-8 D-F).

These findings indicate that at least some of the introduced posttranslational modifications of LSD-1 and LSD-2 are phosphorylations. The observation that the spots are not completely shifted towards the predicted position on the gel can be explained either by an insufficient dephosphorylation or by other modifications present on these proteins.

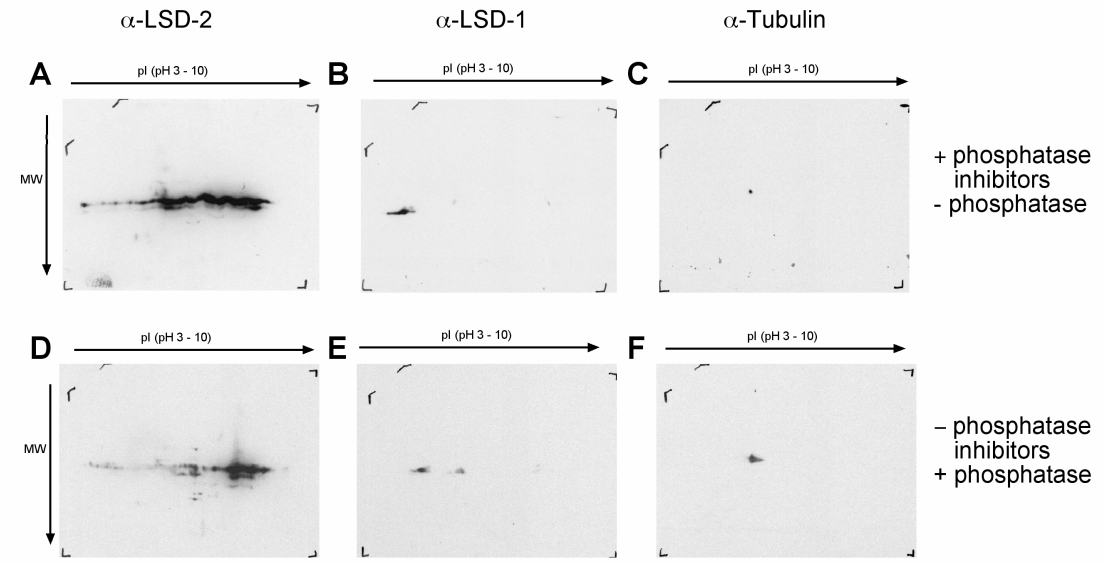

Fig. 2-8: Posttranslational modification of LSD-proteins

2D-Western blots of larval fat body extracts (material and methods 3.4.11). Extracts have been prepared in the presence (A-C) or the absence (D-F) of phosphatase inhibitors. If no inhibitor was added (D-F), an additional incubation step with calf intestine phosphatase (CIP) was included (see material and methods 3.4.11). In (A) and (D) the blot was probed with the LSD-2 specific antiserum, followed by reprobing first with the LSD-1 specific antiserum (B and E) and finally with an antibody detecting ß-tubulin (C and F). In the presence of phosphatase inhibitors the LSD-2 protein is represented by different isoforms, characteristic for phosphorylated proteins (A; predicted pI 8.53), whereas the LSD-1 protein is represented by

a distinct spot (B), shifted towards the acidic end (pI 8.66). The control ß-tubulin is not showing such an altered spot location (C, predicted pI 4.5). Repeating the experiments in the absence of phosphatase inhibitors, but in the presence of CIP, shows that the signals corresponding to LSD-1 and –2 are shifted towards the basic end (D, E). Again the ß-tubulin signal is detected on the predicted position (F).

The results reported so far show that LSD-2 is involved in adjusting the organismic TAG content and that posttranslational modified isoforms of LSD-2 might be involved in regulating its activity as observed for Perilipin. The amount of LSD-2 protein cannot be generally correlated with the amount of stored organismic TAG. These findings are in agreement with the hypothesis that additional regulatory factors reside on the surface of lipid droplets and that they are part of the regulatory system that controls the TAG content of the organism. In order to uncover the proteome associated with lipid droplets, I isolated them and determined the identity of the proteome components by mass spectroscopy.

2.9 The lipid droplet-associated proteome of *Drosophila* larvae

Analysis of the protein composition of given complexes or cells on a large scale is generally called proteomics. Done with enriched cellular organelles or compartments, these approaches are described as subcellular proteomic screens. The advantages of subcellular as compared to whole cell proteome analysis is outlined e.g. in two recent publications (Brunet et al., 2003; Dreger, 2003).

In order to assess a stage- and tissue-specific lipid droplet proteome of *Drosophila melanogaster*, I used lipid droplet preparations from manually prepared third instar larval fat bodies, free of obvious contaminating organs that were purified by sucrose step gradient ultracentrifugation (see material and methods 3.4.3). The efficiency of this purification protocol, and the resulting purity of the enriched lipid droplets, was already shown in 2.3. Proteins were identified by various techniques using mass spectroscopy (gel-based and gel-less; see material and methods 3.4.12.1 and 3.4.12.2)

2.10 Characterization of the lipid droplet proteome by gel-based techniques

In order to assay for the resolving capacity of the 2D gel-separation process of the very lipid-rich material from the larval fat bodies, 500 µg of the complete postnuclear supernatant protein extracts were used. The fat body extracts were delipidated, and proteins were precipitated as described in material and methods 3.4.6 prior to separation using 2D gel electrophoresis (material and methods 3.4.7). After staining the proteins with the fluorescent dye Sypro Ruby (material and methods 3.4.9) a complex spot pattern can be seen (Fig. 2-9 A).

The proteome of purified lipid droplets was first separated on a standard 1D SDS-PAGE. For this purpose, 300 µg of the proteins present in the lipid droplet fraction were delipidated and precipitated. After separation, proteins were visualized using the fluorescent Sypro Ruby stain (Fig. 2-9 B), showing a reduced complexity as compared to the total cellular extract separated in Fig. 2-9 A. Approximately 90 to 100 bands could be detected, probably representing even more proteins since each band might contain several proteins. Therefore too many protein bands were present for a rapid, comprehensive identification using standard techniques. In order to identify the lipid droplet-associated proteins by peptide mass fingerprinting (PMF), a separation of 300 µg of the lipid droplet-associated proteins using 2D-PAGE was carried out as described above (see scheme in Fig. 2-10 A). This separation revealed 90 to 100 spots of different intensities (Fig. 2-9 C), again showing a reduced complexity as compared to the total postnuclear supernatant.

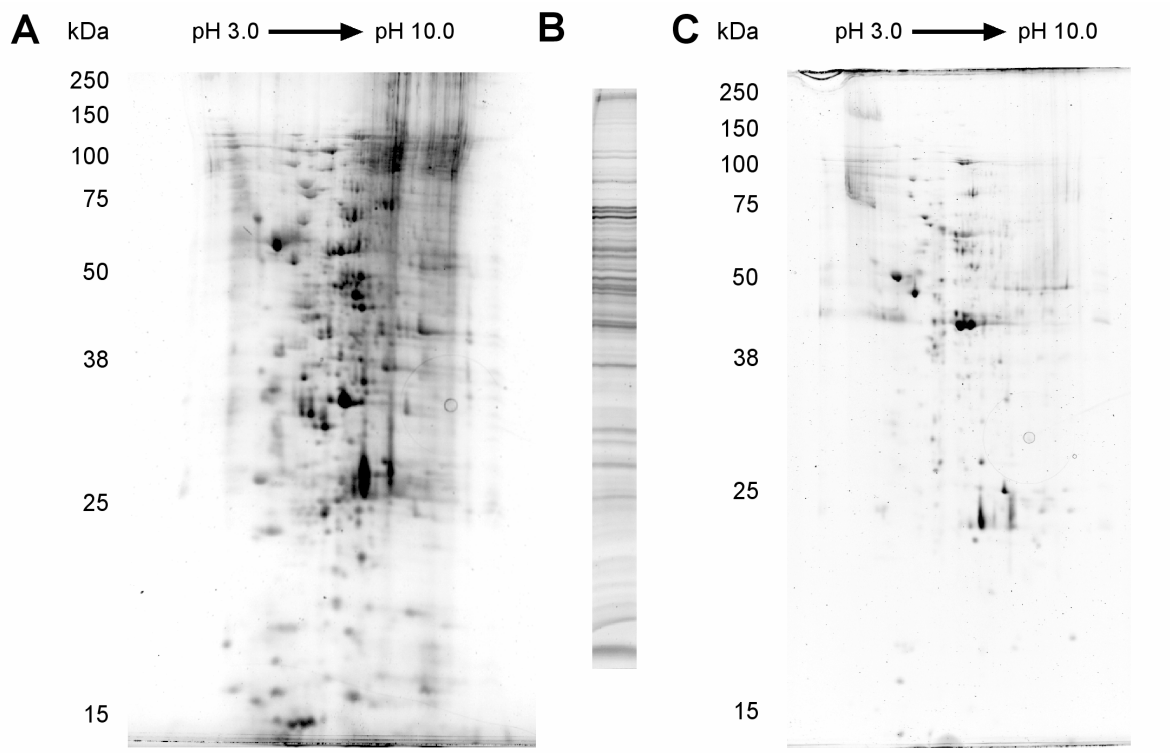

Fig. 2-9: Gel-separated fat body/lipid droplet proteomes

(A) 2D-PAGE separated proteins of *Drosophila* third instar larval fat bodies. The fat bodies have been manually dissected and 500 µg of the delipidated and precipitated proteins of the postnuclear supernatant were separated on an IPG strip ranging from pH 3–10 for the first dimension and a 10 % SDS-PAGE for the second dimension as described under material and methods 3.4.7. (B, C) 300 µg of the proteins associated with purified lipid droplets (see material and methods 3.4.3) were separated by either 1D SDS-PAGE (B) or 2D-PAGE (C), as described in (A). All gels have been stained with the fluorescent dye Sypro Ruby (Berggren et al., 2000) as described in material and methods 3.4.9.

From this 2D lipid droplet proteome map, 18 individual proteins have been identified after in-gel digestion of picked spots followed by mass spectroscopy (material and methods 3.4.12.1; appendix I). Among the identified proteins were members of the storage proteins like Fat Body Protein 1 (FBP1), chaperones, and several others, whereas no spots corresponded to the already described lipid droplet-associated proteins LSD-1 or LSD-2. Additionally, comparison of the 2D-separated lipid droplet proteome with the one separated by 1D SDS-PAGE, revealed the relatively low efficiency of recovery in the 2D gel representing maximal 50 % of the SDS-PAGE separated proteins (approx. 40 to 50 band forming spots - obtained by a theoretical conversion of the 2D-PAGE into a 1D SDS-PAGE - versus approximately 90 to 100 bands in the 1D SDS-PAGE; Fig. 2-9 B, C). This

relatively low recovery of proteins might be linked to the physicochemical properties of the proteins and the sample as a whole, as the sample still contained a considerable amount of lipids after the methanol-chloroform extraction as revealed by later experiments (see 2.11). The results, however, show that the extraction procedures enrich for proteins that are associated with the lipid droplet fraction.

2.11 Gel-less and "semi gel-less" characterization of the lipid droplet-associated proteome

The recent development of gel-less peptide separation techniques using liquid chromatography directly linked to the identification using mass spectroscopy (LC-MS/MS), enables to overcome the loss of proteins that derives from the gel separation process (in particular during the IEF-process). This procedure starts with the proteolytic digestion of a protein mixture with given complexity. The resulting peptides are separated by chromatographic means and are subjected to tandem mass spectroscopy leading to sequence information. This technique has the advantage of a rapid identification, delivering high confidence information as compared to the more conventional peptide mass fingerprinting.

2.11.1 Protein and peptide separation

An overview of the strategies used for the separation and identification of the lipid droplet proteome is shown in Fig. 2-10. After a series of pilot experiments using only the portion of proteins insoluble in the 2D-sample buffer (2-10 B), the complete lipid droplet proteome was used for identification by the LC-MS/MS technique (Fig. 2-10 C). Therefore, the complete protein pellet after the methanol–chloroform precipitation (see material and methods 3.4.6) was digested with trypsin prior to identification. However, it turned out that the remaining chemical compounds in the peptide mixture were competing with the peptides for binding in the LC-columns, resulting in low efficiency identifications. As these compounds were co-eluted under hydrophobic elution

conditions (as seen in the UV-channel, data not shown), the contaminating agent was very likely residual lipid.

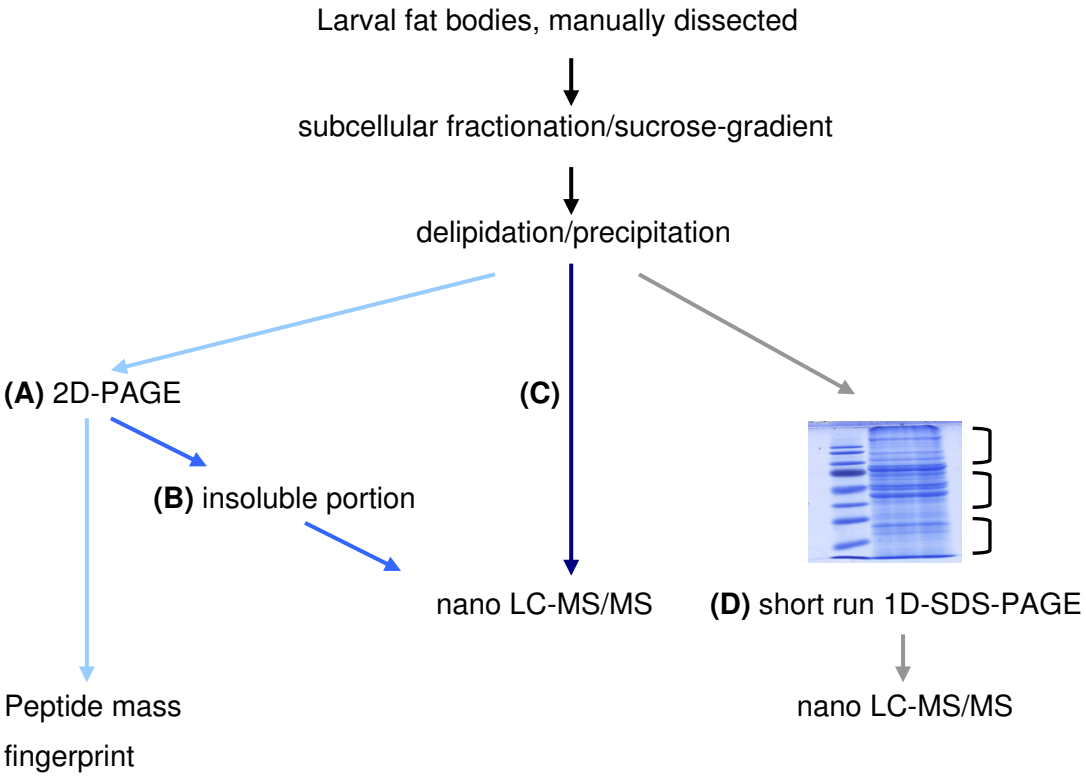

Fig. 2-10: Strategies used for the separation and identification of lipid droplet-associated proteins

For all protein separation strategies larval fat bodies were manually dissected and the lipid droplets purified using sucrose gradient ultracentrifugation. The proteins were delipidated and precipitated prior to identification using the following strategies:
(A) 2D-PAGE coupled to peptide mass fingerprinting as described in 2.10. (B) Only insoluble proteins were used for the nano LC-MS/MS identifications, whereas in (C) the complete precipitated proteome was used as described in 2.11. (D) The precipitated proteins were pre-fractionated and purified from the residual lipid by an introduced short run 1D-SDS-PAGE separation (see 2.11) prior to nano LC-MS/MS identification.

In order to improve the sensitivity and reliability of the protein identification, the precipitated proteins were incompletely separated by a short run 1D SDS-PAGE prior to digestion in order to purify the proteins from the lipids and achieve a pre-fractionation to reduce complexity (Fig. 2-10 D). Each gel lane was then divided in three equally sized regions. They were cut out, followed by standard tryptic in-gel digestion of the partially separated proteins (material and methods 3.4.12.2).

The eluted peptides were separated using a nano-LC system, directly coupled to the mass spectroscopy-based identification using a nano electro-spray-

injection quadrupol time-of-flight (ESI-Q-TOF) device (material and methods 3.4.12.2). In the subsequent ion scan, the m/z values (unit of the mass to charge ratio; “mass of the peptide” normalized to the fold-charge of the selected ion) of the separated peptides can be detected (Fig 2-11).

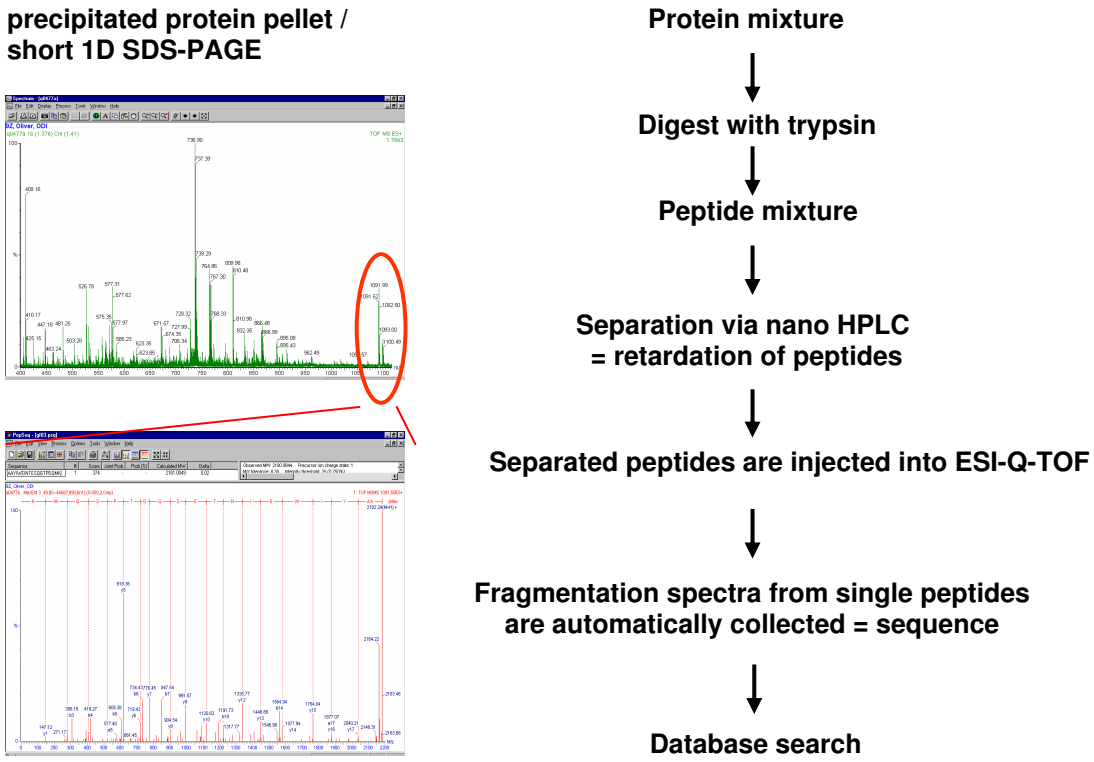

Fig 2-11: nano LC-MS/MS identification scheme

The upper spectrum represents an m/z ion scan. The red-marked ion was used for collecting the fragmentation spectrum shown below. For details see paragraph 2.11.1.

Single peptides were then automatically chosen and fragmented, leading to sequence information by analyzing the m/z values of the resulting peptide ladder. The resulting fragmentation spectra were used to search the non-redundant *Drosophila* or complete NCBI proteome database using the MASCOT algorithm resulting in a statistical Bayesian weighed score of the protein identification (Chamrad et al., 2004; Perkins et al., 1999).

2.11.2 Protein identification

Four rounds of protein identifications have been performed using the nano LC-MS/MS technique including proteins derived from fat body preparations of the wildtype (*OregonR; OreR*), the lean *LSD-2[51]* loss-of-function mutant and

two obese mutants. On of them was generated by fat body specific *Lsd-2:EGFP* overexpression, the other was the obese *adp[60]* loss-of-function mutant (Häder et al., 2003). For each genotype, two separate lipid droplet-purifying gradients were run, each separating extracts of 70 fat bodies. Three independent preparations were carried out. As a control for the reproducibility of protein identification, different vials of the first preparation were used twice for identifications (labeled with “x” and “y” in the following tables). 61 % of the first identifications (105 of $\Sigma x = 171$ identified proteins) and 70 % of the second identifications (105 of $\Sigma y = 151$ identified proteins) were shared ($\Sigma xy = 105$). Thus, some variability of proteins is due to the identification procedure or the protein preparation. The identifications from the second preparation are labeled by a “z” in the following tables and the ones from the third by “k”. Identifications were judged to be significant if the MASCOT threshold value of 27 for the *Drosophila* proteome was reached after a careful manual re-examination of the data.

In a first descriptive approach, all identified proteins were considered as being part of the “storage lipid droplet proteome” of *Drosophila* larval fat bodies, irrespective of the genotype they were extracted from. This way, effects caused by the genotype, and differences caused by proteins present only at low levels, were eliminated. One example of such low abundance effects might be the Brummer protein (synonym: CG5295), which was identified only in one preparation. Previous overexpression studies, however, showed that a Brummer-EGFP variant is localized to the surface of lipid droplets *in vivo* (S. Grönke, in preparation), suggesting that it might be endogenously present only at very low levels. Its presence indicates that proteins can be detected, even if they are at the border of detection limit set by the method used.

In total, 271 different proteins have been identified (see appendix II). They include 160 proteins from the wildtype *OreR*, 144 proteins from the *adp[60]* mutant, 167 proteins from the *Lsd-2:EGFP* overexpression and 161 proteins from the *Lsd-2[51]* mutant. Among the 271 candidate proteins, 39 homologues of the approximately 100 previously identified lipid droplet-associated proteins have been found (Table 2-1). They include the *Drosophila*

PAT-domain proteins LSD-1 and LSD–2, lipid-metabolizing enzymes and stress-response proteins like chaperones.

Table 2-1: *Drosophila* proteins homologous to previously identified lipid droplet proteins

Yeast/Mammalian protein - name or description:	ID/subtype:	*Drosophila* BLAST hit:	Reference of identification:
Perilipin	gi|28316726	**LSD-1/LSD-2**	Brasaemle et al., 2004
ADRP	Q99541	**LSD-1/LSD-2**	Fujimoto et al., 2004; Umlauf et al., 2004 Brasaemle et al., 2004; Liu et al., 2004; Wu et al., 2000
TIP47	O60664	**LSD-1/LSD-2**	Fujimoto et al., 2004; Umlauf et al., 2004 Brasaemle et al., 2004
Acyl-CoA synthetase long chain member 1, 2, 3	gi|729927 gi|20455039 gi|6172341	**CG3961** CG8732 CG8732	Brasaemle et al., 2004
Acetyl-CoA carboxylase	NP_000655	**CG11198**	Liu et al., 2004; Umlauf et al., 2004
17ß-hydroxosteroid dehydrogenase	type 11: AF126780 / NP_057329 type 7: P56937	CG15629 / third hit **CG2254** CG7221	Fujimoto et al., 2004; Umlauf et al., 2004 Brasaemle et al., 2004; Liu et al., 2004
Lanosterol synthase / synthetase	YHR072w, P48449 / P48449 gi|22122469	CG10363 weak **CG7981 weak** CG13948 weak	Athenstaedt et al., 1999 Fujimoto et al., 2004 Umlauf et al., 2004 Brasaemle et al., 2004; Liu et al., 2004
Patatin domain protein	YMR313c CAC01131 gi|21313274	**CG5295**	Athenstaedt et al., 1999; Umlauf et al., 2004 Liu et al., 2004
Cholesterol Esterase	Q64285	CG17901 weaker hits **CG1112/ CG2505**	Wu et al., 2000
ER carboxylesterase	Q8VCC2	CG6414 weaker hits **CG1112/CG2505**	Wu et al., 2000
Squalene epoxidase	YGR175c AAD10823 gi|6678127	**CG10639**	Athenstaedt et al., 1999; Umlauf et al., 2004 Liu et al., 2004
Pyruvate Carboxylase	gi|200246	**CG1516**	Brasaemle et al., 2004; Wu et al., 2000
Glyceraldehyde-3-P-dehydrogenase	YJL052w,YJR 009c, YGR192c, P04406	**CG12055 CG8893**	Athenstaedt et al., 1999 Fujimoto et al., 2004
Alcohol dehydrogenase		**ADH**	Liu et al., 2004
Fatty acid synthase	NP_032014	**CG3523/3254**	Wu et al., 2000
Aldehyde dehydrogenase	gi|18028981	**CG11140**	Brasaemle et al., 2004
Prediced protein	YKR046c	CG14120 **CG18076 weak**	Athenstaedt et al., 1999
CGI49	AF151807	**CG2604/ CG5167**	Brasaemle et al., 2004; Fujimoto et al., 2004
Predicted protein	FLJ14497	**CG7430**	Fujimoto et al., 2004
Rab	5 1, 6, 7, 10, 18 1, 2, 5, 7, 10, 11, 14, 18 5, 7, 14, 18	**Rab1, 2, 5, 6**, 7, 10, 11, 14, 18	Fujimoto et al., 2004 Umlauf et al., 2004 Liu et al., 2004 Brasaemle et al., 2004

Yeast/Mammalian protein - name or description:	**ID/subtype:**	***Drosophila* BLAST hit:**	**Reference of identification:**
Rap1B	P09526	**CG1956**	Fujimoto et al., 2000
GRP94	P14625	**CG5520**	Umlauf et al., 2004
HSP-90-alpha / -beta	P07900/ P08238	**CG1242**	Umlauf et al., 2004
BiP	P11021 gi|2598562 gi|2506545	**CG4147**	Liu et al., 2004; Umlauf et al., 2004 Brasaemle et al., 2004
HSP70 / HSC70 / HSC 73		**CG4264**	Brasaemle et al., 2004; Wu et al., 2000; Umlauf et al., 2004
HSP60	P10809	**CG12101**	Umlauf et al., 2004
PDI		**CG6988**	Liu et al., 2004; Umlauf et al., 2004
ß-actin	AAH08633	**CG4027**	Umlauf et al., 2004
p53 responsive gene 3 (AMID)	NP_116186	**CG7430 weak**	Umlauf et al., 2004
Related to Prohibitin / Stomatin B-Cell receptor associated protein 37	gi|6671622 gi|6679299 gi|28526501	**CG15081/ CG10691**	Liu et al., 2004 Brasaemle et al., 2004
VDAC-1	gi|10720404	**CG6647**	Liu et al., 2004
TER ATPase	Q01853	**CG2331**	Wu et al., 2000
ERP99	P08113	**CG5520**	Wu et al., 2000
ATP Synthase beta	gi|25052136	**CG11154**	Brasaemle et al., 2004
Collagen type IV / VI	gi|6753484 gi|3913189 gi|3236370	**CG16858** CG14889 CG33103	Brasaemle et al., 2004

The proteins identified in the proteomics screen of this study are shown in bold.

For further analysis, the proteins were manually grouped into nine functional classes (see Fig. 2-12). The largest class of lipid droplet-associated proteins consists of metabolism-related proteins (first class; 73 proteins). Both lipid metabolizing enzymes as well as enzymes of the carbohydrate metabolism are included. The second largest group (second class; 65 proteins) comprises proteins of uncertain function/protein transport-related proteins like Rab proteins or members of the Translocon complex. The third class of proteins consists of chaperones. It includes 20 proteins that may be necessary for a properly folded lipid droplet-associated proteome. The fourth class includes the known lipid droplet resident PAT-domain proteins LSD-1 and LSD–2. Proteins with a predicted function in fatty acid and TAG binding form the fifth class (three proteins). Storage protein metabolism associated proteins (six proteins) are combined in the sixth class.

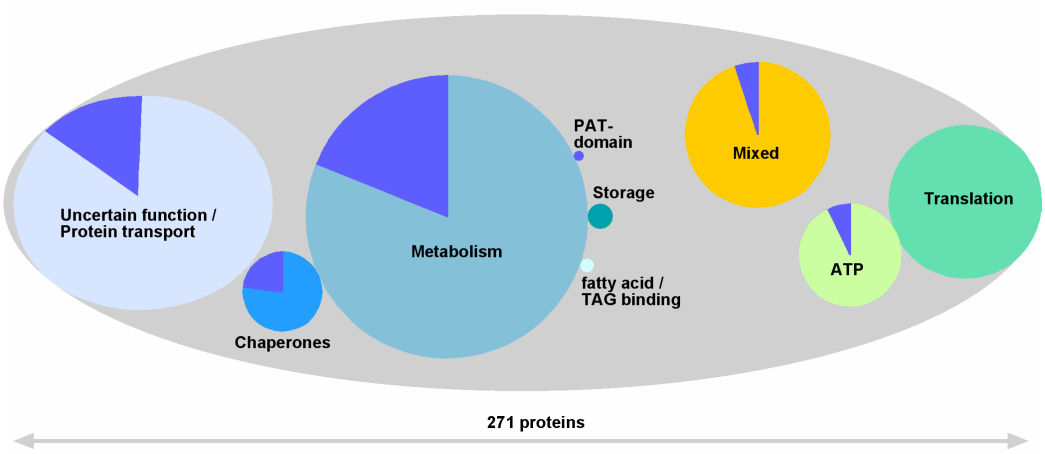

Fig. 2-12: Classification of identified proteins

The 271 nano LC-MS/MS identified proteins have been manually grouped into nine classes. The relative abundance of proteins of each class is shown in comparison to the complete proteins, as the dimension of the x-axis of each oval/circle is proportional to the amount of proteins. Segments of the circles in dark blue indicate the portion of proteins homologous to previously identified lipid droplet proteins (see Table 2-1).
Number of proteins for each group: Uncertain function/protein transport 65 (11 homologues previously identified); Chaperones 20 (6 homologues previously identified); Metabolism 73 (16 homologues previously identified); PAT-domain proteins 2 (for both proteins homologues were previously identified); Storage proteins 6; fatty acid / TAG-binding 3; Mixed 37 (2 homologues previously identified); ATP 26 (2 homologues previously identified) and Translation 39. The bluish colored protein groups are assumed to be lipid droplet-associated and therefore clustered together. For the orange unique standing “Mixed” group such a decision is hard to be made. The two green groups might be co-purified contaminating proteins, e.g. ribonuclear particles.

These six groups might represent the “hard core” lipid droplet-associated proteins, as the majority of the homologues of the previously identified lipid droplet proteins are included (marked as sections of the circles representing the classes in Fig. 2-12). The six classes are clustered in Fig. 2-12.

All other proteins could not be directly linked to lipid droplets. They from the classes “Mixed” (seventh class; 37 proteins), “ATP” (eigth class; 26 proteins) and “Translation” (ninth class; 39 proteins). The presence of these proteins (ribosomal proteins, ATP synthase subunits etc.) can be explained by the co-purification of e.g. ribonucleoprotein complexes. The complete list of the identified proteins is shown in appendix II.

2.12 Comparative lipid droplet proteomics

As for most of the identified proteins no data regarding lipid droplet-association or subcellular localization was available, I increased the stringency for a comparative analysis of the genotype-specific sub-proteomes by only taking proteins into account, which were identified at least in two different genotypes or were found constantly in the lipid droplet fractions of larvae with a distinct genotype. This was done because proteins identified only once could either be “false positives”, or belong to the group of the very low abundant proteins which are just at the detection limit.

Using this criterium, only 182 proteins were left for further analysis (a list of the genotype-specific identifications can be found in appendix IV). Among these, 142 proteins have been identified in the wildtype *OregonR*, 122 in the *adp[60]* mutant, 146 in *Lsd-2[51]* mutant and 147 in *Lsd-2:EGFP* overexpressing individuals. Fig. 2-13 shows the protein distribution between the wildtype and the mutant genotypes. Common to all individuals is a basic set of 76 proteins. These proteins represent most likely “constitutive lipid droplet-associated proteins”, and are likely the most abundant proteins of the lipid droplet enriched fractions. Proteins, which are not present in the lipid droplet fractions of all investigated genotypes, are often associated with samples obtained from individuals of a different TAG-content modifying genotype.

Fig. 2-13 shows that 59 % (39 of 66) of the proteins detected in the wildtype and not shared by all genotypes are also observed in two of the mutant genotypes. Additional 40 % (26 of 66) are still shared by another genotype and only one protein has repeatedly been identified only in the wildtype (CG5320 glutamate dehydrogenase (DH); see appendix IV).

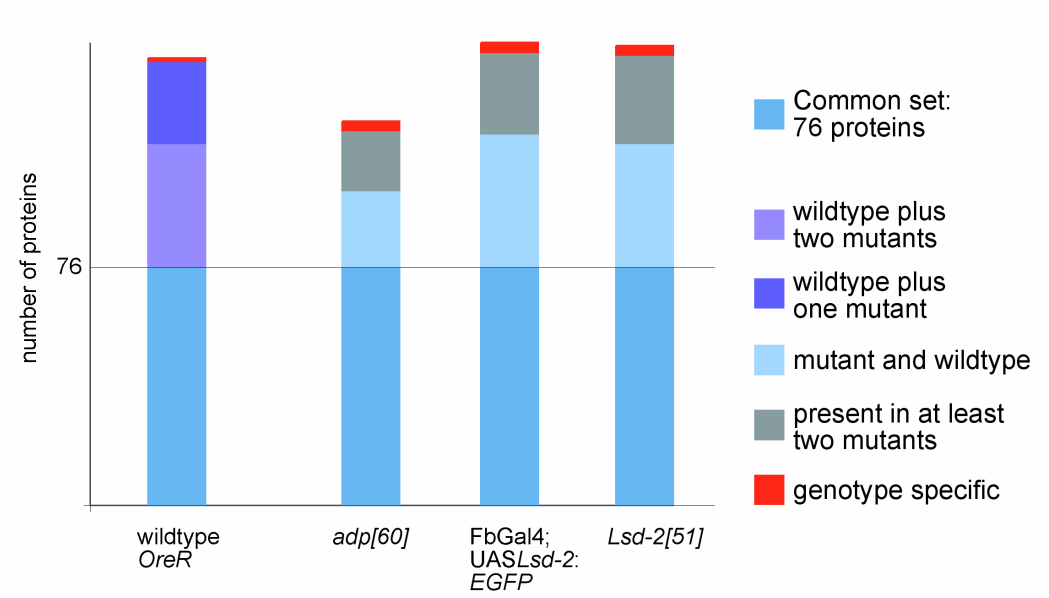

Fig. 2-13: Lipid droplet proteome comparison of the different genotypes
Proteins fulfilling high stringency criteria (no unique identifications, at least identified twice, either in one or at least two genotypes) have been analyzed for presence or absence in the different genotypes. 76 of the overall 182 proteins are present in all genotypes (53 % from the 142 wildtype *OreR* proteins, 62 % of the 122 *adp[60]* proteins, 52 % of the 147 *Lsd-2:EGFP* proteins and 52 % of the 146 *Lsd-2[51]* proteins). The darker as well as the light blue portions of the variable part of the bars are representing proteins shared between the wildtype and one or two of the other genotypes. In dark green, proteins not included in the wildtype but shared by the mutants are shown. Only a small portion of the identified proteins is genotype specific and indicated by the red coloring. The detailed results are shown in appendix IV.

Moreover, the main part of the remaining proteins identified in the mutants, which are not shared with the wildtype, are also present in the other mutant genotypes. Only three proteins of each genotype have been repeatedly identified as unique representatives. These are in the *adp[60]* mutants CG8036 (a transketolase), CG1803 (Regucalcin) and CG8588 (a novel protein) and in the *Lsd-2[51]* mutants these are CG3926 (a serine pyruvate aminotransferase), CG1907 (a carrier protein) and CG3751 (a ribosomal constituent). The samples obtained from *Lsd-2:EGFP* overexpressing larvae revealed CG5590 (a short chain dehydrogenase), CG7430 (a dihydrolipoyl dehydrogenase) and CG15081 (an SPFH/band-7 protein) as unique identifiers (see appendix IV).

2.13 The lipid droplet fraction contains the enzymes of a lipogenic pathway

The analysis of the identified proteins described in 2.11.2 revealed the enzymes of the backwards reactions of the Krebs cycle (see Table 2-2).

Table 2-2: Identified enzymes of the backwards reactions of the Krebs Cycle

OreR	***adp[60]***	***Lsd-2[51]***	***Lsd-2: EGFP***	**FlyBase ID**	**Function**
fatty acid synthesis from glutamate:					
		x		CG4233	aspartate transaminase EC 2.6.1.1
x	xy	xz	xy	CG7176	isocitrate DH EC 1.1.1.42
xz		xz		CG9244	aconitase EC 4.2.1.3
fatty acid synthesis from glucose:					
xyz	xyz	xykz	xy	CG1516	pyruvate Carboxylase 6.4.1.1.
		x	xkz	CG11876	pyruvate DH EC 1.2.4.1
common to both branches:					
xyz	xyz		xyz	CG8322	ATP citrate lyase EC 2.3.3.8 (formerly 4.1.3.8)
yz	xyz	yz	xyz	CG11198	acetyl CoA carboxylase EC6.4.1.2
xyz	xyz	xyz	xyz	CG3523	fatty acid synthase
	xyz	y		CG3524	[acyl-carrier protein] S-acetyltransferase activity (EC:2.3.1.38)
z	y			CG12233	isocitrate DH EC 1.1.1.41

x, y, z and k symbolize the different rounds of identification

This pathway has been demonstrated to be involved in lipogenesis in human and rat adipose tissue, starting both from glucose and glutamate as substrate (Belfiore and Iannello, 1995). However, the function of this pathway in lipogenesis and its subcellular localization is unknown. The association of the involved enzyme components with the lipid droplet fraction suggests that lipogenesis is taking place directly at or close to the surface of the lipid droplets. It also outlines that the pathway might not just be used in vertebrate adipocytes, but also in *Drosophila* fat tissue. Figure 2-14 shows a schematic drawing of the pathway.

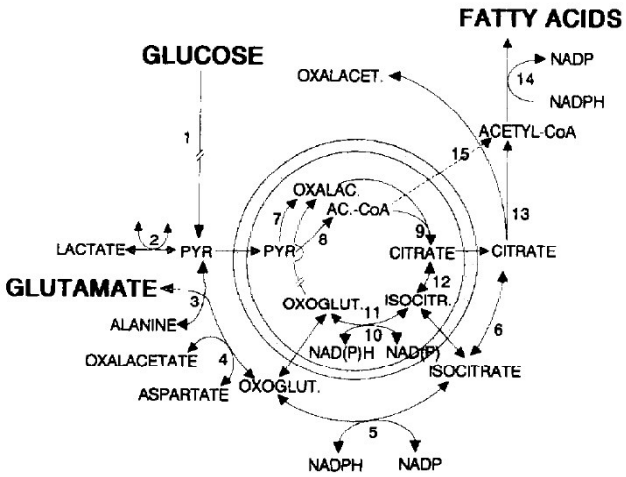

Fig. 2-14: Schematic drawing of the backwards reactions of the Krebs Cycle

The scheme was taken from Belfiore and Iannello (1995). Marked enzymes are: 1 enzymes of glycolysis (EC 2.7.1.1); 2 lactate dehydrogenase (EC 1.1.1.27); 3 alanine amino-transferase (EC 2.6.1.2); 4 aspartate aminotransferase (2.6. 1.1); 5 isocitrate dehydrogenase (cytosolic EC 1.1.1.42); 6 aconitate hydratase (EC 4.2.1.3); 7 pyruvate carboxylase (EC 6.4.1.1); 8 pyruvate dehydrogenase (EC 1.2.4.1); 9 citrate synthase (EC 4.1.3.7); 10 isocitrate dehydrogenase (EC 1.1.1.42 mitochondrial); 11 isocitrate dehydrogenase (EC 1.1.1.41); 12 aconitate hydratase (mitochondrial EC 4.2.1.3); 13 ATP citrate lyase (EC 4.1.3.8); 14 acetyl CoA carboxylase (EC 6.4.1.2) plus fatty acid synthase complex; 15 sequential steps catalyzed by acetyl CoA acetyltransferase (EC 2.3.1.9), acetoacetyl CoA hydrolase (EC 3.1.2.11), 3-ketoacid CoA transferase (EC 2.8.3.5) and again acetyl CoA acetyltransferase. Fatty acid synthesis from glucose: steps 1, 7, 8, 9, 13 and 14. Fatty acid synthesis from glutamate: steps 3, 4, 5, 6, 13 and 14.

Interestingly, two proteins (aconitase and ATP citrate lyase) of this pathway are among the lipid droplet-associated proteins which are altered in larvae of different genotypes which are either lean or obese (repeatedly identified in several genotypes, but not in the others). Homologues of these proteins have been previously described as lipogenic markers (Boll et al., 1996; Karbowska et al., 2001; Meegalla et al., 2002; Swierczynski et al., 2000). This observation led to a search for additional proteins within the identified lipid droplet-associated proteome, which show a differential presence in the one or the other genotype or have other indications for an altered, genotype-specific abundance.

2.14 Indications for genotype-specific quantitative differences in the lipid droplet proteome composition

The mass spectroscopy technique as used in the reported approach is not suited to obtain directly quantitative information. However, differences in the number of identified peptides that derive from a given protein, gives a rough

estimate of its relative abundance in the sample. This means that a protein can already be identified if a unique peptide appears in the fragmentation spectrum. However, if the protein is more abundant the chances of more than one peptide chosen for fragmentation will increase. Therefore, the more identified peptides of a certain protein can be found in a given protein sample, the more abundant the protein should be. Thus the number of identified peptides can serve as a crude measure for the relative abundance of a given protein in comparison to other proteins.

Additionally, proteins repeatedly associated with only one genotype might be enriched in the lipid droplet fraction of the corresponding larvae. Considering that such an evaluation would add some quantitative aspects to the data obtained, I used peptide frequency on proteins that were identified in at least two completely independent preparations. Table 2-3 summarizes 12 proteins that were found to vary significantly with respect to peptide frequency and thus, are likely to represent regulated proteins.

Table 2-3: Candidates for quantitatively regulated lipid droplet-asscociated proteins

Wildtype *OreR*	***adp[60]***	***Lsd-2[51]***	***Lsd-2:EGFP***	**Identified gene**	**Predicted function**	**Mammalian homologue**
x (27-2)	xy (75-1, 56-1)	z (88-1)	xy (96-1, 64-1)	CG5958	Retinol/fatty acid binding	CRALBP
---------	xy (46-2, 17-3)	xz (38-2, 79-3)	xyz (16-3, 60-2, 14-6)	CG9342	Triglyceride binding	microsomal TAG transfer protein
xz (92-1, 82-2)	---------	xz (90-1, 35-2)	---------	CG9244	Aconitase	aconitase
xyz (13-6. 56-2, 46-2)	xyz (30-2, 46-1, 29-3)	---------	xyz (17-4, 15-2, 44-1)	CG8322	ATP citrate lyase	ATP citrate lyase
xz (22-4, 21-3)	---------	xyz (31-2, 52-1, 32-4)	xyz (31-2, 72-1, 24-3)	CG4389	long chain hydroxoacyl CoA DH	long chain hydroxoacyl CoA DH
---------	---------	---------	xz (51-1, 86-1)	CG5590	oxidoreductase short chain DH	hydroxysteroid DH like
---------	xz (69-1, 38-1)	z (28-2)	---------	CG2254	short chain DH	short chain DH9
---------	xyz (63-1, 47-1, 64-1)	y (54-1)	---------	CG3524	[ACP] S-acetyltransferase activity (EC:2.3.1.38)	FAS
---------	yz (40-1, 71-1)	---------	---------	CG8588	no prediction possible	no mammalian homolog C.elegans predicted ER protein
---------	---------	---------	xyz (80-1, 33-2, 61-1)	CG15081	nothing predictable SPFH/band7	B cell receptor associated protein 37 prohibitin / stomatin
xyz (97-1, 69-1, 85-1)	z (68-1)	---------	x (78-1)	CG15825	protein transport/ targeting	nothing mammalian, weaker BLAST hits in Anopheles and Caenorhabditis
---------	xy (53-2, 66-1)	---------	---------	CG1803	Regucalcin	regucalcin / SMP-30

x, y, z and k symbolize the different rounds of identification. The numbers in brackets indicate the rank of identification and the number of peptides identified.

Several proteins have been repeatedly identified in the lipid droplet protein preparations of larvae of only one genotype, like for example the B-cell receptor-associated protein homologue encoded by CG15081, which was only identified in the *Lsd-2:EGFP* overexpression situation or Regucalcin only detected in the *adipose* mutant (Table 2-3). Conversely, proteins such as ATP citrate lyase and aconitase were repeatedly devoid in lipid droplet samples from larvae of a given genotype. These observations suggest that the proteins are upregulated or downregulated in the lipid droplet fraction of larvae of a given genotype, respectively. An upregulation might result in a genotype-specific identification of the protein, whereas downregulation might decrease the amount of the protein below the detection limit.

2.15 Testing selected candidates for their subcellular localization

Verification of the localization of proteins identified in subcellular proteomics screens is an essential step, as contaminating proteins or organelle-remnants might have been co-purified. Since antibodies are most often not available for monitoring the localization of the endogenous candidate protein, overexpression of a fluorescently tagged candidate protein can be used instead to assay the protein distribution pattern in cells. Since the generation of fusion protein expressing transgenic animals is time-consuming and therefore not suited for a high-throughput screening of the candidates, pre-tests were done with tissue culture cells (*Drosophila* Schneider S2 cells; Schneider, 1972). They were transfected with plasmids coding for fluorescently labeled versions of the candidate proteins generated using the recombination cloning system Gateway (see material and methods 3.3). This system allows one to rapidly generate constructs that can be used for the generation of transgenic animals to confirm a positive tissue culture localization at the organismic level.

In order to increase the amount and size of lipid droplets in Schneider S2 cells, they were fed with oleic acid (Weller et al., 1991). After feeding (material and methods 3.5.1), a variable number of lipid droplets sized from 0.3 to 1 µm in diameter, can be detected both by light microscopic examination (e.g. Fig. 2-15 D and H), as well as by staining with the lipid droplet specific dyes Nile

Red (Greenspan et al., 1985; Fig. 2-15 B) or BODIPY (Gocze and Freeman, 1994; Fig. 2-15 E).

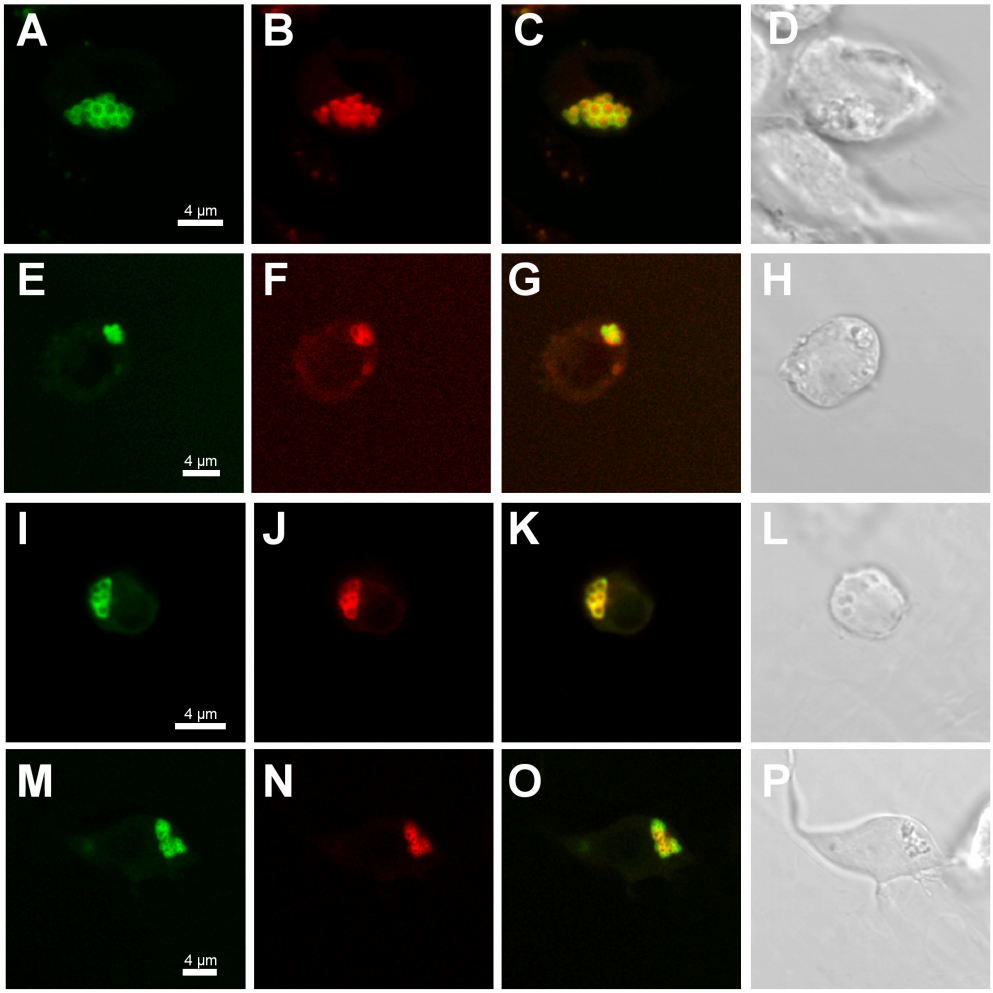

Fig. 2-15: Localization of fluorescent LSD-1 and LSD-2 variants in *Drosophila* Schneider S2 cells

S2 cells were transfected or co-transfected (material and methods 3.5.1) with C-terminal tagged fluorescent variants of LSD-1 and LSD-2. A–D: LSD-1:EGFP transfection (A) counterstained with Nile Red (B). E–H: LSD-2:TdT transfection (F) counterstained with BODIPY (E). I–P double transfections of LSD-1:EGFP (I, M) and LSD-2:TdT (J, N). C, G, K and O are showing the merged channels and in D, H, L and P transmission pictures of the transfected cells are shown. Cells were fixed in 4% PFA (in PBS or in bufferB) and stained with Nile Red (1mg/ml DMSO stock 1:50000 diluted) or BODIPY (1mg/ml ethanol stock 1:50000 diluted). Images were taken with a Leica TCS SP2 confocal microscope.

2.15.1 Lipid droplet membrane localization of LSD proteins in S2 cells

In order to obtain molecular markers for lipid droplet-association of selected candidate proteins that can also be used for co-localization studies, fluorescent variants of the LSD proteins have been generated. Upon

transfection, both proteins localize to the surface of lipid droplets in Schneider S2 cells (Fig. 2-15 A and F). Two localization patterns were observed. First, both proteins are found in association with the same set of lipid droplets (e.g. 2-15 I–K). Secondly, lipid droplets of the same cell were associated with only one of the two proteins in addition to droplets which were decorated with both proteins (e.g. LSD-1 in Fig. 2-15 M–O). These observations suggest that the lipid droplet population of Schneider S2 cells might be heterogenous with respect to their demand for LSD proteins and metabolic state.

2.15.2 Localization of selected candidates

EGFP fusion proteins with four putative lipid droplet-associated proteins have been generated and assayed for their localization in Schneider S2 cells. The first candidate, CG1112, is a protein with a predicted alpha/beta hydrolase fold. It is assumed to function as an esterase or lipase (FlyBase, 2003) and has been identified in all genotypes assayed in the proteomics screen. Fig. 2-16 shows that the EGFP:CG1112 fusion protein has a broad cytoplasmic distribution and accumulates in ring-like sub-structures inside the Schneider cells (Fig.: 2-16 A, E).

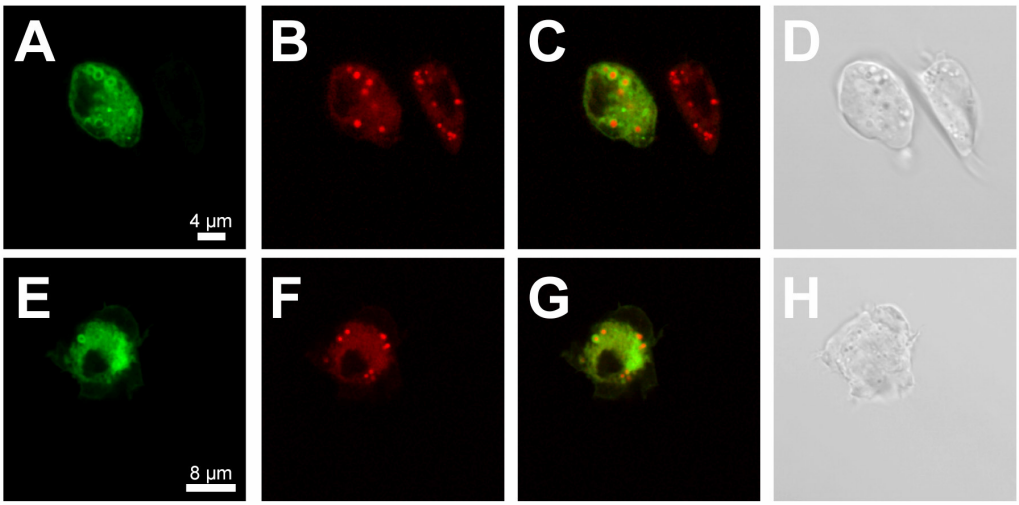

Fig. 2-16: Localization of CG1112 in *Drosophila* Schneider S2 cells
Confocal images of two cells transfected with a construct coding for an N-terminal EGFP tagged form of the CG1112 protein are shown (A-D and E–H). A and E show the EGFP:CG1112 signal, B and F show the red signal of the lipid droplet specific dye Nile red which has been used for counterstaining. C and G show the merged channels and D and H are transmission images. Staining and imaging was performed as described in Fig. 2-15.

Counter-staining with Nile Red (Fig. 2-16 B, F) shows that these ring like structures are lipid droplets and that the EGFP:CG1112 fusion protein demarcates their surface (merged channels in Fig. 2-16 C, G). Interestingly, CG1112:EGFP is not found around all lipid droplets, but labels only a subset.
Two other proteins, assayed for their subcellular localization in the same way, are CG10691 and CG15081 (FlyBase, 2003). They belong to the SPFH/ band7 domain containing protein family which is predicted to participate in membrane protein turnover control (Tavernarakis et al., 1999). Both were classified as members of the uncertain function/protein transport function group of candidate lipid droplet-associated proteins. CG15081 was exclusively identified in LSD-2:EGFP overexpressing individuals, whereas CG10691 was identified in the lipid droplet-associated protein samples of larvae of all investigated genotypes. EGFP:CG10691 shows a weak cytoplasmic distribution and the ring like structures (Fig. 2-17 A, E), which can be counter-stained by Nile Red (Fig. 2-17 B, F), and thus correspond to the lipid droplet surface areas. As in the case of EGFP:CG1112, only a subset of the cellular lipid droplets are decorated. In contrast, EGFP:CG15081 is not enriched around the lipid droplets (Fig. 2-17 I-P). However, it is found in a subcellularly restricted pattern, suggesting an as yet unidentified cellular compartment. In one transfection series, however, also some ring-like structures could be detected (data not shown). This observation is consistent with the proposal that under certain and as yet unidentified conditions, the CG15081 protein can be targeted to the lipid droplet surface.

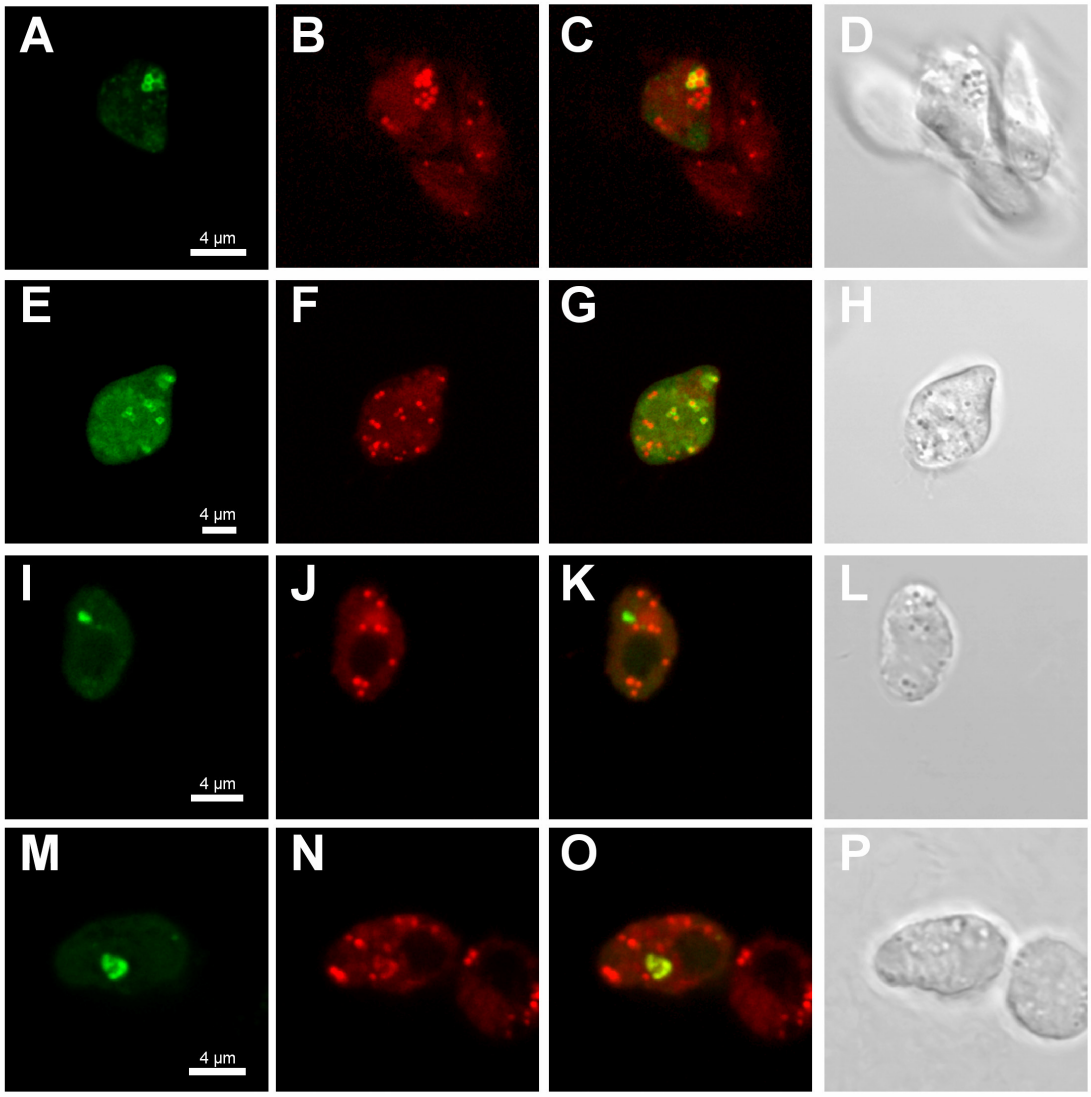

Fig. 2-17: Localization of CG10691 and CG15081 in *Drosophila* Schneider S2 cells

Confocal images of cells transfected with a construct coding for an N-terminal EGFP tagged form of the CG10691 protein (A-D and E–H) or the CG15081 protein (I–L and M–P) are shown. A, E, I and M show the EGFP signal, B, F, J and N show the red signal of the lipid droplet specific dye Nile red which has been used for counterstaining. C, G, K and O show the merged channels and D, H, L and P are transmission images. Staining and imaging was performed as described in Fig. 2-15.

The fourth candidate protein, CG2254, contains a short chain dehydrogenase motif (FlyBase, 2003). It was consistently identified in the *adipose[60]* mutant fat body extracts and once in the *Lsd-2[51]* mutant. The EGFP:CG2254 fusion protein localizes exclusively around lipid droplets (Fig. 2-18), no significant staining was observed in the cytoplasm. As seen with CG1112 and CG10691, not all lipid droplets of a given cell were decorated.

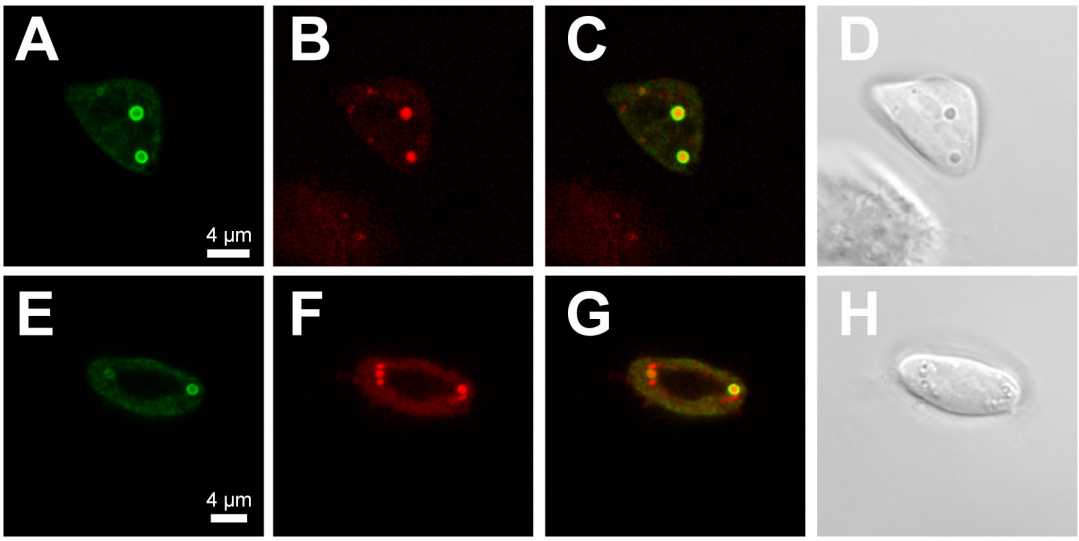

Fig. 2-18: Localization of EGFP:CG2254 in *Drosophila* Schneider S2 cells
Confocal images of two cells transfected with a construct coding for an N-terminal EGFP tagged form of the CG2254 protein are shown (A-D and E–H). A and E show the EGFP signal, B and F show the red signal of the lipid droplet specific dye Nile red which has been used for counterstaining. C and G show the merged channels and D and H are transmission images. Staining and imaging was performed as described in Fig. 2-15.

In summary, the results show that three out of four examined candidate proteins are associated with lipid droplets and are *bona fide* components of the lipid droplet-associated proteomes as revealed by mass spectroscopy analysis combined with fluorescent protein *in vivo* imaging. Aside from supporting the reliability of the biochemical analysis, which provided us with a total of 271 candidates for the lipid droplet-associated proteome, the localization pattern of by now six proteins including the two PAT-domain proteins LSD-1 and LSD-2 strongly suggest that the individual lipid droplets of cells are not homogeneous with respect to the protein composition of their surfaces. Whether the differences are of qualitative nature, and thus may reflect different metabolic subsets of lipid droplets, or only quantitative variations can not be yet decided.

3. Material and Methods

3.1 *Drosophila* genetics

3.1.1 Fly strains and fly culture

All flies were propagated on a complex cornflour-soyflour-molasse medium supplemented with dry yeast at 25 °C and 20–30 % humidity with a 12 h/12 h light/dark cycle and were handled according to standard procedures as outlined in e.g.: Ashburner (1989), Greenspan (1997) or Roberts (1998).
An overview of all fly strains used in this work is given in table 3-1. Further details considering fly strains and marker mutations can be found at the following websites: FlyBase (http://flybase.bio.indiana.edu) and Bloomington stock center (http://flystocks.bio.indiana.edu/). *OregonR*, *Lsd-2[KG00149]* and *white* flies were obtained from the Bloomington *Drosophila* stock center (Bloomington, Indiana, USA). *Lsd-2[51]* and *Lsd-2[40]* deletion mutants (missing *Lsd-2* sequences from pos. –34 to +654 and –34 to +970 relative to putative start ATG) as well as flies carrying the precise excision allele *Lsd-2[+]* were generated by a conventional P-element mobilization scheme (see Fig. 3-1) and molecularly confirmed by sequencing the relevant genomic part of the *Lsd-2* gene using the primer combination SGO181 and RHO206 (see table 3-2).

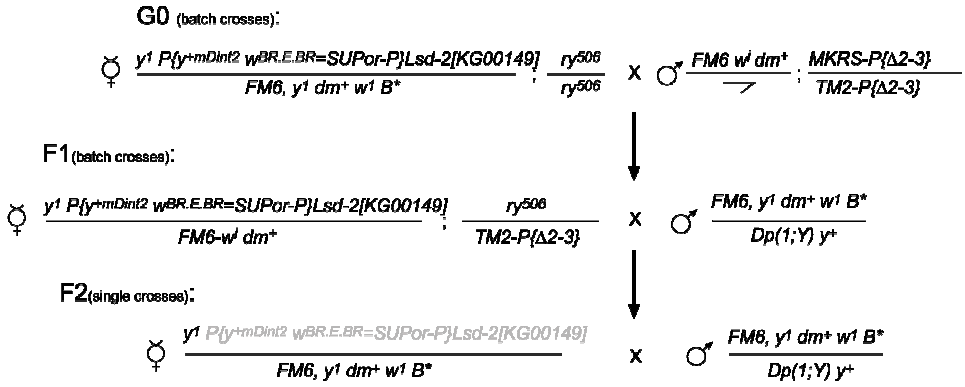

Fig. 3-1: Crossing scheme for the generation of *Lsd-2* mutants and revertants

Lsd-2[KG00149] heterozygous females were mated with male flies carrying the transposase encoding gene (G0 cross). Flies resulting from this cross carrying both, the P-element insertion and the transposase source, were crossed against the *FM6* balancer chromosome

carrying males (Filial generation F1). Remobilization in the progeny of this cross was detected by loss of the *yellow* marker gene, resulting in a yellow body color. Those flies were again crossed against the *FM6* balancer chromosome carrying males (Filial generation F2, loss of the P-element is depicted in light grey) in order to establish genetically stable fly lines, which were then molecularly characterized by PCR.

3.1.2 Generation of transgenic flies

Transgenic fly stocks allowing conditional expression of *Lsd-2* (UAS-*Lsd-2*) were generated in collaboration with S. Grönke (MPI für biophysikalische Chemie, Göttingen). The *Lsd-2* full-length cDNA clone RE58939 (ResGen; Invitrogen, Karlsruhe) was restricted with *Eco*RI/*Kpn*I and cloned into the pUAST vector (Brand and Perrimon, 1993), which was transformed into *Escherichia coli*. The resulting plasmid DNA was isolated using the Qiagen Plasmid Midi Kit (Qiagen, Hilden) followed by phenol/chloroform extraction and ethanol precipitation. Afterwards the construct was mixed with the transposase coding Δ2,3-helper plasmid (Laski et al., 1986) in a ratio of 3:1 (weight/weight). After co-precipitation, the plasmids were dissolved in water and the DNA concentration was adjusted to 450 ng DNA per µl. This solution was injected into pre-blastoderm embryos of the *Drosophila white* mutant strain. After hatching, the flies were again crossed to *white* mutant flies. The progeny of this cross was subsequently screened for transgene-insertion in the germline by reversion of the *white* mutant phenotype, resulting in red eye color. Flies conditionally overexpressing a C-terminal EGFP fusion protein version of LSD-2 (UAS-*Lsd-2*:EGFP) were generated by germ line transformation with pUAST-*Lsd-2*:EGFP. This construct was generated by introducing the *Lsd-2*:EGFP cassette of a pEGFP-N2 *Lsd-2* construct into pUAST. For fat body-targeted *Lsd-2* expression Fb-Gal4 (Gal4-trap inserted at CG1516) and *Adh*-Gal4 (Fischer et al., 1988) lines were used.

Table 3-1: Fly strains used in this study

Name	Genotype	Reference
OregonR	wildtype	Bloomington
Lsd-2[KG00149]	*y[1] P{y[+mDint2] w[BR.E.BR]=SUPor-P}Lsd-2[KG00149] / Dp(1;Y) y[+]* or hom*; ry[506]* float	Spradling et al., 1999
Lsd-2[+]	*y[1] rev P{y[+mDint2]w[BR.E.BR] =SUPor-P}Lsd-2[KG00149] / Dp(1;Y) y[+] or* hom*; ry[506]* float	Grönke et al., 2003
Lsd-2[40]	*y[*] Lsd-2[40] / Dp(1;Y) y[+]* or FM6 float	Grönke et al., 2003
Lsd-2[51]	*Lsd-2[51] / FM7i; P{w[+mC]=ActGFP} JMR3* or hom or *Y*	Grönke et al., 2003
UAS-*Lsd-2*	*w[*] ; P{w[+mC]UAS-Lsd-2} / CyO-hb-beta-gal* float	Grönke et al., 2003
UAS-*Lsd2:EGFP*	*w[*] ; + ; P{w[+mC]UAS-Lsd-2:EGFP} / TM3 Sb[1] e[1]* float	Grönke et al., 2003
***Adh*-Gal4**	*w[+] ; Adh[fn6] cn / Adh[fn6] cn ; P{ry[+] ADH-Gal4}E1 / TM2 Ubx[130] ry[+]*	Fischer et al., 1988
Fb-Gal4	*w[*]; P{w[+mW.hs]=GawB}FB/SNS*	Grönke et al., 2003
brummer[1]	*w[1118]; bmm1/TM3 Sb*	S. Grönke, in preparation
UAS-*brummer*	*w[*]; P{w[+mC]UAST-bmm}*	S. Grönke, in preparation
UAS-*AKHR*	*w[*]; P{UAST AKHR}/TM3 Sb[1] e[1]* float	R. P. Kühnlein, unpublished
UAS-*midway*	*w[*]; P{w[+mC]UAS-mdy}/TM3 Sb[1] e[1]* float	R. P. Kühnlein, unpublished
midway[QX25]	*mdy[QX25] cn[1] bw[1] / CyO, l(2)DTS513[1]*	Buszczak et al., 2002
chico[2]	*y[*] w[*] ; chico[2] / CyO y[+]*	Bohni et al., 1999
adp[60]	*y[*] w[*] ; adp[60] / CyO* float	Häder et al., 2003
white	*w*	Bloomington
Transposase source	*FM6 y* w^{j} dm^{+} *B / Dp(1;Y)* y^{+};; MKRS, *Sb P*[$ry^{+t7.2}$Δ2-3]99B / TM2, ry^{1}P[$ry^{+t7.2}$Δ2-3]99B	Ulrich Schäfer (MPI für biophysikalische Chemie, Göttingen)
FM7i, act-GFP	*C(1)DX, y f/FM7,* y^{93j} sc^{8} *w oc ptg B P*[w^{+mc}*act::GFP]/Y*	Bloomington
FM6	*FM6* y^{1} w^{1} dm^{+} *B / Dp(1;Y)* y^{+}	Bloomington

3.2 Embryology

3.2.1 Collection of embryos

Embryos for stainings were collected in “fly cages” using apple juice agar plates supplemented with yeast. For details of the protocol see Roberts (1998).

3.2.2 Fixation of embryos

Embryos from the agar plates were collected in thin-meshed sieves using a brush.
After excessive washing with water, the chorion was removed by incubating the embryos in 50 % hypochloric solution (50 % Klorix in water; Colgate-Palmolive, Hamburg) for 2–3 minutes with constant perturbation. This dechorionating solution was removed by washing with water before the embryos were transferred into a scintillation vial with 4 ml fixing solution (100 mM Hepes, 2 mM $MgSO_4$, 1 mM EGTA, pH 6.4) and 5 ml heptane. After adding 500 µl of a 37 % formaldehyde solution the embryos were fixed for 20 minutes under rigorous shaking. Following phase separation, the lower aqueous phase was removed and the embryos were devitellinized by the addition of 10 ml methanol and shaking for two minutes. In order to detach last remnants of the vitelline membrane the methanol was replaced by 10 ml fresh methanol, again followed by rigorous shaking. The embryos were then stored in methanol at –20 °C until use.

3.2.3 Developmental expression analysis by RNA *in situ* hybridization

In situ hybridization on whole-mount embryo collections was performed as described in Goldstein and Fyrberg (1994), using a digoxygenin-labeled antisense RNA probe. The *Lsd-2* RNA antisense probe was generated by *in vitro* transcription on a *Cla*I linearized RE58939 *Lsd-2* cDNA template using T3 polymerase and the DIG labeling mix (Roche Diagnostics, Mannheim). For *in situ* hybridization on larval fat body, *OregonR* 3rd instar larvae were

mechanically opened and the exposed fat body tissue fixed in 10 % paraformaldehyde/50 mM EGTA in PBS diluted 1:1 with PBS for 15 minutes before specimens were subjected to the washing, hybridization and staining procedures of the embryo *in situ* hybridization protocol. All buffer volumes were 1 ml and all incubation steps were performed at room temperature if not otherwise mentioned.

Fixed embryos, stored in methanol, were first washed with 50 % methanol/PBT (PBS including 0.1 % Tween 20) and then with 100 % PBT for 5 min. A post-fixation was carried out using a mixture of 500 µl PBT and 500 µl RNA fix solution (PBS including 10 % formaldehyde and 50 mM EGTA) for 20 min, followed by several PBT washing steps. These washing steps were followed by a proteinase K digestion (10 µl of a 5 mg/ml proteinase K solution in 1 ml PBT for 1 min) in order to facilitate penetration by the RNA antisense probe. Afterwards several PBT washes were performed to stop the reaction and a second post fixation step as mentioned above was carried out. The PBT was stepwise replaced by HybeB (50 % Formamid, 5 x SSC (Sambrook and Russel, 2001), 0.1 % Tween 20) and afterwards hybridisation solution (50 % Formamid, 5 x SSC (Sambrook and Russel, 2001), 50 µg/ml Heparin, 200 µg/ml Torula RNA, 0.1 % Tween 20, pH 6.7). Prehybridization was carried out at 58 °C for 30 min to 1 hour. After prehybridization the buffer was removed quantitatively and the RNA antisense probe was added in 30 µl hybridization solution (1–5 µl probe), followed by incubation at 58 °C over night.

The next day embryos or opened larvae were washed once with hybridization solution and then two times with HybeB, which was afterwards diluted with PBT. After re-equilibration, several PBT-washing steps were performed. Meanwhile anti DIG FAB fragments conjugated to alkaline phosphatase (Roche Diagnostics, Mannheim) were preabsorbed against wildtype embryos in order to reduce unspecific binding. The hybridized embryos were incubated with these antibodies for 1 hour (antibodies diluted 1:2000 in PBT). After an additional washing step with PBT the specimens were equilibrated in alkaline phosphatase buffer (AP buffer: 100 mM Tris pH 9.5, 100 mM NaCl, 50 mM $MgCl_2$, 0.1 % Tween 20) three times for 5 min each. The embryos were afterwards incubated in AP buffer containing NBT/BCIP solution (stock solution 1:100 diluted, Roche Diagnostics, Mannheim) until staining took

place. The reaction was stopped by several PBT washing steps and embryos were subjected to a stepwise ethanol dehydration procedure prior to storage in 100 % ethanol or mounting in Canada balsam (Sigma-Aldrich, Taufkirchen).

3.3 Molecular biology

Recombinant DNA was either generated using standard techniques according to Sambrook and Russel (2001) or using the Gateway recombination cloning system (Invitrogen, Karlsruhe) according to the manufacturers instructions. DNA was prepared using the Qiagen Plasmid isolation kits (Qiagen, Hilden; Mini or Midi size) and PCR products were purified using the Qiagen spin columns of the PCR purification kit (Qiagen, Hilden) according to the manufacturers instructions. Restriction endonucleases were either purchased from New England Biolabs (NEB, Frankfurt a.M) or Amersham Biosciences (Freiburg). Recombinant DNA was propagated in the *E. coli* strains DH5α or TOP10.

3.3.1 Polymerase Chain Reaction (PCR)

Polymerase chain reaction was used to amplify DNA prior to cloning and to characterize the deletion mutants generated in the course of the imprecise excision screen (3.1.1). For screening purposes, recombinant Taq Polymerase obtained from Qiagen (Qiagen, Hilden) was used. For generating recombinant DNA, the proofreading capable Expand Polymerase (Roche Diagnostics, Mannheim) was used for amplification. Primers were obtained from MWG–Biotech AG (Ebersberg) and used in a final concentration of 1 µM.

Table 3-2: Primers used in this study

Name	Sequence
SGO181	GCGTCACACAATCCTCGG
RHO206	CAGGATGTCTATGGCAAAGTAA
SGO214	TAGAATTCGATGGCCAGTGCAGAGCAGAA
SGO215	TCGAATTCTACTGAGACGACACCGCCG
*Lsd-2Not*I forward	**GCTTGCGGCCGCCACC**ATGGCCAGTGCAGAGCAGAAAC
*Lsd-2Asc*I no stop	**GCAAGGCGCGCCCCT**GAGACGACACCGCCGGCG

Name	Sequence
*Lsd-1Not*I forward	**GCTTGCGGCCGCCACC**ATGGCAACTGCAACCAGCGGC
*Lsd-1Asc*I no stop	**GCAAGGCGCGCCCGT**AGACGCCGTTGATGTTATTG
CG10691*Not*I forward	**GCTTGCGGCCGCCACC**ATGGCTGCTCAGTTCTTTAATCGC
CG10691*Asc*I reverse	**GCAAGGCGCGCCCCT**ACTGCGCGATGGTCGATGGC
CG15081*Not*I forward	**GCTTGCGGCCGCCACC**ATGGCACAGAGCAAATTGAACG
CG15081*Asc*I reverse	**GCAAGGCGCGCCCCT**ATTTACTTTTGTAAACCTTCTCGG
CG2254*Not*I forward	**GCTTGCGGCCGCCACC**ATGTCGAAAGTGACGCAAAGTG
CG2254*Asc*I reverse	**GCAAGGCGCGCCCGG**ACTTATCGGTATCCACACC
CG1112*Not*I forward	**GCTTGCGGCCGCCACC**ATGAATAAGAACCTCGGCTTTG
CG1112*Asc*I reverse	**GCAAGGCGCGCCCTTA**AAACAATAAATCTTTGTTGTCG

Sequences in bold indicate constant *Not*I / *Asc*I sites and linker regions for Gateway cloning.

Example of a standard PCR protocol:

- 5 minutes 95 °C initial denaturation
- Cycling (30 to 35 cycles):
    - 1 minute 95 °C
    - 30–60 seconds 55–63 °C (annealing temperature depends on the melting temperature of the primers used)
    - 1 minute extension time at 72 °C for each kb using Taq Polymerase (Expand 2 minutes per kb)
- 8 minutes final extension at 72 °C

3.3.2 Isolation of genomic DNA from single flies

For the analysis of the jump-out events mapping the molecular lesion, single fly PCR was performed. For this purpose genomic DNA was isolated according to Gloor et al., (1993). Therefore, a single fly was placed in an eppendorf cup and homogenized in 50 µl of squishing buffer (SB: 10 mM Tris-Cl pH 8.2, 1 mM EDTA, 25 mM NaCl, and 200 µg/ml proteinase K). The homogenate was incubated for 20 to 30 min at 37 °C prior to inactivating proteinase K by heating at 95 °C for 2 min. 1 µl of this solution was used in 20 µl PCR reactions.

3.3.3 Sequencing of DNA

Recombinant DNA and PCR products of the mutant deletion analysis were sequenced on both strands using Cycle Sequencing with an ABI Prism 377/96 Sequencer and the DNA sequencing kit from Applied Biosciences (Foster City, Ca, USA) according to the manufacturers instructions. Sequences were analyzed using the DNA Star software package for the Macintosh platform.

Table 3-3: Plasmids used and generated in this study

Name	Description	Reference
RE58939	*Lsd-2* cDNA	Rubin et al., 2000
GH13950	*CG1112* cDNA	Rubin et al., 2000
RH47744	*CG2254* cDNA	Rubin et al., 2000
LD46344	*CG15081* cDNA	Rubin et al., 2000
GH12454	*CG10691* cDNA	Rubin et al., 2000
GH10767	*Lsd-1* cDNA	Rubin et al., 2000
pUAST	Germ-line transformation vector with upstream activating sequence (UAS) for Gal4-mediated transgene expression	Brand and Perrimon, 1993
Δ2,3 Helper	Transposase encoding helper plasmid for germline transformation, not able to replicate	Laski et al., 1986
pUAST-*Lsd-2*	*Lsd-2* cDNA in pUAST for targeted over/mis-expression *in vivo*	Grönke et al., 2003
pUAST-*Lsd2:EGFP*	*Lsd-2* cDNA tagged with GFP in pUAST for targeted over/mis-expression *in vivo* and *in vivo* localization studies	Grönke et al., 2003
pGEX-4T-3	GST-fusion vector for bacterial protein expression	Amersham Biosciences, Freiburg
GST-LSD-2	*Lsd-2* coding region was PCR amplified and fused to GST for purification using pGEX-4T-3	Grönke et al., 2003
pENTR/D-TOPO	ENTRY vector of Gateway system for recombination cloning	Invitrogen, Karlsruhe
pUbi-Rfa-TdT	TdT coding sequence was cloned for C-terminal fusions together with Gateway *att* recombination sites under control of ubiquitin promotor in pBluescript (Stratagene, Amsterdam, The Netherlands) backbone	Dr. A. Herzig, MPI für biophysikalische Chemie, Göttingen

Name	Description	Reference
pUbi-Rfa-EGFP	EGFP coding sequence was cloned for C-terminal fusions together with Gateway *att* recombination sites under control of ubiquitin promotor in pBluescript (Stratagene, Amsterdam, The Netherlands) backbone	Dr. A. Herzig, MPI für biophysikalische Chemie, Göttingen
pUbi-EGFP-Rfa	EGFP coding sequence was cloned for N-terminal fusions together with Gateway *att* recombination sites under control of ubiquitin promotor in pBluescript (Stratagene, Amsterdam, The Netherlands) backbone	Dr. A. Herzig, MPI für biophysikalische Chemie, Göttingen
pENTR-*Lsd-2*	*Lsd-2* coding region was PCR amplified and *Not*I/*Asc*I directional cloned into pENTR/D-TOPO	This study
pENTR-*Lsd-1*	*Lsd-1* coding region was PCR amplified and *Not*I/*Asc*I directional cloned into pENTR/D-TOPO	This study
pENTR-*CG1112*	*CG1112* coding region was PCR amplified and *Not*I/*Asc*I directional cloned into pENTR/D-TOPO	This study
pENTR-*CG2254*	*CG2254* coding region was PCR amplified and *Not*I/*Asc*I directional cloned into pENTR/D-TOPO	This study
pENTR-*CG10691*	*CG10691* coding region was PCR amplified and *Not*I/*Asc*I directional cloned into pENTR/D-TOPO	This study
pENTR-*CG15081*	*CG15081* coding region was PCR amplified and *Not*I/*Asc*I directional cloned into pENTR/D-TOPO	This study
pUbi-*Lsd-2:TdT*	Derived from Gateway recombination reaction between pENTR-*Lsd-2* and pUbi-Rfa-TdT	This study
pUbi-*Lsd-1:EGFP*	Derived from Gateway recombination reaction between pENTR-*Lsd-1* and pUbi-Rfa-EGFP	This study
pUbi-*CG1112:EGFP*	Derived from Gateway recombination reaction between pENTR-*CG1112* and pUbi-EGFP-Rfa	This study
pUbi-*CG2254:EGFP*	Derived from Gateway recombination reaction between pENTR-*CG2254* and pUbi-EGFP-Rfa	This study
pUbi-*CG10691:EGFP*	Derived from Gateway recombination reaction between pENTR-*CG10691* and pUbi-EGFP-Rfa	This study
pUbi-*CG15081:EGFP*	Derived from Gateway recombination reaction between pENTR-*CG15081* and pUbi-EGFP-Rfa	This study

3.4 Biochemistry

3.4.1 Antiserum production

A LSD-2-specific antiserum was generated in cooperation with S. Grönke. Rabbits were immunized with partially purified GST-LSD-2 fusion protein according to the standard immunization scheme of Eurogentec (Seraing, Belgium). The *Lsd-2* full-length coding region was amplified by PCR using the primer pair SGO214/SGO215 and the *Lsd-2* cDNA clone RE58939 as template before cloning into pGEX-4T-3 (Amersham Biosciences, Freiburg). Recombinant GST-LSD-2 expression was induced in *E.coli* BL21 Codon plus cells (Stratagene, Amsterdam, The Netherlands) according to the manufacturers guidelines. For each round of immunization approximately 100 µg of fusion protein was partially purified using preparative SDS-PAGE.

3.4.2 Triacylglycerol (TAG) assay

TAG content quantification was done using the Infinity kit (Sigma-Aldrich, Taufkirchen) in a microtiter format (Grönke et al., 2003). Batches of 8 male flies of the desired genotypes were subjected to homogenization in 0.05 % Tween 20 using a Fast Prep 120 machine (Bio101, Irvine, USA). Homogenates were subjected to a 70 °C heat-inactivation step and then centrifuged. An aliquot of the supernatant was incubated with Infinity reagent at 37 °C and its absorbance measured at 540 nm using a spectrophotometer. Absolute TAG amounts were determined using Triglyceride standard (Sigma-Aldrich, Taufkirchen) and scaled to the total protein content of the homogenates determined using the BCA protein assay reagent (Perbio Science, Bonn). TAG contents of a representative experiment are depicted as average values of triplicate measurements with corresponding standard deviations. Experiments were repeated at least twice.

3.4.3 Lipid droplet fractionation

For every gradient 60 to 75 fat bodies from wandering late third instar *OregonR* larvae were hand-dissected in phosphate buffered saline (PBS) on ice. The dissected fat bodies were transferred into 100 µl fat body buffer (FBB: 10 mM HEPES pH 7.6, 10 mM KCl, 0.1 mM EDTA, 0.1 mM EGTA and 1 mM DTT) including protease inhibitors (EDTA-free complete protease inhibitors, Roche Diagnostics, Mannheim). Fat bodies were frozen and kept at –80 °C until use. Lysis of the fat bodies was performed by bath sonication until dispersion of fat bodies. Lipid droplets were purified as described by Yu et al., (2000). After sonication the cellular debris was pelleted by centrifugation at 3000 x g for 8 min. The resulting postnuclear supernatant (PNS) was adjusted to a volume of 3 ml, mixed with an equal volume of FBB including 1.08 M sucrose, and afterwards transferred into a 12 ml polyallomer ultracentrifugation tube (Beckman Instruments, Palo Alto, USA). It was then sequentially overlayed with 2 ml of 0.27 M and 0.135 M sucrose each in FBB and top solution (FBB only). The gradient was centrifuged for 1 h 30 min at 4 °C at 30000 rpm in a Beckman SW41.Ti rotor using a Beckman Optima L-90K ultracentrifuge (Beckman Instruments, Palo Alto, USA). After the run 8 fractions, 1.5 ml each, were pipetted from top to bottom: the buoyant lipid droplets (fractions F1 and F2), the mid-zone (F3 and F4) between lipid droplets and cytosol, and the cytosol itself (F5-F8). The protein content of 50 µl of each fraction was measured using the BCA assay.
The desired protein amount of the respective fraction was subsequently precipitated using the method of Wessel and Flügge (see 3.4.6) and protein pellets either frozen at –20 °C or solubilized in the respective buffer.

3.4.4 BCA protein assay

Protein amounts were measured using the Pierce BCA assay kit (Perbio Science, Bonn) according to the manufacturers instructions. Defined amounts of bovine serum albumin were used as standard.
In the BCA assay proteins form a complex with Cu^{2+} in an alkaline solution (Biuret reaction). Together with Bicinchononic acid (BCA) this complex

develops a violet color, which can be measured by spectroscopy at a wavelength of 572 nm.

3.4.5 Electron microscopy of isolated lipid droplets

Electron microscopy of purified lipid droplets was performed in collaboration with Dr. Dietmar Riedel (MPI für biophysikalische Chemie, Göttingen) using Epon embedding carried out as described in Luft (1961). In brief, purified lipid droplets were pelleted by ultracentrifugation and afterwards fixed by immersion in 2 % glutaraldehyde in 0.1 M cacodylate buffer at pH 7.4. Fixation was performed for 60 min at room temperature. The fixed pellet was immobilized with 2 % agarose in cacodylate buffer at pH 7.4. The pellet was cubed and the pieces were carefully washed with buffer, followed by further fixation in 1 % osmium tetroxide. After pre-embedding, the sample was stained with 1 % uranyl acetate, followed by dehydration and embedding in Agar 100 (equivalent to Epon). Thin sections (30-60 nm) were again counterstained with uranyl acetate and lead citrate and examined using a Philips CM 120 BioTwin transmission electron microscope (Philips Inc.Eindhoven, The Netherlands). Images were taken with a 1K slow scan CCD camera (GATAN, Inc., Munich).

3.4.6 Methanol–chloroform protein precipitation

Protein precipitation was carried out according to Wessel and Flügge (1984). 100 µl protein solution was mixed with 400 µl methanol and vortexed thoroughly. After adding 100 µl chloroform and mixing, 300 µl water was added resulting in a precipitation of the proteins at the interphase between organic (bottom) and aqueous phase (top). The lipids remained in the organic phase whereas salts stayed in the aqueous phase. Phase separation was achieved by centrifuging for 5 minutes at room temperature with 13000 rpm after mixing the phases rigorously. The aqueous phase was removed and 400 µl methanol was added before the sample was mixed and centrifuged at 13000 rpm at room temperature for 15 minutes. After the removal of the supernatant, a protein pellet was visible which was vacuum dried (Savant

Speed Vac, GMI, Ramsey, USA). Precipitated proteins were solubilized in the respective sample buffer depending on the protein separation technique used afterwards, namely isoelectric focusing or SDS-PAGE.

3.4.7 2D electrophoresis–Isoelectric focusing

Prior to isoelectric focusing, proteins were precipitated as described in 3.4.6 in order to remove salts and lipids. 500 µg of the postnuclear supernatant (3.4.3) was precipitated for visualizing the overall complexity of the fat body proteins. For the lipid droplet proteome map and subsequent identification by mass spectroscopy approximately 300 µg of the purified lipid droplet proteins were precipitated. Dried protein pellets were solubilized in 125 µl of rehydration solution (9 M Urea, 3 M Thiourea, 4 % CHAPS, 30 mM DTT, 1.7 mM basic Tris, 1 mM PMSF, 1 mM Pefablock) with 0.5 µl Ampholyte added (BioLyte pH 3–10; BioRad, Munich). In some cases the protein solutions were bath sonicated for one to three minutes to increase solubility. After centrifugation at 13000 rpm at room temperature for 5 minutes, the supernatant was transferred to a fresh tube and 1 µl bromphenol blue in rehydration solution was added before the sample was loaded to the focusing chamber (BioRad Protean IEF Cell, BioRad, Munich). Prior to loading, electrodes were covered with water soaked electrode wicks (BioRad, Munich). Isoelectric focusing was carried out using precast 7 cm strips with a pH range from pH 3 to pH 10 (BioRad, Munich). After adding the gel strip, silicon oil was added to avoid evaporation. The gels were swelled using active rehydration at 50 volts for 12 hours at a constant temperature of 20 °C. Afterwards voltage was raised to 4000 V with a 50 µA per gel strip limitation within 2 hours. Focusing was then carried out until accumulation of 20,000 Volt-hours.

After focusing, the silicon oil was removed and gel strips were fully reduced and carbamidomethylated. Full reduction of the proteins was achieved by incubating the gel strips in equilibration solution (50 mM Tris/HCl pH 8.8, 6 M Urea, 30 % glycerol, 2 % SDS) supplemented with 1 % DTT for 10 minutes at room temperature. This treatment was followed by carbamidomethylation, which is necessary to inactivate excessive DTT and to block the reactive sulfhydryl groups of broken disulfide bonds, which can otherwise be

chemically modified in various ways. This targeted modification prevents such unknown modifications and thus facilitates the mass spectroscopic identification. For carbamidomethylation, the gel strips were incubated for 10 minutes in the equilibration solution supplemented with 260 mM iodoacetamide.
After equilibration, gel strips were laid on top of a continous SDS-PAGE and overlayed with 1 % low melting point agarose in Laemmli-SDS running buffer (Laemmli, 1970).

3.4.8 SDS-PAGE

Discontinous and continous SDS-PAGE were performed according to standard protocols (Laemmli, 1970) using the BioRad MiniProtean 2 or the BioRad IIxi gel separation systems (BioRad, Munich).

3.4.9 Fluorescent protein staining using the Sypro Ruby dye

Analytical and preparative 2D- and 1D-gels were stained with the fluorescent protein dye Sypro Ruby (Berggren et al., 2000). This dye is nearly as sensitive as silver staining but provides better compatibility with mass spectroscopy and a wide linear intensity range enabling quantification of proteins.
After the gel run large format gels were equilibrated and fixed in 10 % ethanol/ 7 % acetic acid for one hour at room temperature in a large plastic container. After removing this solution the Sypro Ruby dye (200 ml Sypro Ruby, Molecular probes, Leiden, The Netherlands) was added and incubated over night with gentle agitation. The following day the staining solution was removed and the gel was post-fixed with the ethanol/acetic acid solution mentioned above for 30 minutes. Stained gels were imaged using a CCD equipped LAS-1000plus system (Fuji Photo Film, Düsseldorf) and analyzed with the Fuji ImageGauge software V3.45 (Fuji Photo Film, Düsseldorf).

3.4.10 Western blot analysis

Equal amounts of protein were precipitated using the method of Wessel and Flügge (3.4.6) and separated using standard SDS-PAGE. Separated proteins were transferred onto PVDF membrane (ImmobilonP, Millipore, Schwalbach) at 150 mA per gel for 45 to 60 min. The membranes were washed with PBS including 0.1 % Tween-20 (PBT) and blocking was carried out over night with 5 % BSA in PBT at 4 °C. After additional PBT washing steps primary antibodies were added in dilutions of 1:3000 to 1:5000 respectively in PBT including 2.5 % BSA and incubated for 2 hours at room temperature. Following additional washing steps, the species-specific secondary antibody conjugated with Peroxidase (Perbio Science, Bonn) was added in a dilution of 1:8000 in PBT containing 2.5 % BSA and incubated for 30 to 60 min. Results were visualized using the Super signal West Pico ECL system (Perbio Science, Bonn) and Kodak BioMax XAR-films (Kodak, Stuttgart), which were developed using the Optimax type TR-developing machine (MS-Laborgeräte, Wiesloch) or the CCD equipped LAS-1000plus system (Fuji Photo Film, Düsseldorf) and analyzed with the Fuji ImageGauge software V3.45 (Fuji Photo Film, Düsseldorf).

In experiments where the membrane was successively probed with different antibodies, detection was followed by incubating the membrane for 15 min at room temperature in 10 ml of Restore Western blot stripping solution (Amersham biosciences, Freiburg). This treatment removed the antibodies already detected. After washing the membrane with PBT, another blocking incubation with 5 % BSA/PBT followed at 4 °C over night prior to the next antibody probing which was carried out as described above.

Table 3-4: Antibodies used in this study

Antibody / antigen	Dilution	Reference
anti LSD-2	1:3000	Grönke et al., 2003
anti LSD-1	1:3000	R. P. Kühnlein, unpublished
anti ß-tubulin E7	1:4000	Developmental studies hybridoma bank (DSHB, Iowa, USA)
anti EIF4A	1:4000	Hernandez et al., 2004

Antibody / antigen	Dilution	Reference
anti rabbit POD	1:8000	Perbio Science
anti mouse POD	1:8000	Perbio Science
anti DIG-AP	1:2000	Roche Diagnostics

3.4.11 2D Western blot analysis–detection of phosphorylations

For 2D Western blot analysis, standard 2D-PAGE was carried out using third instar larval fat body extracts as described in 3.4.7. After the separation, proteins were transferred onto the Immobilon membrane as described in 3.4.10. In order to detect phosphorylations these posttranslational modifications were stabilized by the addition of Phosphatase inhibitor cocktails (Inhibitor cocktails I and II from Sigma-Aldrich, Taufkirchen) diluted 1:100 in all buffers.

In order to test, whether the observed modifications were indeed phosphorylations, the experiments were repeated without phosphatase inhibitor cocktails. Instead, Calf intestine phosphatase (CIP) was added (250 units for 500 µg protein; New England Biolabs, Frankfurt a. M.) after disruption of the fat bodies. CIP removes the phosphate moieties from serine, threonine and tyrosine residues of proteins (NEB protocol for dephosphorylation of proteins with CIP). Dephosphorylation was carried out for 1 h at 37 °C. Afterwards precipitation and separation of the proteins and detection by Western blot experiments followed as described.

3.4.12 Identification of lipid droplet-associated proteins by mass spectroscopy

Mass spectroscopy was carried out in collaboration with the proteomics group of the department of Cell Biology (Prof. Jürgen Wehland) at the GBF in Braunschweig by Dr. Lothar Jänsch and Dr. Dirk Wehmhöner.

Gloves were worn at all times when samples subjected to mass spectroscopy were handled in order to avoid contamination with keratin from skin. All surfaces were extensively rinsed with water or 70 % ethanol.

3.4.12.1 Mass spectroscopy of 2D gel spots

Sypro Ruby stained 2D spots were cut out of the gel with a clean scalpel on a 280 nm transilluminator and kept in water. After removing the water, gel pieces were dehydrated using 200 µl of acetonitrile. Dryness of the gel pieces was achieved when they appeared white and opaque. After removing the acetonitrile, gel pieces were washed with 200 µl 0.1 M NH_4HCO_3 and incubated in this buffer for 20 minutes prior to another dehydration step using acetonitrile. Subsequently the acetonitrile was removed and the gel pieces were completely dried in a vacuum centrifuge (Savant Speed Vac, GMI, Ramsey, USA). Afterwards gel pieces were rehydrated with trypsin solution (Promega, Mannheim, sequencing grade; activated by acetic acid according to manufacturers instructions in 50 mM NH_4HCO_3) and incubated at 37 °C over night.

The next day peptides were extracted with 50 µl acetonitrile at 37 °C. The supernatant was removed and kept. The gel piece was now rehydrated with 50 µl 5 % formic acid and after 15 min at 37 °C the same amount of acetonitrile was added. After additional 15 min, this supernatant was removed and combined with the first one. The volume of this peptide solution was then decreased in a vacuum centrifuge (Savant Speed Vac, GMI, Ramsey, USA). In order to increase the peptide concentration and purify the samples from salts, a reversed phase chromatography was applied using Zip-Tips C_{18} (Millipore, Schwalbach). After the purification, the peptides were either spotted on a MALDI-grid together with the crystallization matrix alpha-Cyano-4-hydroxycinnamic acid (Sigma-Aldrich, Taufkirchen) or eluted in solution for analysis using Q-TOF mass spectroscopy.

3.4.12.2 LC-MS/MS of precipitated lipid droplet proteins

After methanol-chloroform precipitation the protein pellet was resuspended in 50 mM NH_4HCO_3 and adjusted to 1 mg/ml by determining the protein concentration using Bradford reagent. The proteins were digested at 37 °C overnight with trypsin (ratio 50:1, sequencing grade, Promega, Mannheim) and diluted to the final concentration with 0.1 % trifluoroacetic acid.

10 µl of each sample (50-500 ng) were injected into the Ultimate nano-HPLC (LC Packings/Dionex) and separated on a C_{18} reversed-phase column (75 µm, 150 mm, PepMap), using a 120 min 0 % - 60 % B gradient (A = 5 % acetonitrile, 0.1 % formic acid, B = 80 % acetonitrile, 0.1 % formic acid) and a flow rate of 200 nl/min. Doubly and triply charged peptide-ions were automatically chosen by the software and fragmented in a Micromass nano-electrospray ionisation Q-TOF II mass spectrometer.

PMF-data and MS/MS-fragmentation data were analysed using an internal MASCOT-server (version 1.9; Matrix Science) or the MASCOT-web interface (http://www.matrixscience.com/search_form_select.html) by searches against the *Drosophila* genome published in the FLYBASE database (http://flybase.bio.indiana.edu). Iterative calibration algorithms on the basis of identified peptides were used to achieve a better average absolute mass accuracy of better than 50 ppm for MS/MS precursor ions. Only peptides with a MASCOT rank of 1 were considered to be significant and used for the combined peptide score.

3.5 Tissue culture

Tissue culture experiments for the investigation of the localization of selected putative lipid droplet-associated proteins were performed using Schneider S2 cells in a 25 °C incubator. All handling of cells was done under sterile conditions using a cell culture sterile hood. Prior to working all materials were disinfected using 70 % technical ethanol.
The cells were kept in 25 cm^2 flasks (Nunc, Wiesbaden), grown in 10 ml of Schneider's Drosophila medium (Gibco Invitrogen, Karlsruhe) supplemented with 10 % Fetal Calf Serum (FCS, PAA, Pasching, Austria) and a penicillin/streptomycin antibiotic mixture (10 mg/ml; PAA, Pasching, Austria). Every 5–6 days cells were split after detaching them from the substrate by pipetting the cells up and down and diluting them 1:10 in fresh medium.

3.5.1 Tissue culture transfection

Cells almost reaching confluency were diluted 1:20 with fresh medium resulting in a final cell concentration of approximately 2–5 x 10^6 cells per ml. 1.5 ml of this cell suspension was pipetted in each well of 6 well plates (Nunc, Wiesbaden) and incubated for 18–24 hours in order to recover. Transfections were performed using the lipofectamine derivate Effectene (Qiagen, Hilden) according to the manufacturers instructions. Therefore 1 µg DNA (concentration 100 ng/µl in TE buffer) of each construct to be transfected was adjusted to 140 µl using the supplied buffer EC. After vortexing 8 µl of the enhancer was added, followed by an additional vortexing step. The mixture was incubated for 5 minutes at room temperature. After spinning down, 10 µl of the Effectene reagent was added followed by rigorous vortexing for 15 seconds. The mixture was incubated for 10 to 20 minutes at room temperature in order to form transfection complexes. After the incubation 850 µl fresh medium was added and the transfection complexes were drop-wise added to the cells. Afterwards the cells were incubated for 48 hours prior to feeding with oleic acid in order to increase the amount of lipid droplets (Weller et al., 1991). 800 µl medium was replaced with the same volume of the oleic acid working solution (1000 x stock solution diluted in fresh medium). After incubation for additional 12-18 hours the cells were stained and imaged.

3.5.2 Lipid droplet staining of Schneider S2 cells

The transfected cells were either imaged for the fluorescent signal of the overexpressed proteins alone or counterstained with lipid specific dyes. Prior to staining or imaging respectively cells were harvested from the six well dishes by centrifugation for 3 minutes at 1000 x g. Afterwards cells were fixed using either 4 % PFA/PBS or buffer B (5 % PFA pH 6.8, 16.7 mM KH_2 PO_4/ K_2HPO_4, 75 mM KCl, 25 mM NaCl, 3.3 mM $MgCl_2$) for 5 minutes. After centrifuging the cells they were washed once with PBT and finally resupended in 500 µl PBT. 100 µl of this suspension was subsequently either directly spun down and mounted for visualization or stained for lipid droplets by adding 1 µl of the diluted stock solution of the specific dyes BODIPY or Nile Red

(Molecular Probes, Leiden; both 1 mg/ml stock solutions 1:500 diluted in PBT). Staining was performed for three minutes before cells were centrifuged and mounted by resuspending in 28 µl of Prolong solution (Molecular Probes, Leiden, The Netherlands) of which 10 µl were dropped on a microscope slide and sealed with a 18x18 mm cover slip. Imaging was done using a Leica TCS SP2 confocal microscope (Leica Microsystems, Bensheim). Images were processed using the Macintosh version of Adobe Photoshop 5.0.

3.6 Statistics and bioinformatics

For the quantitative Western Blotting experiments, two lanes of each genotype were loaded, and three different exposure times of the CCD Imager were used. The Fuji ImageGauge software V3.45 (Fuji Photo Film, Düsseldorf) was used to mark equally sized “regions of interest” containing the detected protein bands. From the several exposures, the groupwise background was substracted and the mean absorption units for each genotype were calculated. The anti ß-tubulin absorption units of the fed wildtype flies were used to normalize the absorption units of the other genotypes and the different antibody detections, which were then expressed in percent of the fed wildtype signal. Error bars were calculated using the standard deviation formula.
The following algorithms and databases were used for DNA or Protein sequence analysis or to retrieve information. Searches were performed according to the respective software documentation with standard settings.

Table 3-5: Algorithms and databases used in this study

Name	Reference	URL
BLAST	Altschul et al., 1990	http://www.ncbi.nlm.nih.gov/BLAST/
NetPhos 2.0	Blom et al., 1999	http://www.cbs.dtu.dk/services/NetPhos/
MotifScan	Pagni et al., 2004	http://myhits.isb-sib.ch/cgi-bin/motif_scan
Wormbase	Harris et al., 2004	http://www.wormbase.org/
Flybase	FlyBase, 2003	http://flybase.bio.indiana.edu/
FlyNet	Bader Lab at Johns Hopkins University	http://www.jhubiomed.org/perl/flynet.pl
BDGP gene expression database	Tomancak et al., 2002	http://www.fruitfly.org/cgi-bin/ex/insitu.pl

Name	Reference	URL
OsPrey	Breitkreutz et al., 2003	http://biodata.mshri.on.ca/osprey/servlet/Index
Mascot	Perkins et al., 1999	http://www.matrixscience.com/search_form_select.html
ProFound	Zhang and Chait, 2000	http://prowl.rockefeller.edu/profound_bin/WebProFound.exe

Furthemore the following software packages were used:

- DNAStar for the Macintosh platform
- GraphViz for the visualization of the Flynet results (http://www.research.att.com/sw/tools/graphviz/)
- Image Gauge (Fuji Photo Film, Düsseldorf) for the densitometry of quantitative Western blots
- moverz for the analysis of peptide mass fingerprints (http://bioinformatics.genomicsolutions.com/moverz.html).

4. Discussion

Lipid droplets represent the lipid storage organelles of eukaryotic cells (e.g. reviewed in: Murphy, 2001). Aside from their important organismic role in providing a pool of stored energy in the form of neutral lipids in specialized storage tissues (Brown, 2001), they are important for general cellular lipid metabolism, delivering lipid precursors for anabolic processes (Servetnick et al., 1995) or the generation of membranes (Murphy, 2001). The growing knowledge of multiple lipid droplet functions is in contrast to the seemingly simple overall structure of these evolutionary conserved organelles. Their structure is defined by a lipid droplet-specific phospholipid monolayer that shields the neutral lipids-containing hydrophobic core and serves as an attachment site for proteins (Murphy and Vance, 1999; see Fig. 1-2).

Members of the lipid droplet-associated proteome are likely to provide the basis for different lipid droplet functions. Little is known about the lipid droplet proteome composition and even less about the function of its individual proteins. The hypothesis that these proteins are important for lipid droplet-specific functions in distinct cell types is supported by recent studies on certain vertebrate members of the lipid droplet-associated PAT-domain protein family. The PAT-domain of yet unknown function (Lu et al., 2001) is named after the three vertebrate representatives, Perilipin, ADRP and TIP47 (see 1.4). Perilipin plays an important role in the regulation of the triacylglycerol (TAG) store mobilization in cells of the fat storing tissue, the adipocytes (e.g. Tansey et al., 2001; see 1.4). Despite the evolutionary conservation of this protein family, no functional data outside of mammals exists. The present study extends the finding that also non-mammalian PAT-domain proteins are localized to lipid droplets (Miura et al., 2002) and shows that also the regulatory potential is conserved. Additionally, subcellular proteomics was used to identify the lipid droplet-associated proteome of *Drosophila melanogaster* larval fat bodies in a systematic manner to unravel putative new regulators of TAG storage for a forthcoming systematic analysis.

4.1 LSD-2 has a Perilipin-like function in regulating organismic TAG storage

Two PAT-domain protein encoding sequences are present in the *Drosophila* genome. They are termed *Lipid storage droplet associated protein 1* and *2* (*Lsd-1* and *Lsd-2*), respectively. Of those, *Lsd-2* was chosen for a detailed functional analysis using both loss-of-function and gain-of-function experiments.

First parallels to the *Perilipin* gene arose during the investigation of the *Lsd-2* RNA expression patterns during embryonic and postembryonic developmental stages showing that transcripts were distributed in a similar spatiotemporally restricted manner (Fig. 2-2). Upon expression in nurse cells during oogenesis, they become maternally provided to the egg and afterwards restricted to the primordial germ cells, the midgut and the fat body of the embryo. In the postembryonic stages, transcripts were mainly restricted to the fat body. This expression pattern is reminiscent of Perilipin, which is only present in the adipose tissue and steroidogenic cells (Greenberg et al., 1991). In contrast, other PAT-domain protein encoding genes such as ADRP and TIP47 are ubiquitously expressed (Brasaemle et al., 1997b; Diaz and Pfeffer, 1998). Interestingly, also the second *Drosophila* PAT-domain protein encoding gene, *Lsd-1*, shows a tissue-specific expression, with even more striking similarities to Perilipin. *Lsd-1* transcripts are restricted to the fat body and the ring gland, a neuroendocrine organ with similar functions as the vertebrate steroidogenic cells (R. P. Kühnlein, personal communication). The tissue-specific expression of the *Lsd* genes poses the yet unsolved question, which *Drosophila* proteins fulfill the functions of the ubiquitous vertebrate PAT-domain proteins ADRP or TIP47.

In addition to the expression pattern, the subcellular localization of LSD-2 revealed another parallel to Perilipin as LSD-2 was found to be most prominent on the surface of lipid droplets and to a lower degree in the cytosol (Fig. 2-3). In contrast, LSD-1 is restricted to the lipid droplets (Fig. 2-3; R. P. Kühnlein, unpublished), an observation reminiscent of the ADRP localization (Brasaemle et al., 1997b). The presence of LSD-2 in different subcellular

compartments might indicate that shuttling between lipid droplet surface and cytosol may be important for LSD-2 function.

Both, localization of LSD-2 to lipid droplets and expression in the fat body suggested a Perilipin-like function, a proposal that could be demonstrated by the analysis of several newly generated *Lsd-2* mutant alleles (see 2.4/2.5). LSD-2 mutant flies contain significantly less TAG as compared to control alleles, a finding similar to results obtained with Perilipin knock-out mice. Transgene-mediated rescue experiments showed the specificity of the *Lsd-2* mutant phenotype. Moreover, the combined loss-of-function and overexpression studies show that *Lsd-2* is not only necessary for adjusting the organismic TAG content, but is also sufficient to modulate the TAG level in a dosage-dependent manner when expressed in fat body cells (see 2.6/Fig. 2-5). However, this dosage-dependency does not seem to be a general mechanism of adjusting TAG content, since a direct correlation between TAG content and LSD-2 amount cannot always be made as shown by quantitative Western blot experiments (Fig. 2-6). Though, this observation does not exclude the possibility that the modulation of LSD-2 amount is important under certain physiological conditions for adjusting the TAG content of the organism. Alternatively, LSD-2 action might be not only regulated on basis of its cellular abundance but by posttranslational modifications of the protein. In fact, different isoforms of the two LSD proteins were identified by 2D-Western blotting experiments (Fig. 2-8), some of which were due to phosphorylation. Such modifications are consistent with corresponding phosphorylation sites as detected by *in silico* analysis of the protein primary sequences (Figs. 2-7, 2-8). Perilipin is regulated by posttranslational modifications in the form of phosphorylation. This action is important for an efficient targeting of the hormone sensitive lipase (HSL) to the lipid droplet surface and the release of Perilipin from the lipid droplets (Greenberg et al., 1991; Souza et al., 2002). Preliminary experiments show that differently modified LSD-2 isoforms localize to the lipid droplet and cytosolic fractions, respectively (data not shown). This observation suggests that these modifications are likely to be involved in the regulation of the subcellular localization of the protein as observed with mammalian Perilipin. Alternatively, the modifications could be important for different LSD-2 actions in the respective compartments and/or to

activate or inactivate LSD-2 action. To unravel the function of these modifications, the causative signaling cascade that leads to phosphorylation or dephosphorylation needs to be identified and the effects of mutations of the modified residues have to be investigated. Corresponding phosphorylation sites of the LSD proteins are already suggested by the *in silico* analysis (Fig. 2-7). Additionally, mass spectroscopy could be used to verify the modified sites. Candidates for a signaling cascade that causes LSD-modification include the adipokinetic hormone and its downstream signaling events involving Protein Kinase A (PKA), the activity of which has been shown to affect TAG storage (Arrese et al., 1999). In addition, Perilipin has been shown to be a target of PKA (Tansey et al., 2003). Regulation of LSD-2 in response to PKA activity would further strengthen the argument that the invertebrate and vertebrate PAT-domain proteins are homologous.

However, there are also clear-cut differences between LSD-2 and Perilipin, as for example the transcript distribution. In addition, the phylogenetic tree shown in Fig. 2-1 already revealed that the *Drosophila* PAT-domain proteins are not easily homologized to the vertebrate counterparts on basis of the protein primary sequence. Also, a functional allocation of the two proteins to the one or the other vertebrate representative is not unambiguous, since LSD-1 for example is more similar to Perilipin with respect to sequence and expression pattern, but the lack of LSD-1 activity does not result in lean individuals as observed with LSD-2 and Perilipin but in obese flies (R. P. Kühnlein, unpublished). This puzzling result can be explained if PAT-domain proteins in *Drosophila* would act in concert in order to adjust TAG storage. This scenario would then be different from the vertebrate system, where Perilipin replaces ADRP upon maturation of the adipocytes (Brasaemle et al., 1997a). Supporting circumstantial evidence for a coordinated action of LSD-1 and LSD-2 comes from the observation that the LSD-1 loss-of-function phenotype could be mediated by LSD-2, since loss-of LSD-1 causes increased levels of LSD-2 (R. P. Kühnlein, unpublished). Also, analysis of the LSD-1 modification state in *Lsd-2* mutant flies suggests that LSD-1 is dephosphorylated in such animals (data not shown). These observations imply that both proteins are under the control of the same signaling pathway or, in case of different pathways, their activities are functionally linked. This aspect of LSD-1 and

LSD-2 action needs a more detailed analysis. Additionally, it needs to be confirmed whether and under which conditions the endogenous forms of the two proteins are associated with the same lipid droplets and whether they can interact physically.

Several lipid droplet-protein encoding genes, as for example *Lsd-2*, are expressed in the primordial germ cells where, at least in the early developmental stages, no lipid droplets are observed (e.g. Fig. 1-1 B). At the same time, however, lipid metabolism seems to be crucial for the spatial and temporal regulation of germ cell migration (Renault et al., 2004; Starz-Gaiano et al., 2001). These findings raise the question whether LSD-1 and/or LSD-2 function also in lipid/protein/RNA complexes as represented in the polar granules. First results pointing in this direction are present for the *Xenopus laevis* PAT-domain protein FATVG (Fat and vegetal pole expressed gene), which is most often homologized to ADRP. It was shown that the *fatvg* RNA is present in such germinal granules (Chan et al., 2001; Kloc et al., 2002) and an involvement in germ cell migration and survival was discussed (Chang et al., 2002).

Irrespective of these possible additional functions, the results presented here demonstrate the ability of both LSD proteins to modulate the organismic TAG content. Their subcellular localization further suggests that the surface of lipid droplets represents an evolutionary conserved cellular compartment-boundary with distinct regulatory potential. This proposal is consistent with the finding of a distinct lipid droplet-associated proteome that emerged from the subcellular proteomics screen presented here.

4.2 Subcellular proteomics of *Drosophila* lipid droplets

The analysis of the LSD PAT-domain proteins suggested that the surface of lipid droplets harbors regulators of organismic TAG storage. To identify additional regulators in a systematic manner, a subcellular proteomics screen was initiated in which the lipid droplet-associated proteome was isolated and the individual components were identified by mass spectroscopy. The purified lipid droplet fractions used in this study were free of contaminating organelles

but may have contained traces of membrane remnants of unknown origin (Fig. 2-3 C).

The analysis of the genotype-specific lipid droplet proteomes (see 2.12) points in a direction that the investigated TAG content-modifying genotypes result in rather small differences with respect to the presence or absence of a given protein. This observation favors the argument that the lipid droplet-dependent fat content regulation is based on quantitative aspects with respect to the identified components and/or coupled with their specific modification and interactions between them. However, for several proteins a differential appearance in larvae of a given genotype was detected (2.12: Fig. 2-13, 2.14: Table 2-3). This observation might be interpreted that these proteins were either up- or downregulated in the respective genotype and thus reach or escape from the sensitivity threshold for protein identification. In wildtype larvae, only one protein (the glutamate dehydrogenase) was present as unique identifier not observed in the mutants. Also, in each mutant genotype only three proteins were differentially present (2.12). Most of these unique proteins could not be easily associated with the observed phenotypes. Only the Regucalcin protein identified in the obese *adipose* mutant showed an already known connection to fat storage, since a mammalian homologue of this protein, senescence marker protein 30 (SMP30), was recently shown to affect mouse lipid storage, leading to an obese phenotype with decreased lifespan upon mutation (Ishigami et al., 2004). SMP30 is a calcium binding protein and has two *Drosophila* counterparts. It remains to be shown whether the identification of this protein is linked to the *adipose* mutant genotype. A possible link between the two proteins could be a mislocalization of the Regucalcin protein in the *adipose* mutants, if Regucalcin would act downstream of *adipose* activity.

To improve the quantitative information content of the proteomics experiments, the genotype specific proteomes could be labeled. It was shown, that techniques like e.g. isotope coded affinity tagging (ICAT) can be used to obtain quantitative information of the relative abundance of certain proteins in mixtures (Righetti et al., 2004; Tao and Aebersold, 2003). Further studies including techniques that allow the quantification of the protein composition could be applied to identify more diagnostic and maybe even causative

protein markers for the different genotypes. Additionally, the ratio of modified versus unmodified forms of the lipid droplet-associated proteins could be investigated by analyzing the peptide fractions.

The 271 identified proteins were regarded as the global lipid droplet-associated proteome, irrespective of their origin, i.e. the genotype of larvae they were isolated from. This assignment seemed justified, since the robust genotype-specific differences in the protein patterns were rather small (see above). In addition to the LSD proteins, the screen revealed 37 homologues of proteins previously identified in the lipid droplet proteomes obtained from different organisms and cell types (see 2.11.2: Table 2-1). Comparison of the results of the present screen with previous lipid droplet proteomic screens revealed that there is a highly variable spectrum of identified proteins. This variation could be based on technical differences or species-specific/cell type-dependent proteome variabilities (see 1.3; appendix VII). The most prominent technical achievement of the present screen is the use of nano LC-MS/MS, which results in substantially more identified proteins, due to the high sensitivity, as compared to the 16 to 33 proteins that were identified in the previous screens.

Only four proteins were found to be shared by four of the seven screens (including this study), although five of these screens used very similar technical setups, namely the identification of the most prominent 1D SDS-PAGE separated lipid droplet protein bands. This low overlap suggests that there are only a few very abundant and generally present lipid droplet-associated proteins, which can be identified irrespective of the technique used. These four common proteins are ADRP, which is the protein related to both LSD-1 and LSD-2, the 17ß-hydroxosteroid dehydrogenase of which the identified *Drosophila* short-chain dehydrogenase CG2254 is a distant relative, the lanosterol synthase/synthetase lacking a clear-cut *Drosophila* homologue and the NADH-cytochrome B5 reductase which, however, was not identified in the present screen and thus could be vertebrate-specific. A larger data set including additional studies with different cell types analyzed in parallel with standardized techniques will be necessary to finally answer the question whether the observed differences in the former screens and the differences between vertebrates and *Drosophila* have a biological meaning.

The largest group of identified proteins in the present screen is associated with metabolism-related processes. Interestingly, the direct homologue of the vertebrate hormone sensitive lipase (HSL), which was thought to be the main catabolic enzyme in TAG mobilization for a long time (Londos et al., 1999), was not identified. However, in the vertebrate system there is also increasing evidence that not only HSL contributes to lipolytic activity since the HSL knock-out mice do not show an obese phenotype (Osuga et al., 2000). Moreover, several additional mammalian lipolytically active lipases were identified in adipose tissue (Fortier et al., 2004; Jenkins et al., 2004; Soni et al., 2004; Villena et al., 2004). Similarly, two predicted alpha esterases, which can also act as lipases, as well as two other predicted lipases (FlyBase, 2003) have been found in the present screen. Thus, it can not be excluded that during the larval stages, lipolysis only plays a minor role, since energy storage is more important during the developmental stages prior to the catabolic shift at beginning of pupation. Furthermore, some of the identified lipolytic enzymes might be used for lipid droplet size control and, additionally, identification of an enzyme does not necessarily imply its active state but rather a “stand-by” localization for its action to come under different physiological conditions.

Not only lipolysis, but also lipogenesis seems to be spatially linked to the lipid droplets since the complete set of components for a lipogenic pathway was identified in the present proteomics screen. This pathway is “the backwards reactions of the Krebs cycle” (Belfiore and Iannello, 1995; see 2.13). The components of this pathway have been localized to the non-mitochondrial fractions in rat and human adipose tissue without going into further detail. Although the extent by which this pathway contributes to total lipogenesis is still unknown (Belfiore and Iannello, 1995), the finding that components of this pathway are associated with lipid droplets suggests that components of the backwards reactions of the Krebs cycle are also active in *Drosophila* fat metabolism. The identification of a complete enzymatic pathway furthermore revealed a very comprehensive coverage of the lipid droplet proteome and suggests a metabolic compartmentalization at the surface of the lipid droplets.

Several enzymes of the backwards reactions of the Krebs cycle have been previously described as lipogenic markers (Meegalla et al., 2002;

Swierczynski et al., 2000), which are regulated upon and after starvation both at the level of transcription and enzymatic activity (Boll et al., 1996; Karbowska et al., 2001). Especially the activities of fatty acid synthase and ATP citrate lyase were shown to decrease dramatically upon starvation in rats (Boll et al., 1996). This decrease is reversible by re-feeding the animals. A similar starvation response for the ATP citrate lyase was shown in *Drosophila* on the level of transcription (appendix III; Zinke et al., 2002). Additionally, it has been demonstrated that after repeated starvation and feeding cycles, a transcriptional counter regulation is active, since both enzymes are transcriptionally upregulated after this treatment (Karbowska et al., 2001). Interestingly, however, ATP citrate lyase was repeatedly absent from the fat body lipid droplet preparations of the *Lsd-2[51]* mutant larvae. This absence might reflect a constant “starvation-type” metabolism that is active in the lean *Lsd-2* mutant animals, as it was seen on the transciptional level upon starvation of wildtype flies. Such a possible downregulation of lipogenic pathways is reminiscent of the metabolic adaptation seen in Perilipin mutant mice, where the level of beta-oxidation is increased in order to possibly remove excess free fatty acids and hepatic glucose production is decreased (Saha et al., 2004).

Therefore, the proteome analysis indicates that a substantial part of cellular metabolic reactions are localized close to or even at the surface of lipid droplets. Thus the results suggest a dynamic and metabolically active character for these organelles. Additional identifications, such as the presence of storage proteins, further support this conclusion. This protein class includes the receptor Fat Body Protein1 (FBP1), which was initially found to be localized at the cytoplasmic membrane (Burmester et al., 1999). Upon binding of the ligand, in the form of the larval serum protein complex, the receptor gets internalized and proteolytically processed by an as yet unknown mechanism (Burmester et al., 1999). The FBP1 receptor was identified among the most abundant proteins in the lipid droplet enriched fractions, which is both reflected by the prominent Sypro Ruby stain signals and frequent identifications in the gel-based experiments (appendix I), as well as the constant high rank identifications in the gel-less experiments.

The result showing that predominantly the processed and internalized fragments of the receptor were found in association with lipid droplets leaves the question of how the receptor is targeted to this site. Nevertheless, it suggests an intracellular trafficking route of the processed receptor from the cytoplasmic membrane to lipid droplets. This finding is reminiscent of earlier reports showing that in human ovarian steroidogenic cells a receptor-ligand pair was found to localize to the surface of lipid droplets, namely the “big Stanniocalcin” hormone isoform and its proposed receptor (Paciga et al., 2003). The specific receptor has not been cloned yet. However, *in situ* ligand binding experiments showed the presence of large quantities of such receptors (Paciga et al., 2003). Stanniocalcin was originally identified in bony fish as a regulator of calcium and phosphate homeostasis (Yamashita et al., 1995). In most mammalian tissues it is widely distributed and becomes translocated to mitochondria where it participates in the regulation of the electron transport (McCudden et al., 2002). In human ovarian cells, however, the big Stanniocalcin hormone isoform is targeted to the lipid droplets together with its receptor and is implicated in steroidogenesis control (Paciga et al., 2003). The association of the oligomeric lipid raft-associated integral membrane protein stomatin is another example for putative membrane spanning proteins which become associated with lipid droplets (Umlauf et al., 2004). It will now be of interest to unravel how these receptors are targeted and become anchored to the lipid droplets, since the droplet-specific phospholipid monolayer is not obviously suited for the classical membrane spanning receptor topology (Brown, 2001).

The close proximity of metabolic pathways and storage metabolism-associated proteins might serve as an unknown regulatory mechanism linking different energy sources and pathways to a complex metabolic interplay. The identification of several Rab proteins in the lipid droplet enriched fraction further supports the hypothesis of an exchange between lipid droplets and other organelles. Although multiple studies identified these proteins in association with lipid droplets (Brasaemle et al., 2004; Liu et al., 2004; Umlauf et al., 2004), the meaning of Rab proteins in this context is still unclear. Currently, Rab proteins are thought to regulate the contact and exchange of lipid droplets with other vesicles (Liu et al., 2004; Umlauf et al., 2004).

Additionally, cytoskeletal components in combination with Rab proteins might be important for a dispersion and/or transport of the lipid droplets facilitating lipolysis (Brasaemle et al., 2004). The identification of fatty acid and TAG binding proteins also favors the connection of intracellular transport processes to the lipid droplets as it suggests that TAG and other lipids are not only synthesized at the ER, where the lipid droplets are born (Murphy and Vance, 1999), or on the surface of lipid droplets. Instead, they may be actively transported to or from the lipid droplets.

The present study also revealed an association of proteins of the SRP/ Translocon complex and the lipid droplet fraction (SRP/Translocon reviewed e.g. in: Johnson and van Waes, 1999; Meacock et al., 2000). In plants, it has been demonstrated that this complex is necessary for the lipid droplet localization of the Oleosin protein family (Abell et al., 2002). Members of this familiy decorate the surface of the plant lipid storage organelles (Murphy, 2001). Together with the observation that various chaperones have been identified in the present screen, this finding might reflect the needs of the larval stage, where the main purpose of the organism is to gain size and weight, demanding for a high level of lipid droplet synthesis to store the lipids. This necessity of a massive production might be reflected by a more prevalent nascent status of the droplets with the quality control assuring chaperones still associated with the target organelles. However, the presence of chaperones has to be critically revised as these proteins are highly abundant and might have also been extracted from remnants of the ER during the purification process. On the other hand, chaperones were also demonstrated to be present and active in the cytosol (Hartl and Hayer-Hartl, 2002), where they could aid in the association of proteins to the lipid droplets independently of the ER. Such an alternative localization mechanism has been proposed, since Perilipin was never found in association with ER membranes (Murphy, 2001). In this view, the components of the Translocon machinery might have also been co-purified in connection with active, specialized regions from the ER, where the lipid droplets are thought to derive from. Several lines of evidence indicated earlier the presence of such specialized, active zones within the ER membrane (Murphy, 2001), a conclusion based on the analysis of the lipid composition of the lipid droplet-surrounding monolayer (Tauchi-Sato et al.,

2002) as well as on earlier proteomics studies (Wu et al., 2000). Additionally, the association of intracellular lipid droplets with ER structures was demonstrated (Blanchette-Mackie et al., 1995). Taking these earlier results into account, it is tempting to postulate the model depicted in Fig. 4-1, which provides a working hypothesis to be addressed by biochemical and *in vivo* studies.

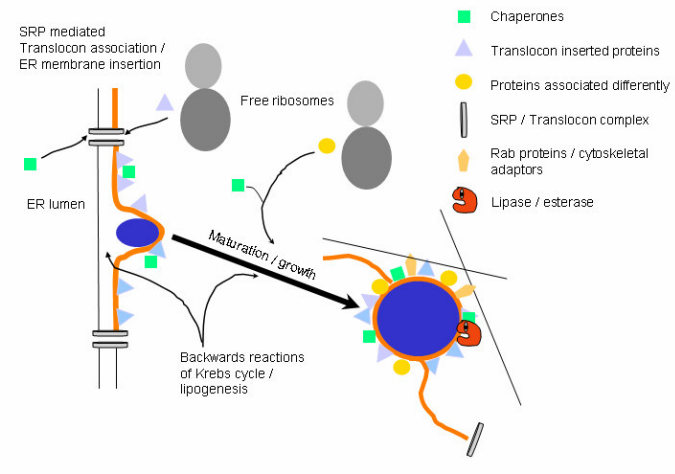

Fig. 4-1: Model of lipid droplet generation and involvement of identified proteins

Identified members of the translocon machinery are part of active ER-zones generating lipid droplets. Free ribosomes, associated with the translocon via the SRP, might have been co-purified. Translated proteins, both inserted by the translocon into the ER membrane, as well as translated in the cytosol and directly associated with the lipid droplets might have been associated with chaperones, ensuring a properly folded conformation. Lipids generated by lipogenic pathways like the backwards reactions of the Krebs cycle are transported into the ER intermembrane space leading to a budding off of the lipid droplets. The lipogenic pathways remain present in close proximity of the lipid droplets to enlarge their volume. Membrane surface enlargement could be caused by fusing individual vesicles. Rab proteins associated to the lipid droplets might be derived from such vesicle membranes. These Rab proteins act as connectors for cytoskeleton components, as well as docking sites for additional fusing vesicles, like for example endocytic vesicles delivering the FBP1 complex. The identified lipases could be necessary for a size and number control or the mobilization of the stored TAG.

Proteins of the groups named “Mixed”, “Translation” and “ATP” in 2.11.2 which add up to a total of 102 proteins, can not be easily linked to any functional aspect of lipid droplets and might be false positives due to the high sensitivity of the technique applied. Several members of translational proteins, which mainly consist of ribosomal structural proteins, might be derived from the Translocon/SRP machinery which seems to be co-purified. On the other hand, these proteins could well be involved in the translation of lipid droplet-associated proteins, a speculation that remains to be shown in further studies. Also, the large amount of ATP generating proteins, mostly ATP synthase

subunits and cytochrome related proteins, might indicate once more a close association of mitochondria with the lipid droplets which has been postulated in several studies, but is not yet conclusively shown (Blanchette-Mackie et al., 1995; Brasaemle et al., 2004; Cohen et al., 2004). The fact that mitochondria were not detected in the electron microscopy studies suggests a breakdown of the mitochondrial membrane during the purification procedure.

In order to obtain first functional data of selected lipid droplet proteome candidates, EGFP-fusion variants of the lipid droplet-associated proteins were overexpressed in *Drosophila* Schneider S2 cells that were fed with oleic acid to increase the number and size of their lipid droplets (see 2.15). Pilot studies on overexpressing fluorescent variants of the LSD proteins in these cells showed their lipid droplet-association (Fig. 2-15). Additionally, co-expression experiments revealed that in many cells the lipid droplets were decorated with only one of the two proteins that were expressed, suggesting heterogeneity of the lipid droplet protein population of these cells. Among the proteins tested for localization were an esterase (CG1112; Fig. 2-16), two proteins of the SPFH/band7 domain protein family (CG10691 and CG15081; Fig. 2-17) and a short chain dehydrogenase (CG2254; Fig. 2-18). For all of these proteins, except for CG15081, localization to the lipid droplets could be unambiguously shown. It has to be noted that CG15081 was only identified in the LSD-2:EGFP overexpressing larvae, suggesting that lipid droplet localization may occur under distinct physiological conditions only. This speculation is consistent with the notion that in one transfection experiment CG15081 was also localized in a ring-like structure. Interestingly, the tested tagged proteins decorated not all cellular lipid droplets inside the S2 cells. Similarly, the LSD proteins did not always co-localize to the same cellular lipid droplets (see 2.15.1). This observation might be indicative of differences and heterogeneity of the proteins associated with cellular lipid droplets, eventually reflecting different physiological states or functionally specialized droplets.

4.3 Did the screen reveal novel regulators of fat storage?

The definite answer to this question has to await functional analysis of at least several of the identified candidate proteins. However, identification of a lipid

droplet-associated esterase (CG1112), as well as other predicted lipid mobilizing enzymes including Brummer, a key protein for lipid mobilisation (S. Grönke, in preparation), can already been taken as first evidence that at least a subset of the proteins associated with the lipid droplet fraction of cells participate in the regulation of lipid homeostasis. In the *Drosophila* genome, ten alpha esterases are found and distinct functions have been discussed (Campbell et al., 2003). Though, it is not yet clear which and how many are indeed involved in lipolysis. One of them, CG1112 was present in the lipid droplet preparations irrespective of the larval genotypes (appendix II). This tight link to lipid droplets suggests that this protein is a general constituent of the lipid droplet proteome and important for one or several aspects of the lipid droplet life cycle. In vertebrates, also a member of this protein family, called CGI-58, has been identified as a lipid droplet resident in a proteomics screen (Liu et al., 2004). This association was further characterized by the association of CGI-58 with Perilipin (Subramanian et al., 2004; Yamaguchi et al., 2004). Furthermore, mutations of the protein are associated with a lipid storage disease and confirm its crucial function in lipid homeostasis (Lefevre et al., 2001). In the present proteomics screen, the *Drosophila* homologue of CGI-58, assigned CG1882, was identified twice in the incomplete gel-less experiments with the proteins insoluble in the 2D sample buffer (data not shown). This result suggests that the *Drosophila* protein may not contribute as much to lipid homeostasis as the vertebrate homologue or that it acts only in a developmentally regulated or stage-specific manner. Alternatively, it may represent a very low abundant member of the lipid droplet proteome in the fly and thus, can only be detected under specific experimental circumstances.

In order to search for possible additional indicators for an involvement of the identified lipid droplet-associated proteins in metabolic homeostasis, the identified proteins were compared to the results of the following screens focusing on lipid storage and human disease aspects: (i) a screen investigating the transcriptional response to starvation of *Drosophila* larvae (Zinke et al., 2002), (ii) *C. elegans* genes with an RNAi phenotype affecting fat storage (Ashrafi et al., 2003) and (iii) evolutionary conserved human disease genes (Homophila database (Chien et al., 2002)). This analysis revealed that 71 of the identified *Drosophila* proteins or their homologues were also found in

one or more of these screens (see appendix III). 39 of the identified proteins have human disease-associated counterparts, of which 17 are lipid-metabolism-associated diseases. Furthermore, 37 proteins were transcriptionally regulated in response to starvation of the *Drosophila* larvae, suggesting that they might be involved directly or indirectly either in lipogenesis or lipid mobilization. In addition, nine of the candidate proteins have homologues which show a lipid phenotype in *C. elegans* when knocked down by RNAi. These observations suggest that the proteomics screen might have identified a number of regulators of the fat storage control in the fly, a conclusion that needs to be confirmed by a detailed functional study of each candidate protein by gain-of-function and loss-of-function studies as demonstrated here for the *Lsd-2* gene.

The newly gathered knowledge of the lipid droplet proteome constituents can also help to build up a “lipid droplet protein interactome”. As most proteins are not able to function independently, it will be of interest to identify the interconnections of the identified proteins. Several attempts have been made to identify genetic and protein interaction networks in different organisms like *yeast* (Tong et al., 2004), *C. elegans* (Lefevre et al., 2004) and *Drosophila* (Giot et al., 2003). In order to assay for putative interactions among the identified proteins, the *Drosophila* protein interactome data (Giot et al., 2003) was analyzed using the Osprey software (Breitkreutz et al., 2003). This analysis revealed 28 interactions among the identified candidates (appendix V). Additional searches, using the FlyNet server (http://www.jhubiomed.org/perl/flynet.pl) which includes additionally to the *Drosophila* proteome data, the yeast proteome as well as the genetic interaction information, revealed a total of 157 interactions among the identified proteins (appendix VI) and several putative functional complexes like the ones shown in Fig. 4-2. The complex containing CG10691 (corresponding to the l(2)37Cc gene) involves proteins predicted to function in vesicle transport control, a process which might well be important for lipid droplet trafficking. The second complex, containing CG11151, involves several lipid-modifying enzymes such as a monooxygenase (CG6178), potentially involved in cholesterol metabolism and steroid synthesis, and a dodecanoyl-CoA isomerase (CG13890).

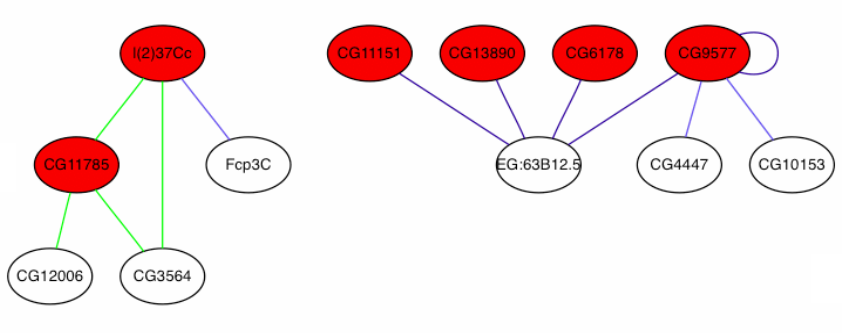

Fig. 4-2: Exemplary interactions among a subset of the identified lipid droplet-associated proteins obtained from the FlyNet server

Interactions obtained from the FlyNet server were analyzed using the graphviz software, leading to hierarchical interaction trees. In red, proteins identified in the present proteomics screen are shown (see appendix II/VI).

l(2)37Cc (CG10691) – SPFH/band7 domain protein; CG11785 – involved in vesicle mediated transport; CG12006 – (phospho-) lipid metabolism/protein lipidation; CG3564 – intracellular protein transport; Fcp3C – follicle cell protein 3c; CG11151 – sterol carrier protein 2; CG13890 – dodecanoyl CoA isomerase; CG6178 – luciferase monooxygenase; CG 9577 – delta5-2,4 dienoyl CoA isomerase, EG:63B12.5 (CG14815) – peroxisome targeting; CG4447/CG10153 – no function known.

It is tempting to speculate that complexes of potentially interacting proteins might be indications for islands of functionally linked proteins on the surface of lipid droplets. This speculation provides a basis for forthcoming studies testing the *in silico*-based interactions by yeast-2-hybrid studies and/or co-immunoprecipitation experiments followed by genetic analysis of the proposed interactions to test their functional means.

4.4 *Drosophila* as a model system for lipid droplet research

The results of the functional analysis of *Lsd-2*, as well as the observation that nearly 40 of the identified lipid droplet-associated proteins have vertebrate or yeast lipid droplet-associated counterparts, suggests that a substantial amount of the functional aspects concerning lipid droplet biology are evolutionary conserved. However, there are also interesting differences to the vertebrate system since, for example, *Lsd-1* and *Lsd-2* cannot be unambiguously homologized with one of the five vertebrate PAT-domain proteins. The functional conservation and the eventually insect-specific modifications emphasize the importance of *Drosophila* as a model system for

an *in vivo* investigation of lipid droplet function using a complex organism. In addition, they allow one to study functional differences and modifications of the system that may have occurred during evolution and the specific adaptation of the lipid storage systems.

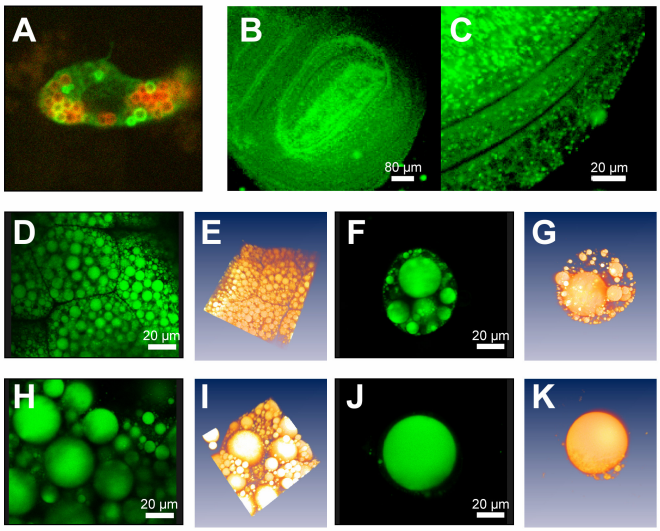

Fig. 4-3: Lipid droplets in different cellular *Drosophila* systems

A S2 cell co-transfected with LSD-2:TdT and EGFP:CG2254; B/C imaginal wing disc; lipid droplets are stained with BODIPY; D/H and F/J third instar larval fat body and adult fat body cell stained with BODIPY. D/F wildtype; H/J *Lsd-1[1]* loss-of-function mutant (A. Bulankina, unpublished), demonstrating the presence of cellular phenotypes since lipid droplets are substantially bigger in the mutant situation as compared to the wildtype. E/G and I/K corresponding 3-dimensional reconstructions using the Amira software package.

Additional cellular systems to the larval fat body, like the adult fat body cells, tissue culture or imaginal discs as well as early embryogenesis together with the increasing evidence for lipids in germ cell formation (Renault et al., 2004; Starz-Gaiano et al., 2001) (Fig. 4-3) provide the unique possibility to study storage and non-storage lipid droplet biology in *Drosophila*. The example of the *Lsd-1* loss-of-function mutation (see Fig. 4-3 D–G compared to H–K) furthermore demonstrates the existence of cellular lipid droplet phenotypes, which complements organismic phenotypes such as obese and lean individuals. The functional analysis of the lipid droplet candidate proteins identified here both at the cellular and organismic level, combined with biochemistry and genetics, will help us to understand the molecular biology of organismic TAG storage control as well as the cell biology of lipid droplet formation and its regulation.

5. Appendix

Appendix I: 2D-PAGE based lipid droplet-protein identification

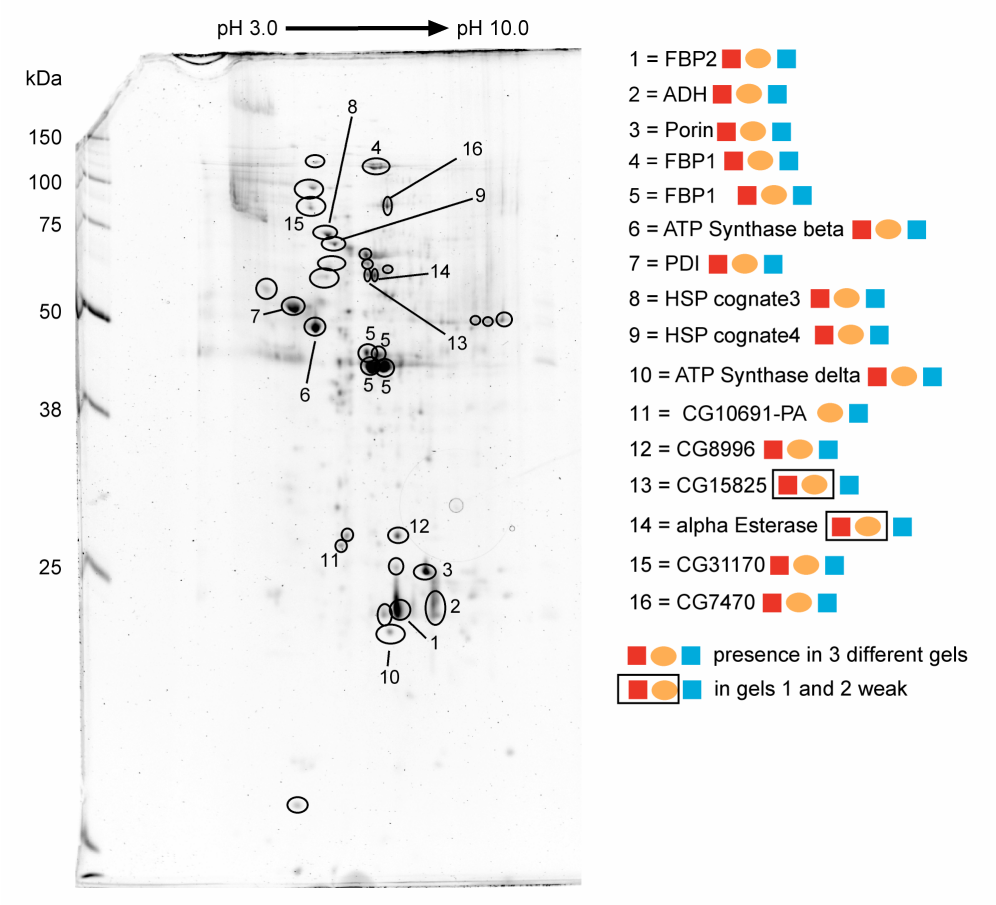

Fig. A-1: 2D Master map of the purified lipid droplet proteome

2D lipid droplet proteome master map from Fig. 2-9 C. Numbered spots have been identified by mass-spectroscopy as described in material and methods 3.4.12.1. Every colored symbol represents the detection of the spot in a separated experiment.

Peptide mass fingerprint spectra were analyzed with the MASCOT algorithm (Perkins et al., 1999) using the *Drosophila* proteome annotation from the Flybase database (2003). A MOWSE score greater than 57 was necessary for a significant identification. The following default settings were used for database searches: (i) one allowed missed trypsin cleavage site (ii) carbamidomethylation as fixed modification and (iii) methionine oxidation as variable modification. The error tolerance was set to 100 ppm (spot Nr. 1 and 3: 200 ppm). The table A-1 shows examples of significant identifications if several identifications were made (several dates) with the respective

sequence coverage and MOWSE score reached. LIFT represents a post-source-decay (PSD) sequenced peptide. Additionally the predicted function is given, as found in Flybase (2003).

Table A-1: Proteins identified from 2D-PAGE

Nr.:	gene / Protein:	kDa / pI	Identified in:	Seq. Cov.(%) / MOWSE score:	Function:
1	Fat body protein 2	30 / 6,7	07 / 2002 12 / 2002	34 / 67	storage protein of fat body nutrient reservoir activity /oxidoreductase activity
2	CG3481-PA ADH	27.7 / 7.94	07 / 2002 12 / 2002	64 / 112	ethanol oxidation
3	Porin	30.5 / 6.77	12 / 2002	33 / 67	mt outer membrane inferred from sequence
4	FBP1	120 unproc. / 6.25	07 / 2002 12 / 2002 04 / 2003	26 /164	protein transporter transcriptional Ecdysone target is processed after incorporation
5	FBP1		04 / 2003	21 / 74	
6	ATP Synthaseß	54.2 / 5.20	12 / 2002 02 / 2003	58 / 212	proton transport
7	PDI	55.8 / 4.62	07 / 2002 12 / 2002 02 / 2003	42 / 198	protein folding
8	CG4147 HSP cognate3 78 KD GRP	72.2 / 5.15	12 / 2002	35 / 154	stress response / protein folding
9	CG4264 HSP cognate4	71.1 / 5.30	12 / 2002	25 / 83	stress response / protein folding
10	ATP Synthase delta CG6030-PA	20 / 6,4	04 / 2003	41 / 71	proton transport
11	CG10691-PA	30 / 5,5	04 / 2003	61 / 166	SPFH- / band 7- domain; regulating targeted protein turnover in stomatins and other membrane associated proteins /
12	CG8996-PB	34 / 8,3	04 / 2003	LIFT / 73 25 / 52	Electron transporter / uncoupling mito predicted
13	CG15825	58 / 6,7	04 / 2003	LIFT / 67	no domains / predicted annotation
14	alpha Esterase-7 CG1112-PA / PB	65 / 6,3 46 / 6,4	04 / 2003	26 / 42	Esterase / Co-Esterase / carboxylesterase carboxylesterase
15	CG31170	69 / 4,9	04 / 2003	20 / 73	ENTH domain, binds lipids (PtdIns- P2 and P3) lipid monolayer. endocytosis / cytoskeleton lipid bending curvature Epsin binds inner leaflet
16	CG7470-PA	84 / 6,5	04 / 2003	25 / 107	mt inner membrane target based on

Appendix II: Complete list of nano LC-MS/MS identified proteins

Table A-2: nano LC-MS/MS identified proteins

OregonR	*adp[60]*	*Lsd-2[51]*	*Lsd-2:EGFP*	gene	function	class
xykz	xyz	xykz	xykz	CG10374	LSD-1	PAT-domain
xykz	xyz		xykz	CG9057	LSD-2	PAT-domain
xz	y	z		CG11064	Retinol / fatty acid binding	fatty acid / TAG binding
x	xy	kz	xy	CG5958	Retinol / fatty acid binding	fatty acid / TAG binding
	xy	xz	xyz	CG9342	Triglyceride binding	atty acid / TAG binding
yz	z	ykz	yz	CG1112	alpha esterase 7	metabolism
	x		y	CG2505	alpha esterase 2	metabolism
			z	CG5295	brummer LD ass. TAG lipase	metabolism
	y			CG9186	Esterase / Lipase	metabolism
	yz	y	yk	CG11151	SCP2	metabolism
	xyz	y		CG3524	[acyl-carrier protein] S-acetyltransferase activity (EC:2.3.1.38)	metabolism
xyz	xyz	xyz	xyz	CG3523	fatty acid synthase	metabolism
			x	CG3961	long chain fatty acid CoA ligase	metabolism
xz		xyz	xyz	CG4389	long chain hydroxoacyl CoA DH	metabolism
xk	x	yk	y	CG4581	long-chain-3-hydroxyacyl-CoA dehydrogenase activity	metabolism
x		xy	x	CG7461	Very long chain acyl CoA DH	metabolism
yz	xyz	yz	xyz	CG11198	Acetyl CoA carboxylase	metabolism
y	y		y	CG10622	Succinate CoA Ligase	metabolism
xyz	xyz	xykz	xy	CG1516	Pyruvate Carboxylase	metabolism
z				CG4600	acetyl-CoA C-acyltransferase activity	metabolism
	x			CG9390	Acetyl Coenzyme A synthase	metabolism
z		z	xz	CG5887	fatty acid desaturase	metabolism
xyz	xz	xyz	ykz	CG7113	3-hydroxyacyl-CoA dehydrogenase activity Scully	metabolism
xyz	xyz		xyz	CG8322	ATP citrate lyase	metabolism
xz	z	yz	y	CG13890	Dodecanoyl-CoA-Isomerase	metabolism
z				CG12428	carnitine O-octanoyltransferase activity	metabolism
z		yz	x	CG7920	4-hydroxybutyrate CoA transferase	metabolism
z		y	z	CG2604	NAD binding	metabolism
xyz	xy	xyz	xykz	CG5167	NAD binding	metabolism
			z	CG11661	oxoglutarate DH (lipoamide) activity	metabolism
	xz	z		CG2254	short chain DH	metabolism
			x	CG6020	NADH DH	metabolism
x				CG9762	NADH DH	metabolism
		y	z	CG3415	estradiol 17-beta-dehydrogenase activity	metabolism
			xz	CG5590	oxidoreductase short chain DH	metabolism
y	z	z		CG10639	Oxidoreductase	metabolism
	z	y		CG11567	NADPH hemoprotein reductase	metabolism
xz	xyz	xyk	xyz	CG32954	ADH	metabolism
xyz	xz	xz	xyz	CG3752	Aldehyde DH	metabolism
		x	z	CG11140	Aldehyde DH typeIII	metabolism
		x	xkz	CG11876	Pyruvate DH	metabolism
z	y			CG12233	isocitrate DH	metabolism
x	xy	xz	xy	CG7176	Isocitrate DH	metabolism
yz	yz	xyz	yz	CG4067	formate-tetrahydrofolate DH	metabolism
xy				CG5320	Glutamate DH	metabolism
z	x	z	x	CG5362	Malate DH	metabolism

OregonR	*adp[60]*	*Lsd-2[51]*	*Lsd-2:EGFP*	gene	function	class
yz	xz	xyk	x	CG7998	L-Malate DH	metabolism
z		y	xy	CG6343	NADH ubiquinone reductase	metabolism
			z	CG3999	glycine dehydrogenase (decarboxylating) activity	metabolism
			yz	CG7430	dihydrolipoyl DH	metabolism
xz	z	x	x	CG8256	Glycerol-3-P-DH	metabolism
x	x	xz	xz	CG9042	Glycerol-3-P-DH	metabolism
	y			CG12055	Glyceraldehyde-3-P-DH	metabolism
xy	xz	xykz	xyk	CG8893	Glyceraldehyde-3-P-DH	metabolism
z		z		CG8251	phosphogluconate DH	metabolism
xyz	xy	x	xz	CG4104	Trehalose-6-P-Synthase	metabolism
xyz	xyz	yz	xyz	CG7070	Pyruvate Kinase	metabolism
			z	CG4302	UDP-Glucuronosyltransferase	metabolism
xyz	xyz	xykz	xykz	CG6543	Enoyl-CoA-Hydratase	metabolism
z				CG7254	glycogen phosphorylase activity	metabolism
	xy			CG8036	Transketolase	metabolism
xz		xz		CG9244	Aconitase	metabolism
z				CG10120	malic enzyme	metabolism
yz	z	xz	z	CG31305	Malate transporter	metabolism
			z	CG10449	catecholamines up	metabolism
		y		CG10527	farnesoic acid O methyltransferase	metabolism
			z	CG15102	juvenile hormone epoxide hydrolase activity	metabolism
z	xz	x		CG7399	Phenylalanine-4-monooxygenase	metabolism
	x	xkz	xz	CG17654	Enolase	metabolism
x				CG6188	Glycine N-methyltransferase	metabolism
x		y	xz	CG6415	aminomethyltransferase	metabolism
			z	CG17970	Cyp4ac2	metabolism
			z	CG2062	Cytochrome P450-4e1	metabolism
xkz		kz	z	CG2140	CytB5	metabolism
z	z		xyz	CG3656	cytochrom P450 4D1	metabolism
z			z	CG4105	Cytochrome P450-4e3	metabolism
			z	CG8864	Cyp28a5	metabolism
x				CG9081	Cyp4s3	metabolism
xykz	xyz	xykz	xykz	CG17285	FBP1	storage
xyz	xyz	xyz	xy	CG2559	LSP1alpha	storage
xykz	xyz	xykz	xykz	CG3763	FBP2	storage
xyz	xy	xykz	xy	CG4178	LSP1beta	storage
		x	x	CG6806	LSP 2	storage
xyz	xyz	xyz	xykz	CG6821	LSP1gamma	storage
x			z	CG10130	Sec61beta	Uncertain / transport
x			x	CG11642	SRP cotranslational membrane targeting	Uncertain / transport
xz			x	CG2331	transitional ER ATPase TER94	Uncertain / transport
yz	x		y	CG3152	HSP90 TRAP1	Uncertain / transport
xz	z	yz	yz	CG32701	SRP binding	Uncertain / transport
x				CG33162	SRP receptor beta	Uncertain / transport
xz	xy	kz	xz	CG5474	SSR beta	Uncertain / transport
x				CG5677	signal peptidase	Uncertain / transport
			x	CG5885	SSR complex	Uncertain / transport
x	yz	xk	xy	CG9035	TAP delta	Uncertain / transport
			z	CG1104	no prediction possible	Uncertain / transport
z			k	CG12084	no prediction possible	Uncertain / transport
	xy	y		CG1648	no prediction possible	Uncertain / transport
		z		CG1665	no prediction possible	Uncertain / transport
z	yz		k	CG15610	no prediction possible	Uncertain / transport
	y			CG17443	no prediction possible	Uncertain / transport
		y		CG18410	no prediction possible	Uncertain / transport
y		z		CG2267	no prediction possible	Uncertain / transport
			x	CG31714	no prediction possible	Uncertain / transport
	z	x	y	CG33129	no prediction possible	Uncertain / transport

OregonR	*adp[60]*	*Lsd-2[51]*	*Lsd-2:EGFP*	gene	function	class
		x		CG33140	no prediction possible	Uncertain / transport
		y		CG6652	no prediction possible	Uncertain / transport
	yz			CG8588	no prediction possible	Uncertain / transport
			x	CG10105	nothing predictable Stress-activated map kinase interacting protein 1 (SIN1)	Uncertain / transport
			x	CG12734	nothing predictable spectrin repeat	Uncertain / transport
	x			CG31288	no prediction possible DUF227 just present in *D. melanogaster* and *C. elegans*	Uncertain / transport
x	z	xz	xz	CG33113	no prediction possible Reticulon domain	Uncertain / transport
	y			CG6164	no prediction possible ML-domain lipid recognition Niemann Pick type 2 disease	Uncertain / transport
z		x	z	CG9007	no prediction possible Phd finger	Uncertain / transport
z				CG13995	no prediction possible LRR	Uncertain / transport
			z	CG8002	ARM repeat	Uncertain / transport
			xykz	CG15081	nothing predictable SPFH / band7	Uncertain / transport
x	x	xy	x	CG10691	l(2)37CC SPFH / band7	Uncertain / transport
k	z	k		CG15092	Perilipin homology (Short)	Uncertain / transport
xyz	z		xk	CG15825	protein transport / targeting	Uncertain / transport
z			k	CG2093	protein vacuolar targeting (?)	Uncertain / transport
	z			CG11785	vesicle mediated transport	Uncertain / transport
x				CG3320	Rab1	Uncertain / transport
	x			CG3269	Rab2	Uncertain / transport
	z			CG7576	Rab3	Uncertain / transport
	y	k		CG3664	Rab5	Uncertain / transport
	z			CG6601	Rab6	Uncertain / transport
			z	CG18076	shot actin / microtubule binding	Uncertain / transport
y				CG10718	nebbish	Uncertain / transport
xz	z		z	CG18212	cell cycle transport cytoskelet	Uncertain / transport
	z			CG1913	alpha-Tubulin at 84B	Uncertain / transport
y	y	y	x	CG4027	actin 5c	Uncertain / transport
y				CG6392	cmet microtubule motor	Uncertain / transport
z	z	y	x	CG1977	alpha spectrin	Uncertain / transport
xyz	xyz	y	z	CG5870	beta spectrin	Uncertain / transport
z		z	xz	CG9325	HTS	Uncertain / transport
z		z		CG10882	serine endopeptidase	Uncertain / transport
xz	z		xyz	CG5261	Dihydrolipoamide-S-acetyltransferase	Uncertain / transport
x		k	x	CG7592	Obp 99b	Uncertain / transport
		z		CG7111	Receptor of activated protein kinase C 1	Uncertain / transport
		y		CG1956	GTP binding RAS family roughened	Uncertain / transport
	y			CG7935	RAN prot binding small GTPase interacting regulatory	Uncertain / transport
z	y			CG9012	Clathrin HC	Uncertain / transport
		x		CG9280	Glutactin precursor	Uncertain / transport
	z			CG3200	Reg-2	Uncertain / transport
	xy			CG1803	regucalcin	Uncertain / transport
		x	y	CG2139	aralar1 Ca binding	Uncertain / transport
xyz	xy	yz	xyz	CG9429	Calreticulin	Uncertain / transport
z			x	CG12497	ligand binding of LDL-R	Uncertain / transport
z	x	xy	xz	CG17320	SCP-X	Uncertain / transport
y	y	xyz	z	CG12101	HSP60	Chaperones
xyz	xyz	xy	xyz	CG1242	HSP83	Chaperones
		yk	y	CG5436	HSP68	Chaperones
xyz	xyz	xykz	xykz	CG4147	78kDa grp	Chaperones
x	x	x	x	CG5834	Hsp70Bbb	Chaperones

OregonR	*adp[60]*	*Lsd-2[51]*	*Lsd-2:EGFP*	gene	function	class
		y	x	CG8542	Hsc 70-5	Chaperones
y	z	y		CG8937	HSC 70-1	Chaperones
xy	xyz	xyz	xykz	CG4264	HSC-4	Chaperones
xyz	xyz	xyz	xyz	CG5520	Gp93	Chaperones
	y	ykz	y	CG1683	sesB	Chaperones
xyz	xz	xz	xz	CG16944	sesB	Chaperones
xz	xz	xy	xy	CG2918	Chaperone	Chaperones
		z	k	CG7235	chaperone	Chaperones
xykz	xyz	xykz	xykz	CG6988	PDI	Chaperones
xyz	x	xykz	xyk	CG8983	PDI Erp60	Chaperones
z			y	CG5809	PDI like	Chaperones
y				CG14715	Peptidyl-Prolyl Cis-trans isomerase	Chaperones
	x	yk	y	CG2852	Peptidyl-Prolyl Cis-trans isomerase	Chaperones
xz		x	z	CG9577	Delta5-2,4dienoylCoA isomerase	Chaperones
z				CG11958	calnexin 99A	Chaperones
			z	CG11739	tricarboxylate carrier	mixed
x			z	CG8782	Ornithine aminotransferase	mixed
		y		CG11527	Tiggrin	mixed
		z		CG10302	bicoid stability factor	mixed
	y			CG12005	nucleic acid binding	mixed
y				CG12157	TOM	mixed
			x	CG12703	ABC transporter	mixed
x			z	CG16858	Collagen type IV alpha	mixed
z				CG17259	serine-tRNA ligase activity	mixed
		z	xz	CG1742	microsomal GST like	mixed
xy	xyz	xykz	ykz	CG17949	His2B	mixed
	z			CG18104	arginase activity	mixed
		yz		CG1907	carrier	mixed
	z			CG1922	RNA polymerase II transcription factor activity	mixed
y		z		CG2718	Glutamine Synthetase	mixed
z		xz		CG2736	Scavenger Receptor	mixed
kz		k		CG30415	Trypsin	mixed
z	x	z	xk	CG3140	Adenylate Kinase 2	mixed
xz			z	CG31618	histone H2A	mixed
			y	CG3373	hemomucin	mixed
z	x	xz		CG3379	Histone H4 replacement	mixed
x		z		CG3606	caz	mixed
		xy		CG3926	Serine pyruvate aminotransferase	mixed
		y		CG3989	adeS	mixed
		x		CG4233	Aspartate transaminase	mixed
z				CG4545	serotonin transporter activity	mixed
	z	z	xz	CG4994	Phoshate transporter precursor	mixed
xy	xz	xz		CG5170	ssDNA binding	mixed
k			xk	CG5499	HisH2A variant	mixed
			y	CG5826	Peroxidase	mixed
		y		CG5999	Glucoronosyltransferase	mixed
	y			CG6178	Luciferase monooxygenase	mixed
		z		CG6342	Iron regulatory protein 1B	mixed
			z	CG6850	UDP-glucose:glycoprotein glucosyltransferase activity	mixed
xyz	x	yz	xy	CG7008	tudor	mixed
xyz	xyz	xyz	xykz	CG7470	Glutamate Kinase	mixed
xz	yz	xz	xyz	CG7981	Trol	mixed
x		xk	z	CG10664	Cytochrome C oxidase	ATP
z	z	xz	xz	CG14724	CytC Oxidase subunit Va	ATP
	z			CG17280	cytochrome-c oxidase activity	ATP
		z		CG3560	Ubiquinol CytC reductase	ATP

OregonR	*adp[60]*	*Lsd-2[51]*	*Lsd-2:EGFP*	gene	function	class
xz	z	yz	xyz	CG4169	Ubiquinol CytC reductase	ATP
xykz	xyz	xykz	xykz	CG3612	bellwether	ATP
z	y	x		CG12140	electron transfer	ATP
z		x	z	CG13279	Cytb5 Red	ATP
x	x	x	x	CG14028	Cyclope	ATP
xkz	z	z	z	CG4769	Electron transporter	ATP
xyz	yz	xyz	xz	CG2968	ATPase	ATP
k		xkz	z	CG3321	ATPase	ATP
yz	z	yk	kz	CG4692	ATPase	ATP
x	x	kz	xk	CG6105	ATPase	ATP
xz		xykz	xyz	CG4307	Oscp ATPase	ATP
xk	y	xyk	x	CG5389	hydrogen exporting ATPase	ATP
xykz	xyz	xykz	xykz	CG6030	ATP Synthase delta	ATP
	x	kz	xz	CG7610	ATP Synthase gamma	ATP
xyz		xz	x	CG8189	ATP synthase beta	ATP
z				CG8048	Vacuolar H+ ATPase 44kD C subunit	ATP
xykz	xyz	xykz	xykz	CG11154	ATPsynthase beta	ATP
x	y	ykz	x	CG3731	Mito proc. Peptidase	ATP
xykz	xyz	xykz	xyk	CG6647	Mito Porin	ATP
xyz	y	y	yz	CG7834	electron transfer	ATP
y	x	xykz	xkz	CG8996	walrus	ATP
		z		CG9160	mitochondrial acyl carrier protein 1	ATP
	z			CG10305	Ribosomal protein	Translation
			y	CG11276	Ribosomal protein	Translation
		y	y	CG11522	Ribosomal protein	Translation
	x	yz	xz	CG11901	Translation elongation factor 1 gamma	Translation
y				CG14206	Ribosomal protein	Translation
	y	xz	y	CG14792	Ribosomal protein	Translation
xyk	xy			CG1524	Ribosomal protein	Translation
x		x		CG15697	Ribosomal protein	Translation
x	y	y		CG17521	Ribosomal protein	Translation
z			z	CG1883	Ribosomal protein	Translation
y				CG2168	Ribosomal protein	Translation
xz	xyz	xyz	xyz	CG2238	eEF2	Translation
xy		x	y	CG2960	Ribosomal protein L40	Translation
xy		xk	z	CG2998	Ribosomal protein	Translation
		z		CG3195	Ribosomal protein	Translation
		z		CG3314	Ribosomal protein	Translation
		xz		CG3751	Ribosomal protein	Translation
		y		CG3922	Ribosomal protein	Translation
xy	z	xy		CG4046	Ribosomal protein	Translation
x	xz	xkz	xy	CG4087	RpP2	Translation
		x		CG4897	Ribosomal protein	Translation
	x			CG5119	Polyadenylate binding protein	Translation
xz	yz	xz	xz	CG5502	60s Ribosomal protein	Translation
z	z			CG5920	Ribosomal protein	Translation
	z	x	yz	CG6253	Ribosomal protein	Translation
	x		y	CG6341	EF1beta	Translation
	z			CG6510	Ribosomal protein	Translation
xyz	yz	k	y	CG7283	Ribosomal protein	Translation
		z	xy	CG7434	Ribosomal protein	Translation
xyz	xyz	xyz	yz	CG7490	Ribosomal protein P0	Translation
		x	y	CG7622	Ribosomal protein	Translation
xy	xz	y	k	CG7726	Ribosomal protein	Translation
	z		y	CG7977	Ribosomal protein	Translation
xyz	xyz	xykz	xyz	CG8280	EF1alpha 48D	Translation
	x			CG8615	Ribosomal protein	Translation
xz	x	x	x	CG8900	Ribosomal protein S18	Translation
xy	x	xz	xz	CG9282	Ribosomal protein	Translation

OregonR	*adp[60]*	*Lsd-2[51]*	*Lsd-2:EGFP*	gene	function	class
			z	CG9354	Ribosomal protein	Translation

x, y, k and z represent the different rounds of identifications

Appendix III: Indicators for identified regulators of lipid storage

In order to obtain among the identified proteins indications for regulators of TAG storage, a search among the 271 nano LC-MS / MS-identified proteins for homologous genes, previously shown to be involved in human disease or fat storage regulation was performed. For this purpose, the identifications were compared to the Homophila database of *Drosophila* homologues of human disease genes (Chien et al., 2002) and the results of a genome wide RNAi screen done in *Caenorhabditis elegans* focusing on fat storage effects (Ashrafi et al., 2003) (reduced or increased fat content; in the table the respective *C. elegans* homologue is given). Additionally, identifications were compared to the results of a whole transcriptome investigation of starvation response in *Drosophila* larvae (Zinke et al., 2002, downregulated or upregulated upon starvation or no change (nc)). In total, 39 proteins are part of the Homophila database and 9 proteins have *C. elegans* homologs, which showed a fat storage phenotype upon RNAi. 37 genes coding for identified proteins showed a transcriptional regulation upon starvation (at least two of the three timepoints regulated in same direction).

Table A-3: Indicators for TAG storage regulators

gene	function	class	Homophila homologue	*C.elegans* RNAi	larval starvation microarray
CG10374	LSD-1	PAT-domain			downregulated
CG5958	Retinol / fatty acid binding	fatty acid / TAG binding	Yes		downregulated
CG9342	Triglyceride binding	fatty acid / TAG binding	Yes		downregulated
CG5295	brummer LD ass. TAG lipase	metabolism			upregulated
CG4389	long chain hydroxoacyl CoA DH	metabolism	Yes	reduced T08B2.7	nc
CG4581	long-chain-3-hydroxyacyl-CoA dehydrogenase activity	metabolism	Yes		nc
CG7461	Very long chain acyl CoA DH	metabolism	Yes		nc
CG1516	Pyruvate Carboxylase	metabolism	Yes		nc
CG4600	acetyl-CoA C-acyltransferase activity	metabolism	Yes		nc
CG9390	Acetyl Coenzyme A synthase	metabolism	Yes	reduced C36A4.9	nc
CG8322	ATP citrate lyase	metabolism			downregulated

gene	function	class	Homophila homologue	*C.elegans* RNAi	larval starvation microarray
CG3415	estradiol 17-beta-dehydrogenase activity	metabolism	Yes	increased E04F6.3	nc
CG3752	Aldehyde DH	metabolism	Yes		nc
CG11140	Aldehyde DH typeIII	metabolism	Yes		nc
CG4067	formate-tetrahydrofolate DH	metabolism	Yes		upregulated
CG5320	Glutamate DH	metabolism	Yes		nc
CG3999	glycine dehydrogenase (decarboxylating) activity	metabolism	Yes		nc
CG7430	dihydrolipoyl DH	metabolism	yes		nc
CG8256	Glycerol-3-P-DH	metabolism	Yes		nc
CG8893	Glyceraldehyde-3-P-DH	metabolism		reduced K10B3.7	downregulated
CG8251	phosphogluconate DH	metabolism	Yes		nc
CG7070	Pyruvate Kinase	metabolism	yes		nc
CG8036	Transketolase	metabolism	Yes		nc
CG15102	juvenile hormone epoxide hydrolase activity	metabolism	yes		nc
CG7399	Phenylalanine-4-monooxygenase	metabolism	yes		nc
CG17654	Enolase	metabolism	Yes		nc
CG6415	aminomethyltransferase	metabolism	Yes		downregulated
CG4105	Cytochrome P450-4e3	metabolism			upregulated
CG4178	LSP1beta	storage			downregulated
CG10130	Sec61beta	Uncertain / transport			downregulated
CG11642	SRP cotranslational membrane targeting	Uncertain / transport		increased C24F3.1	nc
CG2331	transitional ER ATPase TER94	Uncertain / transport			downregulated
CG32701	SRP binding	Uncertain / transport			downregulated
CG5474	SSR beta	Uncertain / transport			downregulated
CG5885	SSR complex	Uncertain / transport			downregulated
CG9035	TAP delta	Uncertain / transport			downregulated
CG1648	no prediction possible	Uncertain / transport			upregulated
CG6164	no prediction possible ML-domain lipid recognition Niemann Pick type 2 disease	Uncertain / transport			upregulated
CG15081	nothing predictable SPFH / band7	Uncertain / transport			downregulated
CG10691	l(2)37CC SPFH / band7	Uncertain / transport	Yes		downregulated
CG3269	Rab2	Uncertain / transport		reduced F11A5.1	upregulated
CG18076	shot actin / microtubule binding	Uncertain / transport	Yes		upregulated
CG1913	alpha-Tubulin at 84B	Uncertain / transport		reduced T28D6.2	nc
CG1977	alpha spectrin	Uncertain / transport	Yes		nc
CG5261	Dihydrolipoamide-S-acetyltransferase	Uncertain / transport	Yes		nc
CG3200	Reg-2	Uncertain / transport			upregulated
CG2139	aralar1 Ca binding	Uncertain / transport	Yes		nc
CG9429	Calreticulin	Uncertain / transport			downregulated
CG12101	HSP60	Chaperones			downregulated
CG1242	HSP83	Chaperones			downregulated

gene	function	class	Homophila homologue	*C.elegans* RNAi	larval starvation microarray
CG5436	HSP68	Chaperones			downregulated
CG8542	Hsc 70-5	Chaperones			downregulated
CG5520	Gp93	Chaperones			downregulated
CG16944	sesB	Chaperones	Yes		nc
CG8983	PDI Erp60	Chaperones			downregulated
CG5809	PDI like	Chaperones			downregulated
CG11958	calnexin 99A	Chaperones			downregulated
CG8782	Ornithine aminotransferase	mixed	Yes		nc
CG12703	ABC transporter	mixed	Yes		nc
CG16858	Collagen type IV alpha	mixed	Yes		nc
CG17259	serine-tRNA ligase activity	mixed			downregulated
CG3379	Histone H4 replacement	mixed		reduced ZK131.8	nc
CG3606	caz	mixed	Yes		nc
CG3926	Serine pyruvate aminotransferase	mixed			upregulated
CG3989	ade5	mixed			upregulated
CG5499	HisH2A variant	mixed			downregulated
CG6178	Luciferase monooxygenase	mixed		reduced AH10.1	nc
CG7008	tudor	mixed			downregulated
CG7470	Glutamate Kinase	mixed	Yes		nc
CG7981	Trol	mixed	Yes		nc
CG12140	electron transfer	ATP	Yes		nc
CG7834	electron transfer	ATP	Yes		nc
CG8996	walrus	ATP	Yes		nc
CG11276	Ribosomal protein	Translation	Yes		nc

x, y, k and z represent the different rounds of identification

Appendix IV: Detailed results of the comparative aspects of the proteomics screen

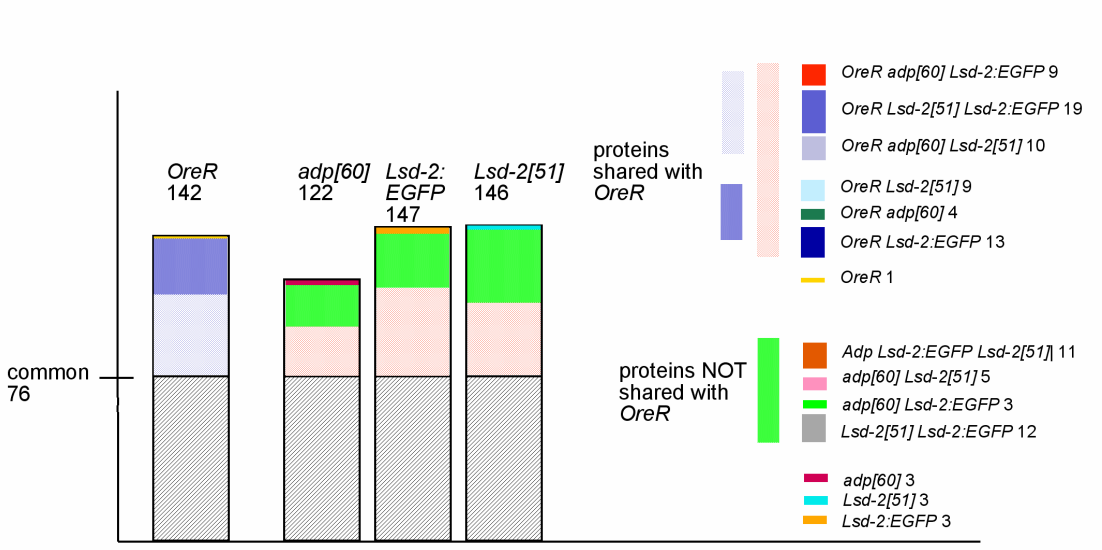

Fig. A-2: Detailed version of Fig. 2-13
On the right side of the graph, the detailed numeric results of the comparison of the genotype-specific proteomes are given. For further details see table A-4.

Table A-4: Genotype specific proteome comparison

OregonR	*adp[60]*	*Lsd-2[51]*	*Lsd-2:EGFP*	gene	function	class
xykz	xyz	xykz	xykz	CG10374	LSD-1	PAT-domain
x	xy	kz	xy	CG5958	Retinol / fatty acid binding	fatty acid / TAG binding
x	xy	xz	xy	CG7176	Isocitrate DH	metabolism
x	x	xz	xz	CG9042	Glycerol-3-P-DH	metabolism
xk	x	yk	y	CG4581	long-chain-3-hydroxyacyl-CoA dehydrogenase activity	metabolism
xyz	xyz	xykz	xy	CG1516	Pyruvate Carboxylase	metabolism
xyz	xyz	xyz	xyz	CG3523	fatty acid synthase	metabolism
xyz	xz	xz	xyz	CG3752	Aldehyde DH	metabolism
xyz	xy	x	xz	CG4104	Trehalose-6-P-Synthase	metabolism
xyz	xy	xyz	xykz	CG5167	NAD binding	metabolism
xyz	xyz	xykz	xykz	CG6543	Enoyl-CoA-Hydratase	metabolism
xyz	xyz	yz	xyz	CG7070	Pyruvate Kinase	metabolism
xyz	xz	xyz	ykz	CG7113	3-hydroxyacyl-CoA DH activity Scully	metabolism
xz	z	yz	y	CG13890	Dodecanoyl-CoA-Isomerase	metabolism
xy	xz	xykz	xyk	CG8893	Glyceraldehyde-3-P-DH	metabolism
xz	xyz	xyk	xyz	CG32954	ADH	metabolism
xz	z	x	x	CG8256	Glycerol-3-P-DH	metabolism
yz	z	ykz	yz	CG1112	alpha esterase 7	metabolism
yz	xyz	yz	xyz	CG11198	Acetyl CoA carboxylase	metabolism
yz	z	xz	z	CG31305	Malate transporter	metabolism
yz	yz	xyz	yz	CG4067	formate-tetrahydrofolate DH	metabolism
yz	xz	xyk	x	CG7998	L-Malate DH	metabolism
z	x	z	x	CG5362	Malate DH	metabolism
xyz	xyz	xyz	xy	CG2559	LSP1alpha	storage
xyz	xy	xykz	xy	CG4178	LSP1beta	storage
xyz	xyz	xyz	xykz	CG6821	LSP1gamma	storage
xykz	xyz	xykz	xykz	CG17285	FBP1	storage

xykz	xyz	xykz	xykz	CG3763	FBP2	storage
x	x	xy	x	CG10691	I(2)37CC SPFH / band7	Uncertain / transport
x	z	xz	xz	CG33113	no prediction possible Reticulon domain	Uncertain / transport
xyz	xyz	y	z	CG5870	beta spectrin	Uncertain / transport
xyz	xy	yz	xyz	CG9429	Calreticulin	Uncertain / transport
y	y	y	x	CG4027	actin 5c	Uncertain / transport
z	x	xy	xz	CG17320	SCP-X	Uncertain / transport
z	z	y	x	CG1977	alpha spectrin	Uncertain / transport
x	yz	xk	xy	CG9035	TAP delta	Uncertain / transport
xz	z	yz	yz	CG32701	SRP binding	Uncertain / transport
xz	xy	kz	xz	CG5474	SSR beta	Uncertain / transport
x	x	x	x	CG5834	Hsp70Bbb	Chaperones
xy	xyz	xyz	xykz	CG4264	HSC-4	Chaperones
xyz	xyz	xy	xyz	CG1242	HSP83	Chaperones
xyz	xz	xz	xz	CG16944	sesB	Chaperones
xyz	xyz	xykz	xykz	CG4147	78kDa grp	Chaperones
xyz	xyz	xyz	xyz	CG5520	Gp93	Chaperones
xyz	x	xykz	xyk	CG8983	PDI Erp60	Chaperones
xz	xz	xy	xy	CG2918	Chaperone	Chaperones
xykz	xyz	xykz	xykz	CG6988	PDI	Chaperones
y	y	xyz	z	CG12101	HSP60	Chaperones
xy	xyz	xykz	ykz	CG17949	His2B	mixed
xyz	x	yz	xy	CG7008	tudor	mixed
xyz	xyz	xyz	xykz	CG7470	Glutamate Kinase	mixed
xz	yz	xz	xyz	CG7981	Trol	mixed
z	x	z	xk	CG3140	Adenylate Kinase 2	mixed
x	x	x	x	CG14028	Cyclope	ATP
x	y	ykz	x	CG3731	Mito proc. Peptidase	ATP
x	x	kz	xk	CG6105	ATPase	ATP
xk	y	xyk	x	CG5389	hydrogen exporting ATPase	ATP
xkz	z	z	z	CG4769	Electron transporter	ATP
xyz	yz	xyz	xz	CG2968	ATPase	ATP
xyz	y	y	yz	CG7834	electron transfer	ATP
xykz	xyz	xykz	xykz	CG11154	ATPsynthase beta	ATP
xykz	xyz	xykz	xykz	CG3612	bellwether	ATP
xykz	xyz	xykz	xykz	CG6030	ATP Synthase delta	ATP
xykz	xyz	xykz	xyk	CG6647	Mito Porin	ATP
xz	z	yz	xyz	CG4169	Ubiquinol CytC reductase	ATP
y	x	xykz	xkz	CG8996	walrus	ATP
yz	z	yk	kz	CG4692	ATPase	ATP
z	z	xz	xz	CG14724	CytC Oxidase subunit Va	ATP
x	xz	xkz	xy	CG4087	RpP2	Translation
xyz	yz	k	y	CG7283	Ribosomal protein	Translation
xyz	xyz	xyz	yz	CG7490	Ribosomal protein P0	Translation
xyz	xyz	xykz	xyz	CG8280	EF1alpha 48D	Translation
xz	xyz	xyz	xyz	CG2238	eEF2	Translation
xy	xz	y	k	CG7726	Ribosomal protein	Translation
xy	x	xz	xz	CG9282	Ribosomal protein	Translation
xz	yz	xz	xz	CG5502	60s Ribosomal protein	Translation
xz	x	x	x	CG8900	Ribosomal protein S18	Translation
OregonR	***adp[60]***	***Lsd-2[51]***	***Lsd-2:EGFP***	**gene**	**function**	**class**
xykz	xyz		xykz	CG9057	LSD-2	PAT-domain
z	z		xyz	CG3656	cytochrom P450 4D1	metabolism
y	y		y	CG10622	Succinate CoA Ligase	metabolism
xyz	xyz		xyz	CG8322	ATP citrate lyase	metabolism

yz	x		y	CG3152	HSP90 TRAP1	Uncertain / transport
z	yz		k	CG15610	no prediction possible	Uncertain / transport
xz	z		z	CG18212	cell cycle transport cytoskelet	Uncertain / transport
xz	z		xyz	CG5261	Dihydrolipoamide-S-acetyltransferase	Uncertain / transport
xyz	z		xk	CG15825	protein transport / targeting	Uncertain / transport
OregonR	***adp[60]***	***Lsd-2[51]***	***Lsd-2:EGFP***	**gene**	**function**	**class**
z		y	z	CG2604	NAD binding	metabolism
z		z	xz	CG5887	fatty acid desaturase	metabolism
z		y	xy	CG6343	NADH ubiquinone reductase	metabolism
xkz		kz	z	CG2140	CytB5	metabolism
xz		xyz	xyz	CG4389	long chain hydroxoacyl CoA DH	metabolism
z		yz	x	CG7920	4-hydroxybutyrate CoA transferase	metabolism
x		y	xz	CG6415	aminomethyltransferase	metabolism
x		xy	x	CG7461	Very long chain acyl CoA DH	metabolism
z		x	z	CG9007	no prediction possible Phd finger	Uncertain / transport
z		z	xz	CG9325	HTS	Uncertain / transport
x		k	x	CG7592	Obp 99b	Uncertain / transport
xz		x	z	CG9577	Delta5-2,4dienoyl CoA isomerase	Chaperones
k		xkz	z	CG3321	ATPase	ATP
z		x	z	CG13279	Cytb5 Red	ATP
xz		xykz	xyz	CG4307	Oscp ATPase	ATP
x		xk	z	CG10664	Cytochrome C oxidase	ATP
xyz		xz	x	CG8189	ATP synthase beta	ATP
xy		x	y	CG2960	Ribosomal protein L40	Translation
xy		xk	z	CG2998	Ribosomal protein	Translation
OregonR	***adp[60]***	***Lsd-2[51]***	***Lsd-2:EGFP***	**gene**	**function**	**class**
xz	y	z		CG11064	Retinol / fatty acid binding	fatty acid / TAG binding
y	z	z		CG10639	Oxidoreductase	metabolism
z	xz	x		CG7399	Phenylalanine-4-monooxygenase	metabolism
k	z	k		CG15092	Perilipin homology (Short)	Uncertain / transport
y	z	y		CG8937	HSC 70-1	Chaperones
xy	xz	xz		CG5170	ssDNA binding	mixed
z	x	xz		CG3379	Histone H4 replacement	mixed
z	y	x		CG12140	electron transfer	ATP
x	y	y		CG17521	Ribosomal protein	Translation
xy	z	xy		CG4046	Ribosomal protein	Translation
OregonR	***adp[60]***	***Lsd-2[51]***	***Lsd-2:EGFP***	**gene**	**function**	**class**
	xy	xz	xyz	CG9342	Triglyceride binding	fatty acid / TAG binding
	x	xkz	xz	CG17654	Enolase	metabolism
	yz	y	yk	CG11151	SCP2	metabolism
	z	x	y	CG33129	no prediction possible	Uncertain / transport
	x	yk	y	CG2852	Peptidyl-Prolyl Cis-trans	Chaperones

					isomerase	
	y	ykz	y	CG1683	sesB	Chaperones
	z	z	xz	CG4994	Phoshate transporter precursor	mixed
	x	kz	xz	CG7610	ATP Synthase gamma	ATP
	x	yz	xz	CG11901	Translation elongation factor 1 gamma	Translation
	y	xz	y	CG14792	Ribosomal protein	Translation
	z	x	yz	CG6253	Ribosomal protein	Translation
OregonR	***adp[60]***	***Lsd-2[51]***	***Lsd-2:EGFP***	**gene**	**function**	**class**
z	y			CG12233	isocitrate DH	metabolism
z	y			CG9012	Clathrin HC	Uncertain / transport
z	z			CG5920	Ribosomal protein	Translation
xyk	xy			CG1524	Ribosomal protein	Translation
OregonR	***adp[60]***	***Lsd-2[51]***	***Lsd-2:EGFP***	**gene**	**function**	**class**
z			z	CG4105	Cytochrome P450-4e3	metabolism
xz			x	CG2331	transitional ER ATPase TER94	Uncertain / transport
x			x	CG11642	SRP cotranslational membrane targeting	Uncertain / transport
x			z	CG10130	Sec61beta	Uncertain / transport
z			k	CG12084	no prediction possible	Uncertain / transport
z			k	CG2093	protein vacuolar targeting (?)	Uncertain / transport
z			x	CG12497	ligand binding of LDL-R	Uncertain / transport
z			y	CG5809	PDI like	Chaperones
xz			z	CG31618	histone H2A	mixed
k			xk	CG5499	HisH2A variant	mixed
x			z	CG16858	Collagen type IV alpha	mixed
x			z	CG8782	Ornithine aminotransferase	mixed
z			z	CG1883	Ribosomal protein	Translation
OregonR	***adp[60]***	***Lsd-2[51]***	***Lsd-2:EGFP***	**gene**	**function**	**class**
xz		xz		CG9244	Aconitase	metabolism
z		z		CG8251	phosphogluconate DH	metabolism
y		z		CG2267	no prediction possible	Uncertain / transport
z		z		CG10882	serine endopeptidase	Uncertain / transport
x		z		CG3606	caz	mixed
kz		k		CG30415	Trypsin	mixed
y		z		CG2718	Glutamine Synthetase	mixed
z		xz		CG2736	Scavenger Receptor	mixed
x		x		CG15697	Ribosomal protein	Translation
OregonR	***adp[60]***	***Lsd-2[51]***	***Lsd-2:EGFP***	**gene**	**function**	**class**
		x	z	CG11140	Aldehyde DH typeIII	metabolism
		y	z	CG3415	estradiol 17-beta-DH activity	metabolism
		x	xkz	CG11876	Pyruvate DH	metabolism
		x	x	CG6806	LSP 2	storage

		x	y	CG2139	aralar1 Ca binding	Uncertain / transport
		yk	y	CG5436	HSP68	Chaperones
		z	k	CG7235	chaperone	Chaperones
		y	x	CG8542	Hsc 70-5	Chaperones
		z	xz	CG1742	microsomal GST like	mixed
		y	y	CG11522	Ribosomal protein	Translation
		z	xy	CG7434	Ribosomal protein	Translation
		x	y	CG7622	Ribosomal protein	Translation
OregonR	***adp[60]***	***Lsd-2[51]***	***Lsd-2:EGFP***	**gene**	**function**	**class**
	xz	z		CG2254	short chain DH	metabolism
	xyz	y		CG3524	[acyl-carrier protein] S-acetyltransferase activity (EC:2.3.1.38)	metabolism
	z	y		CG11567	NADPH hemoprotein reductase	metabolism
	xy	y		CG1648	no prediction possible	Uncertain / transport
	y	k		CG3664	Rab5	Uncertain / transport
OregonR	***adp[60]***	***Lsd-2[51]***	***Lsd-2:EGFP***	**gene**	**function**	**class**
	x		y	CG2505	alpha esterase 2	metabolism
	x		y	CG6341	EF1beta	Translation
	z		y	CG7977	Ribosomal protein	Translation
OregonR	***adp[60]***	***Lsd-2[51]***	***Lsd-2:EGFP***	**gene**	**function**	**class**
			xz	CG5590	oxidoreductase short chain DH	metabolism
			yz	CG7430	dihydrolipoyl DH	metabolism
			xykz	CG15081	nothing predictable SPFH / band7	Uncertain / transport
OregonR	***adp[60]***	***Lsd-2[51]***	***Lsd-2:EGFP***	**gene**	**function**	**class**
		xy		CG3926	Serine pyruvate aminotransferase	mixed
		yz		CG1907	carrier	mixed
		xz		CG3751	Ribosomal protein	Translation
OregonR	***adp[60]***	***Lsd-2[51]***	***Lsd-2:EGFP***	**gene**	**function**	**class**
	xy			CG8036	Transketolase	metabolism
	xy			CG1803	regucalcin	Uncertain / transport
	yz			CG8588	no prediction possible	Uncertain / transport
OregonR	***adp[60]***	***Lsd-2[51]***	***Lsd-2:EGFP***	**gene**	**function**	**class**
xy				CG5320	Glutamate DH	metabolism

x, y, k and z represent the different rounds of identification

Appendix V: Interactions identified using the Osprey software

Physical interactions among the 271 identified lipid droplet-associated proteins based on genome-wide yeast-2-hybrid screens (Giot et al., 2003). The identified proteins were analyzed using the Osprey software (Breitkreutz et al., 2003) resulting in the identification of 28 interactions and subsequently sorted using the Gene Ontology (GO) terms.

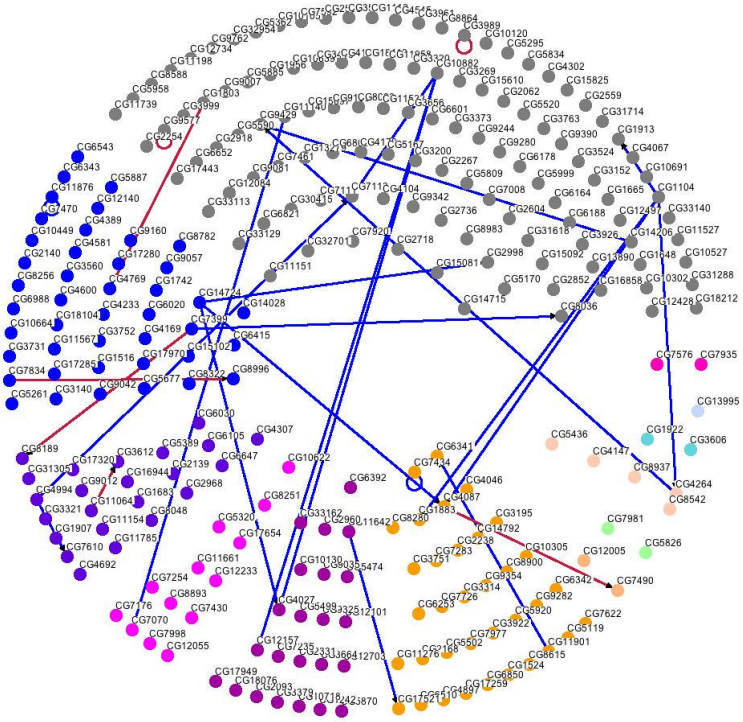

Fig. A-3: Interactions among the identified proteins on basis of the *Drosophila* protein interaction map

Each node represents an identified protein. The proteins are grouped according to the GO (Gene ontology) terms. Color code (clockwise): grey: unknown; darker pink: protein transport; light blue: signal transduction; green: transcription; rose: stress response; light green: cell growth and/or maintenance; apricot: DNA repair; orange: protein biosynthesis; violet: cell organization and biogenesis; light violet: carbohydrate metabolism; blue: transport; lighter blue: metabolism.

Appendix VI: Interactions identified using the FlyNet server

Interactions among the 271 identified lipid droplet-associated proteins as analyzed using the FlyNet server (http://www.jhubiomed.org/perl/flynet.pl) which includes both: all 20405 *Drosophila* protein interactions (Giot et al., 2003), as well as 15570 yeast interactions. In addition to the interactions

shown in appendix V, interactions are shown with *Drosophila* proteins not identified in the present lipid droplet proteomics screen, and additionally the orthologous interactions found in the yeast interactome, both on the genetic and on the physical level. Analysis was done using standard FlyNet settings. Visualization of the results was achieved by using the Graphviz software . 157 interactions among the identified proteins (shown in red ovals) have been detected. Clear ovals show interactors not identified in the screen. Blue interconnections mark yeast-2-hybrid interactions found with *Drosophila* proteins, green interconnections mark yeast-2-hybrid or genetic interactions found with the yeast orthologs.

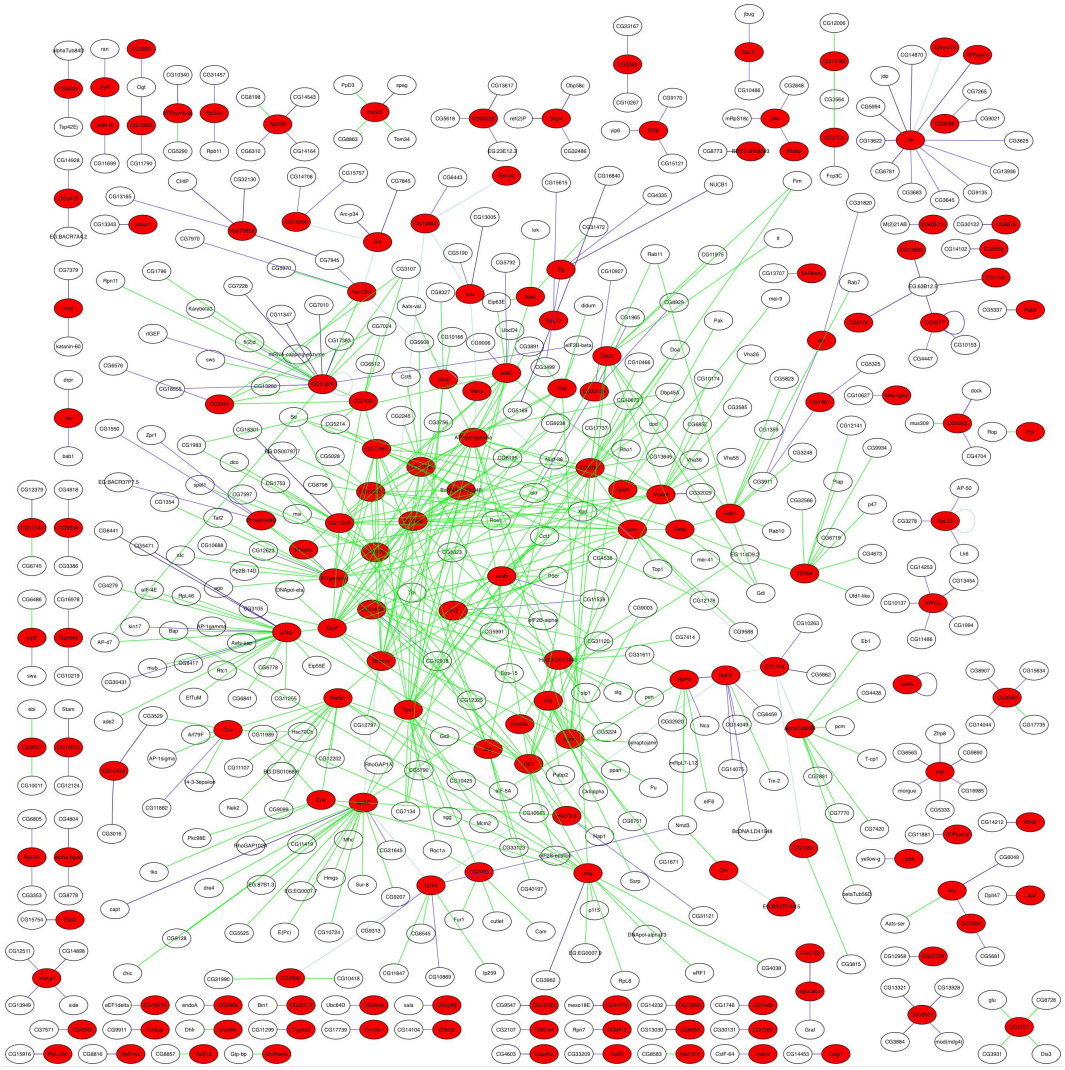

Fig. A-4: Interactions of the identified proteins on basis of the FlyNet server

The hierarchical arrangement of the interactions reveals substantial interconnections of the proteins identified, as shown in the examples below:

Example 1:

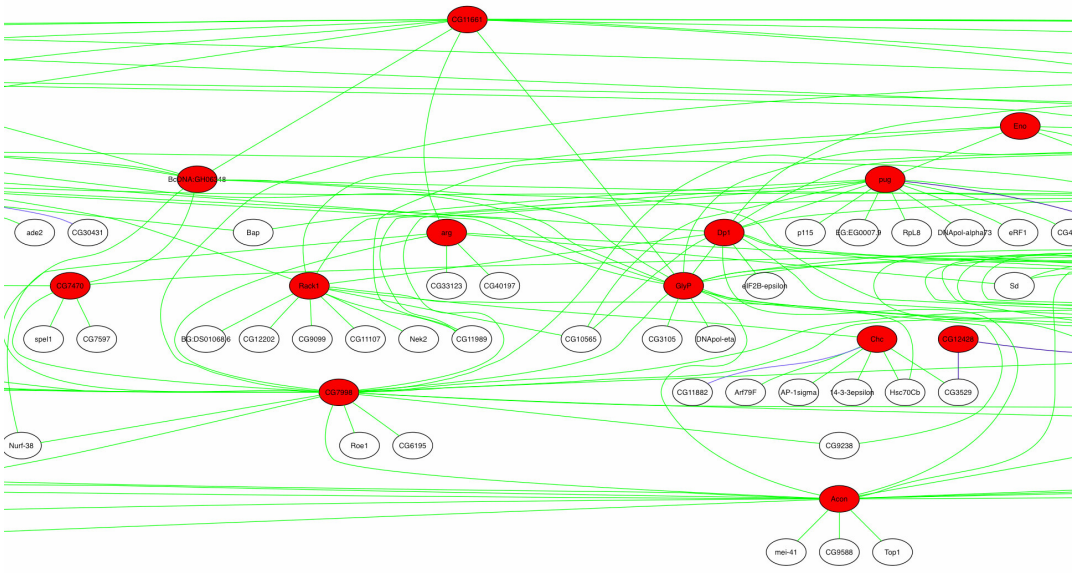

Example 2:

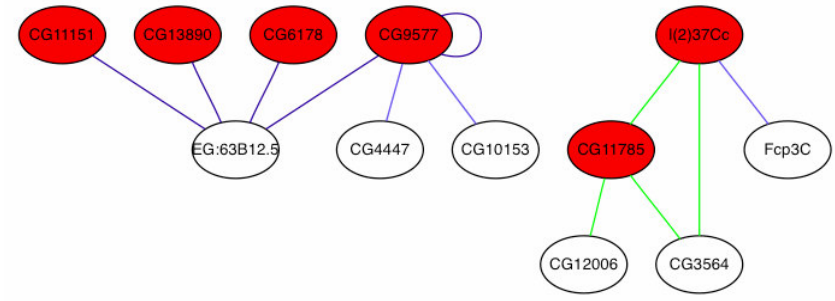

Appendix VII: Proteins identified in previous lipid droplet proteomics screens

Table A-5: Previously identified lipid droplet-associated proteins from other organisms

Protein	ID / subtype	Best *Drosophila* BLAST hit	Reference
Perilipin	gi|28316726	**LSD-1** / **LSD-2**	Brasaemle et al., 2004
ADRP	Q99541	**LSD-1** / **LSD-2**	Fujimoto et al., 2004; Umlauf et al., 2004 Brasaemle et al., 2004; Liu et al., 2004; Wu et al., 2000
TIP47	O60664	**LSD-1** / **LSD-2**	Fujimoto et al., 2004; Umlauf et al., 2004 Brasaemle et al., 2004
S3-12	gi|10181204	CG18331 (weak)	Brasaemle et al., 2004; Liu et al., 2004
long-chain fatty acid CoA ligase	YOR317c, YMR246w	 CG8732	Athenstaedt et al., 1999; Liu et al., 2004
Very long-chain fatty acid activator; fatty acid transport protein	YBR041c	CG7400	Athenstaedt et al., 1999
Acyl-CoA synthetase long chain member 1, 2, 3	gi|729927 gi|20455039 gi|6172341	**CG3961** CG8732 CG8732	Brasaemle et al., 2004
Acetyl-CoA carboxylase	NP_000655	**CG11198**	Liu et al., 2004; Umlauf et al., 2004
3ß-hydroxosteroid DH	Q15738 gi|8473695	CG7724 (weak)	Fujimoto et al., 2004; Umlauf et al., 2004 Brasaemle et al., 2004
17ß-hydroxosteroid DH	type 11: AF126780 / NP_057329 type 7: P56937	CG15629 / third hit **CG2254** CG7221	Fujimoto et al., 2004; Umlauf et al., 2004 Brasaemle et al., 2004; Liu et al., 2004
Lanosterol synthase / synthetase	YHR072w, P48449 / P48449 gi|22122469	CG10363 weak **CG7981 weak** CG13948 weak	Athenstaedt et al., 1999 Fujimoto et al., 2004 Umlauf et al., 2004 Brasaemle et al., 2004; Liu et al., 2004
Patatin domain protein	YMR313c CAC01131 gi|21313274	**CG5295**	Athenstaedt et al., 1999; Umlauf et al., 2004 Liu et al., 2004
Hormone sensitive lipase HSL	gi|6754552	CG11055	Brasaemle et al., 2004
Triacylglycerol lipase	YKL140w	CG8823	Athenstaedt et al., 1999
Lipase	YOR059c	CG32333 weak	Athenstaedt et al., 1999
Cholesterol Esterase	Q64285	CG17901 weaker hits **CG1112** / **CG2505**	Wu et al., 2000
ER carboxylesterase	Q8VCC2	CG6414 weaker hits **CG1112** / **CG2505**	Wu et al., 2000
1-acylglycerol-3-P-acyltransferase	YDL052c	CG3812	Athenstaedt et al., 1999
lysophospholipase	YKL094w	CG3744 / CG1882 weak	Athenstaedt et al., 1999
Squalene epoxidase	YGR175c AAD10823 gi|6678127	 **CG10639**	Athenstaedt et al., 1999; Umlauf et al., 2004 Liu et al., 2004
Sterol-delta 24-methyltransferase	YML008c	CG8076 CG4755	Athenstaedt et al., 1999; Liu et al., 2004

Protein	**ID / subtype**	**Best *Drosophila* BLAST hit**	**Reference**
Pyruvate Carboxylase	gi|200246	**CG1516**	Brasaemle et al., 2004; Wu et al., 2000
GAPDH	YJL052w,YJR009c, YGR192c, P04406	**CG12055** **CG8893**	Athenstaedt et al., 1999 Fujimoto et al., 2004
oxidoreductase / short chain DH	YIL124w	CG3699 CG12171 weak	Athenstaedt et al., 1999; Liu et al., 2004
prediced protein	YKR046c	CG14120 **CG18076 weak**	Athenstaedt et al., 1999
acyl-CoA synthetase3/4	O95573 O60488	CG8732	Fujimoto et al., 2004
P63 ER membrane protein	S33377	CG15792 weak	Fujimoto et al., 2004
predicted protein	BC006145 gi|28436938 gi|23600211	CG10372	Fujimoto et al., 2004 Liu et al., 2004 Brasaemle et al., 2004
CGI49	AF151807	**CG2604** / **CG5167**	Brasaemle et al., 2004; Fujimoto et al., 2004
predicted protein	FLJ14497	**CG7430**	Fujimoto et al., 2004
NADH-cytochrome B5 reductase / Diaphorase	P00387 gi|19745150	CG5946	Fujimoto et al., 2004; Umlauf et al., 2004 Brasaemle et al., 2004; Liu et al., 2004
annexin II	P07355	CG5730	Fujimoto et al., 2004
Rab	5 1, 6, 7, 10, 18 1, 2, 5, 7, 10, 11, 14, 18 5, 7, 14, 18	**Rab1, 2, 5, 6**, 7, 10, 11, 14, 18	Fujimoto et al., 2004 Umlauf et al., 2004 Liu et al., 2004 Brasaemle et al., 2004
B-cell receptor ass prot. 31	P51572	CG13887	Fujimoto et al., 2004
Rap1B	P09526	**CG1956**	Fujimoto et al., 2004
Protein Kinase D2	NP_057541	CG7125	Umlauf et al., 2004
GRP94	P14625	**CG5520**	Umlauf et al., 2004
HSP-90-alpha / -beta	P07900 / P08238	**CG1242**	Umlauf et al., 2004
BiP	P11021 gi|2598562 gi|2506545	**CG4147**	Liu et al., 2004; Umlauf et al., 2004 Brasaemle et al., 2004
HSP70 / HSC70 / HSC 73		**CG4264**	Brasaemle et al., 2004; Wu et al., 2000; Umlauf et al., 2004
HSP60	P10809	**CG12101**	Umlauf et al., 2004
PDI		**CG6988**	Liu et al., 2004; Umlauf et al., 2004
ß-actin	AAH08633	**CG4027**	Umlauf et al., 2004
CGI-58	NP_057090 gi|13385690	CG1882	Brasaemle et al., 2004; Umlauf et al., 2004
p53 responsive gene 3 (AMID)	NP_116186	**CG7430 weak**	Umlauf et al., 2004
stomatin	P27105	CG32245	Umlauf et al., 2004
calcium binding protein p22	Q99653	CG2185	Umlauf et al., 2004
Palmitoyl-protein thioesterase	gi|6679451	CG12108	Liu et al., 2004
Alcohol DH		**ADH**	Liu et al., 2004
Sec22	gi|6755448	CG7359	Liu et al., 2004
alpha-SNAP	gi|13385392	CG6625	Liu et al., 2004
RalA	gi|9507025	RalA	Liu et al., 2004
P50 RhoGap	gi|22122649	CG6811	Liu et al., 2004
14-3-3	gi|26344914	14-3-3	Liu et al., 2004

Protein	ID / subtype	Best *Drosophila* BLAST hit	Reference
Related to Prohibitin Stomatin B-Cell receptor associated protein 37	gi|6671622 gi|6679299 gi|28526501	**CG15081** / **CG10691**	Liu et al., 2004 Brasaemle et al., 2004
unknown	gi|28204956	nothing significant	Liu et al., 2004
Dolichyl-phosphate ß-glucosyltransferase	gi|26325938	CG7870	Liu et al., 2004
VDAC-1	gi|10720404	**CG6647**	Liu et al., 2004
AAA family protein	gi|26351449	CG33101	Liu et al., 2004
TER ATPase	Q01853	**CG2331**	Wu et al., 2000
Fibrinogen gamma	NP_598623	CG30280 / CG8642 equal hits	Wu et al., 2000
Gephyrin	NP_766540	CG2945	Wu et al., 2000
ERP99	P08113	**CG5520**	Wu et al., 2000
Dynein intermediate chain	XP_110968	CG3732	Wu et al., 2000
Motor protein	not traceable		Wu et al., 2000
TIF32	not traceable		Wu et al., 2000
Heterotrimeric G protein ß	not traceable		Wu et al., 2000
ERP29	NP_080405	CG7225	Wu et al., 2000
Peroxiredoxin IV	NP_058044	CG1274	Wu et al., 2000
Fatty acid synthase	NP_032014	**CG3523** / **3254**	Wu et al., 2000
Gelsolin	AAH79472	CG1106	Wu et al., 2000
Xanthine DH	Q00519	CG7642	Wu et al., 2000
Butyrophilin	XP_139886	CG31814	Wu et al., 2000
Vimentin	gi|55408	CG6944	Brasaemle et al., 2004
ancient ubiquitous protein	gi|6671604	CG3209 weak	Brasaemle et al., 2004
Calnexin	gi|6671664	CG11985	Brasaemle et al., 2004
EHD2	gi|18203333	CG6148	Brasaemle et al., 2004
Fat specific gene 27	gi|2829467	CG1975 weak	Brasaemle et al., 2004
Ribophorin 1	gi|16359229	CG33303	Brasaemle et al., 2004
ATP Synthase beta	gi|25052136	**CG11154**	Brasaemle et al., 2004
Collagen type IV / VI	gi|6753484 gi|3913189 gi|3236370	**CG16858** CG14889 CG33103	Brasaemle et al., 2004
Fatty acid translocase	gi|3273897	CG2727	Brasaemle et al., 2004
Lipoprotein Lipase	gi|15030193	CG5966	Brasaemle et al., 2004
Polymerase I	gi|6679567	CG15792	Brasaemle et al., 2004
Aldehyde dehydrogenase	gi|18028981	**CG11140**	Brasaemle et al., 2004
Caveolin-1	gi|6705981	CG3714 weak	Brasaemle et al., 2004
Tubulin beta5	gi|7106439	CG9277	Brasaemle et al., 2004
Tumor Protein D54	gi|12850393	CG5174	Brasaemle et al., 2004
UFP007 family	YBR177c	CG8058	Athenstaedt et al., 1999
mito inner membrane protease	YMR152w	CG17221	Athenstaedt et al., 1999
similar to vilin 2	AAH13903	CG10701	Umlauf et al., 2004
Ca2+ channel protein	YDL193w	CG4775	Athenstaedt et al., 1999
cytokeratin 8 / 18	P05783 / P05787	CG10119 / CG6944	Umlauf et al., 2004

97 proteins identified (plus isoforms): of these 25 identified in multiple screens 39 in the present screen. Proteins found in the present screen are shown in bold.

6. Summary

Energy homeostasis in biological systems depends fundamentally on the regulated balance of fat storage and mobilization both at the cellular and organismic level. Fat storage involves the formation of lipid droplets. These organelles have a stereotyped structure: a hydrophobic lipid core that is surrounded by a phospholipid monolayer and attached proteins. Lipid droplets are enriched in specialized cells, termed adipocytes, which are the building blocks of the organismic fat storage tissue. In vertebrates, proteins attached to lipid droplets were shown to regulate organismic energy homeostasis. Here, I describe the evolutionary conserved function of the *Drosophila* lipid droplet-associated PAT-domain protein LSD-2, which is related to vertebrate Perilipin. *Lsd-2* mutant flies are lean as observed for Perilipin mutant mice, whereas tissue-specific overexpression of LSD-2 causes a dosage-dependant increase of the organismic triacylglycerol- (TAG-) based fat storage. The results provide functional evidence for the conserved regulatory potential of the lipid droplet surface in *Drosophila*.

In order to assess the lipid droplet-associated proteome in a systematic manner, I isolated lipid droplets from fat body cells of wildtype and genetically manipulated third instar larvae and identified the associated proteins by mass spectroscopy. In total, 271 proteins were identified. They include previously identified lipid droplet-associated as well as novel proteins, i.e. small GTPases of the Rab family and enzymes of a lipogenic pathway. The results support the conclusion that lipid droplets are metabolically active organelles of cells. Tissue culture transfection studies with proteins that were fused to the green fluorescent protein reporter confirm their lipid droplet-association *in vivo* and imply functional specialization through heterogeneity of the lipid droplet population in these cells. The results suggest that protein complexes localize to the lipid droplet surface which may function in the biogenesis of lipid droplets, the storage of fat and its mobilization.

7. References

Abell, B.M., High, S. and Moloney, M.M. (2002) Membrane protein topology of oleosin is constrained by its long hydrophobic domain. *J Biol Chem*, **277**, 8602-8610.

Altschul, S.F., Gish, W., Miller, W., Myers, E.W. and Lipman, D.J. (1990) Basic local alignment search tool. *J Mol Biol*, **215**, 403-410.

Arrese, E.L., Flowers, M.T., Gazard, J.L. and Wells, M.A. (1999) Calcium and cAMP are second messengers in the adipokinetic hormone-induced lipolysis of triacylglycerols in *Manduca sexta* fat body. *J Lipid Res*, **40**, 556-564.

Arrese, E.L. and Wells, M.A. (1994) Purification and properties of a phosphorylatable triacylglycerol lipase from the fat body of an insect, *Manduca sexta*. *J Lipid Res*, **35**, 1652-1660.

Ashburner, M. (1989) *Drosophila: A Laboratory Handbook and Manual. Two volumes.* Cold Spring Harbor Laboratory Press, Cold Spring Harbor, New York.

Ashrafi, K., Chang, F.Y., Watts, J.L., Fraser, A.G., Kamath, R.S., Ahringer, J. and Ruvkun, G. (2003) Genome-wide RNAi analysis of *Caenorhabditis elegans* fat regulatory genes. *Nature*, **421**, 268-272.

Athenstaedt, K., Zweytick, D., Jandrositz, A., Kohlwein, S.D. and Daum, G. (1999) Identification and characterization of major lipid particle proteins of the yeast *Saccharomyces cerevisiae*. *J Bacteriol*, **181**, 6441-6448.

Barbero, P., Buell, E., Zulley, S. and Pfeffer, S.R. (2001) TIP47 is not a component of lipid droplets. *J Biol Chem*, **276**, 24348-24351.

Belfiore, F. and Iannello, S. (1995) Fatty acid synthesis from glutamate in the adipose tissue of normal subjects and obese patients: an enzyme study. *Biochem Mol Med*, **54**, 19-25.

Bellen, H.J., Levis, R.W., Liao, G., He, Y., Carlson, J.W., Tsang, G., Evans-Holm, M., Hiesinger, P.R., Schulze, K.L., Rubin, G.M., Hoskins, R.A. and Spradling, A.C. (2004) The BDGP gene disruption project: single transposon insertions associated with 40% of *Drosophila* genes. *Genetics*, **167**, 761-781.

Berggren, K., Chernokalskaya, E., Steinberg, T.H., Kemper, C., Lopez, M.F., Diwu, Z., Haugland, R.P. and Patton, W.F. (2000) Background-free, high sensitivity staining of proteins in one- and two-dimensional sodium dodecyl sulfate-polyacrylamide gels using a luminescent ruthenium complex. *Electrophoresis*, **21**, 2509-2521.

Blanchette-Mackie, E.J., Dwyer, N.K., Barber, T., Coxey, R.A., Takeda, T., Rondinone, C.M., Theodorakis, J.L., Greenberg, A.S. and Londos, C. (1995) Perilipin is located on the surface layer of intracellular lipid droplets in adipocytes. *J Lipid Res*, **36**, 1211-1226.

Blom, N., Gammeltoft, S. and Brunak, S. (1999) Sequence and structure-based prediction of eukaryotic protein phosphorylation sites. *J Mol Biol*, **294**, 1351-1362.

Bloomington *Drosophila* Stock Center. *http://flystocks.bio.indiana.edu/*.

Bohni, R., Riesgo-Escovar, J., Oldham, S., Brogiolo, W., Stocker, H., Andruss, B.F., Beckingham, K. and Hafen, E. (1999) Autonomous control of cell and organ size by CHICO, a *Drosophila* homolog of vertebrate IRS1-4. *Cell*, **97**, 865-875.

Boll, M., Weber, L.W. and Stampfl, A. (1996) Nutritional regulation of the activities of lipogenic enzymes of rat liver and brown adipose tissue. *Z Naturforsch [C]*, **51**, 859-869.

Brand, A.H. and Perrimon, N. (1993) Targeted gene expression as a means of altering cell fates and generating dominant phenotypes. *Development*, **118**, 401-415.

Brasaemle, D.L., Barber, T., Kimmel, A.R. and Londos, C. (1997a) Post-translational regulation of perilipin expression. Stabilization by stored intracellular neutral lipids. *J Biol Chem*, **272**, 9378-9387.

Brasaemle, D.L., Barber, T., Wolins, N.E., Serrero, G., Blanchette-Mackie, E.J. and Londos, C. (1997b) Adipose differentiation-related protein is an ubiquitously expressed lipid storage droplet-associated protein. *J Lipid Res*, **38**, 2249-2263.

Brasaemle, D.L., Dolios, G., Shapiro, L. and Wang, R. (2004) Proteomic analysis of proteins associated with lipid droplets of basal and lipolytically-stimulated 3T3-L1 adipocytes. *J Biol Chem*, **279**, 46835-46842.

Brasaemle, D.L., Rubin, B., Harten, I.A., Gruia-Gray, J., Kimmel, A.R. and Londos, C. (2000) Perilipin A increases triacylglycerol storage by decreasing the rate of triacylglycerol hydrolysis. *J Biol Chem*, **275**, 38486-38493.

Breitkreutz, B.J., Stark, C. and Tyers, M. (2003) Osprey: a network visualization system. *Genome Biol*, **4**, R22.

Brown, D.A. (2001) Lipid droplets: proteins floating on a pool of fat. *Curr Biol*, **11**, R446-449.

Brunet, S., Thibault, P., Gagnon, E., Kearney, P., Bergeron, J.J. and Desjardins, M. (2003) Organelle proteomics: looking at less to see more. *Trends Cell Biol*, **13**, 629-638.

Burmester, T., Antoniewski, C. and Lepesant, J.A. (1999) Ecdysone-regulation of synthesis and processing of fat body protein 1, the larval serum protein receptor of *Drosophila melanogaster*. *Eur J Biochem*, **262**, 49-55.

Buszczak, M., Lu, X.H., Segraves, W.A., Chang, T.Y. and Cooley, L. (2002) Mutations in the midway gene disrupt a *Drosophila* acyl coenzyme A: Diacylglycerol acyltransferase. *Genetics*, **160**, 1511-1518.

Campbell, P.M., Robin G.C., Court, L.N., Dorrian, S.J., Russell, R.J. and Oakeshott, J.G. (2003) Developmental expression and gene/enzyme identifications in the alpha esterase gene cluster of *Drosophila melanogaster*. *Insect Mol Biol*, **12**, 459-471.

Campos-Ortega J.A. and Hartenstein V. (1997) *The embryonic development of Drosophila melanogaster*. Springer, Berlin.

Canavoso, L.E., Jouni, Z.E., Karnas, K.J., Pennington, J.E. and Wells, M.A. (2001) Fat Metabolism in Insects. *Annu Rev Nutr*, **21**, 23-46.

Chamrad, D.C., Korting, G., Stuhler, K., Meyer, H.E., Klose, J. and Bluggel, M. (2004) Evaluation of algorithms for protein identification from sequence databases using mass spectrometry data. *Proteomics*, **4**, 619-628.

Chan, A.P., Kloc, M., Bilinski, S. and Etkin, L.D. (2001) The vegetally localized mRNA fatvg is associated with the germ plasm in the early embryo and is later expressed in the fat body. *Mech Dev*, **100**, 137-140.

Chang A. P., Kloc M., Larabell C. A. and Etkin L. D. (2002) The maternally localized RNA fatvg plays a dual role both in axis specification and germ cell formation. *Second International Göttingen Meeting on Protein and Membrane Transport in the Secretory Pathway (SFB523)*.

Chien, S., Reiter, L.T., Bier, E. and Gribskov, M. (2002) Homophila: human disease gene cognates in *Drosophila*. *Nucleic Acids Res*, **30**, 149-151.

Clifford, G.M., Londos, C., Kraemer, F.B., Vernon, R.G. and Yeaman, S.J. (2000) Translocation of hormone-sensitive lipase and perilipin upon lipolytic stimulation of rat adipocytes. *J Biol Chem*, **275**, 5011-5015.

Clifford, G.M., McCormick, D.K., Londos, C., Vernon, R.G. and Yeaman, S.J. (1998) Dephosphorylation of perilipin by protein phosphatases present in rat adipocytes. *FEBS Lett*, **435**, 125-129.

Cohen, A.W., Razani, B., Schubert, W., Williams, T.M., Wang, X.B., Iyengar, P., Brasaemle, D.L., Scherer, P.E. and Lisanti, M.P. (2004) Role of caveolin-1 in the modulation of lipolysis and lipid droplet formation. *Diabetes*, **53**, 1261-1270.

Demerec, M. (1994) *Biology of Drosophila. [Facsimile edition.]*. Cold Spring Harbor Press, Cold Spring Harbor.

Diaz, E. and Pfeffer, S.R. (1998) TIP47: a cargo selection device for mannose 6-phosphate receptor trafficking. *Cell*, **93**, 433-443.

Dreger, M. (2003) Proteome analysis at the level of subcellular structures. *Eur J Biochem*, **270**, 589-599.

Fischer, J.A., Giniger, E., Maniatis, T. and Ptashne, M. (1988) GAL4 activates transcription in *Drosophila*. *Nature*, **332**, 853-856.

Flatt, J.P. (1995) Use and storage of carbohydrate and fat. *Am J Clin Nutr*, **61**, 952S-959S.

FlyBase (2003) The FlyBase database of the *Drosophila* genome projects and community literature. *Nucleic Acids Res*, **31**, 172-175.

Fortier, M., Wang, S.P., Mauriege, P., Semache, M., Mfuma, L., Li, H., Levy, E., Richard, D. and Mitchell, G.A. (2004) Hormone-sensitive lipase-independent adipocyte lipolysis during beta-adrenergic stimulation, fasting, and dietary fat loading. *Am J Physiol Endocrinol Metab*, **287**, E282-288.

Friedman, J.M. (2003) A war on obesity, not the obese. *Science*, **299**, 856-858.

Fujimoto, Y., Itabe, H., Sakai, J., Makita, M., Noda, J., Mori, M., Higashi, Y., Kojima, S. and Takano, T. (2004) Identification of major proteins in the lipid droplet-enriched fraction isolated from the human hepatocyte cell line HuH7. *Biochim Biophys Acta*, **1644**, 47-59.

Gao, J. and Serrero, G. (1999) Adipose differentiation related protein (ADRP) expressed in transfected COS-7 cells selectively stimulates long chain fatty acid uptake. *J Biol Chem*, **274**, 16825-16830.

Gibbons, G.F., Islam, K. and Pease, R.J. (2000) Mobilisation of triacylglycerol stores. *Biochim Biophys Acta*, **1483**, 37-57.

Giot, L. *et al.* (2003) A protein interaction map of *Drosophila melanogaster*. *Science*, **302**, 1727-1736.

Gloor, G.B., Preston, C.R., Johnson-Schlitz, D.M., Nassif, N.A., Phillis, R.W., Benz, W.K., Robertson, H.M. and Engels, W.R. (1993) Type I repressors of P element mobility. *Genetics*, **135**, 81-95.

Gocze, P.M. and Freeman, D.A. (1994) Factors underlying the variability of lipid droplet fluorescence in MA-10 Leydig tumor cells. *Cytometry*, **17**, 151-158.

Goldstein, L.S.B. and Fyrberg, E.A. (1994) *Drosophila melanogaster: Practical uses in cell and molecular biology*. Academic Press, San Diego.

Görg, A., Obermaier, C., Boguth, G., Harder, A., Scheibe, B., Wildgruber, R. and Weiss, W. (2000) The current state of two-dimensional electrophoresis with immobilized pH gradients. *Electrophoresis*, **21**, 1037-1053.

Greenberg, A.S., Egan, J.J., Wek, S.A., Garty, N.B., Blanchette-Mackie, E.J. and Londos, C. (1991) Perilipin, a major hormonally regulated adipocyte-specific phosphoprotein associated with the periphery of lipid storage droplets. *J Biol Chem*, **266**, 11341-11346.

Greenspan, P., Mayer, E.P. and Fowler, S.D. (1985) Nile red: a selective fluorescent stain for intracellular lipid droplets. *J Cell Biol*, **100**, 965-973.

Greenspan, R.J. (1997) *Fly Pushing*. Cold Spring Harbour Laboratory Press, Cold Spring Harbour.

Grönke, S., Beller, M., Fellert, S., Ramakrishnan, H., Jäckle, H. and Kühnlein, R.P. (2003) Control of fat storage by a *Drosophila* PAT domain protein. *Curr Biol*, **13**, 603-606.

Häder, T., Müller, S., Aguilera, M., Eulenberg, K.G., Steuernagel, A., Ciossek, T., Kühnlein, R.P., Lemaire, L., Fritsch, R., Dohrmann, C., Vetter, I.R., Jäckle, H., Doane, W.W. and Brönner, G. (2003) Control of triglyceride storage by a WD40/TPR-domain protein. *EMBO Rep*, **4**, 511-516.

Harris, T.W. *et al.* (2004) WormBase: a multi-species resource for nematode biology and genomics. *Nucleic Acids Res*, **32 Database issue**, D411-417.

Hartl, F.U. and Hayer-Hartl, M. (2002) Molecular chaperones in the cytosol: from nascent chain to folded protein. *Science*, **295**, 1852-1858.

Heid, H.W., Schnolzer, M. and Keenan, T.W. (1996) Adipocyte differentiation-related protein is secreted into milk as a constituent of milk lipid globule membrane. *Biochem J*, **320**, 1025-1030.

Hernandez, G., Lalioti, V., Vandekerckhove, J., Sierra, J.M. and Santaren, J.F. (2004) Identification and characterization of the expression of the translation initiation factor 4A (eIF4A) from *Drosophila melanogaster*. *Proteomics*, **4**, 316-326.

Hickenbottom, S.J., Kimmel, A.R., Londos, C. and Hurley, J.H. (2004) Structure of a lipid droplet protein; the PAT family member TIP47. *Structure (Camb)*, **12**, 1199-1207.

Hill, J.O., Wyatt, H.R., Reed, G.W. and Peters, J.C. (2003) Obesity and the environment: where do we go from here? *Science*, **299**, 853-855.

Holm, C. (2003) Molecular mechanisms regulating hormone-sensitive lipase and lipolysis. *Biochem Soc Trans*, **31**, 1120-1124.

Imamura, M., Inoguchi, T., Ikuyama, S., Taniguchi, S., Kobayashi, K., Nakashima, N. and Nawata, H. (2002) ADRP stimulates lipid accumulation and lipid droplet formation in murine fibroblasts. *Am J Physiol Endocrinol Metab*, **283**, E775-783.

Ishigami, A., Kondo, Y., Nanba, R., Ohsawa, T., Handa, S., Kubo, S., Akita, M. and Maruyama, N. (2004) SMP30 deficiency in mice causes an accumulation of neutral lipids and phospholipids in the liver and shortens the life span. *Biochem Biophys Res Commun*, **315**, 575-580.

Janke, C., Beck, M., Holzer, M., Bigl, V. and Arendt, T. (2000) Analysis of the molecular heterogeneity of the microtubule-associated protein tau by two-dimensional electrophoresis and RT-PCR. *Brain Res Brain Res Protoc*, **5**, 231-242.

Jenkins, C.M., Mancuso, D.J., Yan, W., Sims, H.F., Gibson, B. and Gross, R.W. (2004) Identification, cloning, expression, and purification of three novel human calcium-independent phospholipase A2 family members possessing triacylglycerol lipase and acylglycerol transacylase activities. *J Biol Chem*, papers in press.

Johnson, A.E. and van Waes, M.A. (1999) The translocon: a dynamic gateway at the ER membrane. *Annu Rev Cell Dev Biol*, **15**, 799-842.

Karbowska, J., Kochan, Z. and Swierczynski, J. (2001) Increase of lipogenic enzyme mRNA levels in rat white adipose tissue after multiple cycles of starvation-refeeding. *Metabolism*, **50**, 734-738.

Kloc, M., Dougherty, M.T., Bilinski, S., Chan, A.P., Brey, E., King, M.L., Patrick, C.W., Jr. and Etkin, L.D. (2002) Three-dimensional ultrastructural analysis of RNA distribution within germinal granules of *Xenopus*. *Dev Biol*, **241**, 79-93.

Laemmli, U.K. (1970) Cleavage of structural proteins during the assembly of the head of bacteriophage T4. *Nature*, **227**, 680-685.

Laski, F.A., Rio, D.C. and Rubin, G.M. (1986) Tissue specificity of *Drosophila* P element transposition is regulated at the level of mRNA splicing. *Cell*, **44**, 7-19.

Lefevre, C. *et al.* (2004) A map of the interactome network of the metazoan *C. elegans*. *Science*, **303**, 540-543.

Liu, P., Ying, Y., Zhao, Y., Mundy, D.I., Zhu, M. and Anderson, R.G. (2004) Chinese hamster ovary K2 cell lipid droplets appear to be metabolic organelles involved in membrane traffic. *J Biol Chem*, **279**, 3787-3792.

Londos, C., Brasaemle, D.L., Schultz, C.J., Adler-Wailes, D.C., Levin, D.M., Kimmel, A.R. and Rondinone, C.M. (1999) On the control of lipolysis in adipocytes. *Ann N Y Acad Sci*, **892**, 155-168.

Lu, X., Gruia-Gray, J., Copeland, N.G., Gilbert, D.J., Jenkins, N.A., Londos, C. and Kimmel, A.R. (2001) The murine perilipin gene: the lipid droplet-associated perilipins derive from tissue-specific, mRNA splice variants and define a gene family of ancient origin. *Mamm Genome*, **12**, 741-749.

Luft, J.H. (1961) Improvements in epoxy resin embedding methods. *J Biophys Biochem Cytol*, **9**, 409-414.

Martinez-Botas, J., Anderson, J.B., Tessier, D., Lapillonne, A., Chang, B.H., Quast, M.J., Gorenstein, D., Chen, K.H. and Chan, L. (2000) Absence of *perilipin* results in leanness and reverses obesity in *Lepr*(*db*/*db*) mice. *Nat Genet*, **26**, 474-479.

Marx, J. (2003) Cellular warriors at the battle of the bulge. *Science*, **299**, 846-849.

McCudden, C.R., James, K.A., Hasilo, C. and Wagner, G.F. (2002) Characterization of mammalian stanniocalcin receptors. Mitochondrial targeting of ligand and receptor for regulation of cellular metabolism. *J Biol Chem*, **277**, 45249-45258.

Meacock, S.L., Greenfield, J.J. and High, S. (2000) Protein targeting and translocation at the endoplasmic reticulum membrane-through the eye of a needle? *Essays Biochem*, **36**, 1-13.

Meegalla, R.L., Billheimer, J.T. and Cheng, D. (2002) Concerted elevation of acyl-coenzyme A:diacylglycerol acyltransferase (DGAT) activity through independent stimulation of mRNA expression of DGAT1 and DGAT2 by carbohydrate and insulin. *Biochem Biophys Res Commun*, **298**, 317-323.

Miura, S., Gan, J.W., Brzostowski, J., Parisi, M.J., Schultz, C.J., Londos, C., Oliver, B. and Kimmel, A.R. (2002) Functional conservation for lipid storage droplet association among Perilipin, ADRP, and TIP47 (PAT)-related proteins in mammals, *Drosophila*, and *Dictyostelium*. *J Biol Chem*, **277**, 32253-32257.

Murphy, D.J. (2001) The biogenesis and functions of lipid bodies in animals, plants and microorganisms. *Prog Lipid Res*, **40**, 325-438.

Murphy, D.J. and Vance, J. (1999) Mechanisms of lipid-body formation. *Trends Biochem Sci*, **24**, 109-115.

Osuga, J., Ishibashi, S., Oka, T., Yagyu, H., Tozawa, R., Fujimoto, A., Shionoiri, F., Yahagi, N., Kraemer, F.B., Tsutsumi, O. and Yamada, N. (2000) Targeted disruption of hormone-sensitive lipase results in male sterility and adipocyte hypertrophy, but not in obesity. *Proc Natl Acad Sci U S A*, **97**, 787-792.

Paciga, M., McCudden, C.R., Londos, C., DiMattia, G.E. and Wagner, G.F. (2003) Targeting of big stanniocalcin and its receptor to lipid storage droplets of ovarian steroidogenic cells. *J Biol Chem*, **278**, 49549-49554.

Passier, P.C., Vullings, H.G., Diederen, J.H. and Van der Horst, D.J. (1995) Modulatory effects of biogenic amines on adipokinetic hormone secretion from locust corpora cardiaca in vitro. *Gen Comp Endocrinol*, **97**, 231-238.

Perkins, D.N., Pappin, D.J., Creasy, D.M. and Cottrell, J.S. (1999) Probability-based protein identification by searching sequence databases using mass spectrometry data. *Electrophoresis*, **20**, 3551-3567.

Renault, A.D., Sigal, Y.J., Morris, A.J. and Lehmann, R. (2004) Soma-germ line competition for lipid phosphate uptake regulates germ cell migration and survival. *Science*, **305**, 1963-1966.

Resing, K.A. (2002) Analysis of signaling pathways using functional proteomics. *Ann N Y Acad Sci*, **971**, 608-614.

Righetti, P.G., Campostrini, N., Pascali, J., Hamdan, M. and Astner, H. (2004) Quantitative proteomics: a review of different methodologies. *Eur J Mass Spectrom (Chichester, Eng)*, **10**, 335-348.

Robenek, M.J., Severs, N.J., Schlattmann, K., Plenz, G., Zimmer, K.P., Troyer, D. and Robenek, H. (2004) Lipids partition caveolin-1 from ER membranes into lipid droplets: updating the model of lipid droplet biogenesis. *Faseb J*, **18**, 866-868.

Roberts, D.B. (1998) *Drosophila A practical approach*. IRL Press, Oxford.

Roseman, R.R., Johnson, E.A., Rodesch, C.K., Bjerke, M., Nagoshi, R.N. and Geyer, P.K. (1995) A P element containing suppressor of hairy-wing binding regions has novel properties for mutagenesis in *Drosophila melanogaster*. *Genetics*, **141**, 1061-1074.

Rubin, G.M., Hong, L., Brokstein, P., Evans-Holm, M., Frise, E., Stapleton, M. and Harvey, D.A. (2000) A *Drosophila* complementary DNA resource. *Science*, **287**, 2222-2224.

Ryder, E. and Russell, S. (2003) Transposable elements as tools for genomics and genetics in *Drosophila*. *Brief Funct Genomic Proteomic*, **2**, 57-71.

Saha, P.K., Kojima, H., Martinez-Botas, J., Sunehag, A.L. and Chan, L. (2004) Metabolic adaptations in the absence of *perilipin*: Increased beta-oxidation and decreased hepatic glucose production associated with peripheral insulin resistance but normal glucose tolerance in *perilipin*-null mice. *J Biol Chem*, **279**, 35150-35158.

Sambrook, J. and Russel D.W. (2001) *Molecular cloning*. Cold Spring Harbour Laboratory Press, Cold Spring Harbour.

Schneider, I. (1972) Cell lines derived from late embryonic stages of *Drosophila melanogaster*. *J Embryol Exp Morphol*, **27**, 353-365.

Schultz, C.J., Torres, E., Londos, C. and Torday, J.S. (2002) Role of adipocyte differentiation-related protein in surfactant phospholipid synthesis by type II cells. *Am J Physiol Lung Cell Mol Physiol*, **283**, L288-296.

Servetnick, D.A., Brasaemle, D.L., Gruia-Gray, J., Kimmel, A.R., Wolff, J. and Londos, C. (1995) Perilipins are associated with cholesteryl ester droplets in steroidogenic adrenal cortical and Leydig cells. *J Biol Chem*, **270**, 16970-16973.

Soni, K.G., Lehner, R., Metalnikov, P., O'Donnell, P., Semache, M., Gao, W., Ashman, K., Pshezhetsky, A.V. and Mitchell, G.A. (2004) Carboxylesterase 3 (EC 3.1.1.1) Is a Major Adipocyte Lipase. *J Biol Chem*, **279**, 40683-40689.

Souza, S.C., Muliro, K.V., Liscum, L., Lien, P., Yamamoto, M.T., Schaffer, J.E., Dallal, G.E., Wang, X., Kraemer, F.B., Obin, M. and Greenberg, A.S. (2002) Modulation of hormone-sensitive lipase and protein kinase A-mediated lipolysis by perilipin A in an adenoviral reconstituted system. *J Biol Chem*, **277**, 8267-8272.

Spradling, A.C., Stern, D., Beaton, A., Rhem, E.J., Laverty, T., Mozden, N., Misra, S. and Rubin, G.M. (1999) The Berkeley *Drosophila* genome project gene disruption project. Single P-element insertions mutating 25% of vital *Drosophila* genes. *Genetics*, **153**, 135--177.

Starz-Gaiano, M., Cho, N.K., Forbes, A. and Lehmann, R. (2001) Spatially restricted activity of a *Drosophila* lipid phosphatase guides migrating germ cells. *Development*, **128**, 983-991.

Subramanian, V., Rothenberg, A., Gomez, C., Cohen, A.W., Garcia, A., Bhattacharyya, S., Shapiro, L., Wang, R., Lisanti, M.P. and Brasaemle, D.L. (2004) Perilipin A mediates the reversible binding of CGI-58 to lipid droplets in 3T3-L1 adipocytes. *J Biol Chem*, **279**, 42062-42071.

Swierczynski, J., Goyke, E., Wach, L., Pankiewicz, A., Kochan, Z., Adamonis, W., Sledzinski, Z. and Aleksandrowicz, Z. (2000) Comparative study of the lipogenic potential of human and rat adipose tissue. *Metabolism*, **49**, 594-599.

Sztalryd, C., Xu, G., Dorward, H., Tansey, J.T., Contreras, J.A., Kimmel, A.R. and Londos, C. (2003) Perilipin A is essential for the translocation of hormone-sensitive lipase during lipolytic activation. *J Cell Biol.*, **161(6)**, 1093-1103.

Tansey, J.T., Huml, A.M., Vogt, R., Davis, K.E., Jones, J.M., Fraser, K.A., Brasaemle, D.L., Kimmel, A.R. and Londos, C. (2003) Functional studies on native and mutated forms of perilipins. A role in protein kinase A-mediated lipolysis of triacylglycerols. *J Biol Chem*, **278**, 8401-8406.

Tansey, J.T., Sztalryd, C., Gruia-Gray, J., Roush, D.L., Zee, J.V., Gavrilova, O., Reitman, M.L., Deng, C.X., Li, C., Kimmel, A.R. and Londos, C. (2001) Perilipin ablation results in a lean mouse with aberrant adipocyte lipolysis, enhanced leptin production, and resistance to diet-induced obesity. *Proc Natl Acad Sci U S A*, **98**, 6494-6499.

Tao, W.A. and Aebersold, R. (2003) Advances in quantitative proteomics via stable isotope tagging and mass spectrometry. *Curr Opin Biotechnol*, **14**, 110-118.

Tauchi-Sato, K., Ozeki, S., Houjou, T., Taguchi, R. and Fujimoto, T. (2002) The surface of lipid droplets is a phospholipid monolayer with a unique fatty acid composition. *J. Biol. Chem.*, **46**, 44507-44512.

Tavernarakis, N., Driscoll, M. and Kyrpides, N.C. (1999) The SPFH domain: implicated in regulating targeted protein turnover in stomatins and other membrane-associated proteins. *Trends Biochem Sci*, **24**, 425-427.

Taylor, S.W., Fahy, E. and Ghosh, S.S. (2003) Global organellar proteomics. *Trends Biotechnol*, **21**, 82-88.

Teixeira, L., Rabouille, C., Rorth, P., Ephrussi, A. and Vanzo, N.F. (2003) *Drosophila* Perilipin/ADRP homologue Lsd2 regulates lipid metabolism. *Mech Dev*, **120**, 1071-1081.

Tomancak, P., Beaton, A., Weiszmann, R., Kwan, E., Shu, S., Lewis, S.E., Richards, S., Ashburner, M., Hartenstein, V., Celniker, S.E. and Rubin, G.M. (2002) Systematic determination of patterns of gene expression during *Drosophila* embryogenesis. *Genome Biol*, **3**, RESEARCH0088.1-0088.14.

Tong, A.H. *et al.* (2004) Global mapping of the *yeast* genetic interaction network. *Science*, **303**, 808-813.

Umlauf, E., Csaszar, E., Moertelmaier, M., Schuetz, G.J., Parton, R.G. and Prohaska, R. (2004) Association of stomatin with lipid bodies. *J Biol Chem*, **279**, 23699-23709.

van der Horst, D.J., van Doorn, J.M., Passier, P.C., Vork, M.M. and Glatz, J.F. (1993) Role of fatty acid-binding protein in lipid metabolism of insect flight muscle. *Mol Cell Biochem*, **123**, 145-152.

van Meer, G. (2001) Caveolin, cholesterol, and lipid droplets? *J Cell Biol*, **152**, F29-34.

Villena, J.A., Roy, S., Sarkadi-Nagy, E., Kim, K. and Sul, H. (2004) Desnutrin, an adipocyte gene encoding a novel patatin-domain containing protein, is induced by fasting and glucocorticoids. Ectopic expression of desnutrin increases triglyceride hydrolysis. *J Biol Chem*, **279**, 47066-47075.

Weller, P.F., Ryeom, S.W., Picard, S.T., Ackerman, S.J. and Dvorak, A.M. (1991) Cytoplasmic lipid bodies of neutrophils: formation induced by cis-unsaturated fatty acids and mediated by protein kinase C. *J Cell Biol*, **113**, 137-146.

Welte, M.A., Gross, S.P., Postner, M., Block, S.M. and Wieschaus, E.F. (1998) Developmental regulation of vesicle transport in *Drosophila* embryos: forces and kinetics. *Cell*, **92**, 547-557.

Wessel, D. and Flügge, U.I. (1984) A method for the quantitative recovery of protein in dilute solution in the presence of detergents and lipids. *Anal Biochem*, **138**, 141-143.

Wolins, N.E., Rubin, B. and Brasaemle, D.L. (2001) TIP47 associates with lipid droplets. *J Biol Chem*, **276**, 5101-5108.

Wolpert, L. (2001) *Principles of development*. Oxford university press, Oxford.

Wu, C.C., Howell, K.E., Neville, M.C., Yates, J.R., 3rd and McManaman, J.L. (2000) Proteomics reveal a link between the endoplasmic reticulum and lipid secretory mechanisms in mammary epithelial cells. *Electrophoresis*, **21**, 3470-3482.

Yamaguchi, T., Omatsu, N., Matsushita, S. and Osumi, T. (2004) CGI-58 interacts with perilipin and is localized to lipid droplets. Possible involvement of CGI-58 mislocalization in Chanarin-Dorfman syndrome. *J Biol Chem*, **279**, 30490-30497.

Yamashita, K., Koide, Y., Itoh, H., Kawada, N. and Kawauchi, H. (1995) The complete amino acid sequence of chum salmon stanniocalcin, a calcium-regulating hormone in teleosts. *Mol Cell Endocrinol*, **112**, 159-167.

Yu, W., Cassara, J. and Weller, P.F. (2000) Phosphatidylinositide 3-kinase localizes to cytoplasmic lipid bodies in human polymorphonuclear leukocytes and other myeloid-derived cells. *Blood*, **95**, 1078-1085.

Zhang, W. and Chait, B.T. (2000) ProFound: an expert system for protein identification using mass spectrometric peptide mapping information. *Anal Chem*, **72**, 2482-2489.

Zinke, I., Schutz, C.S., Katzenberger, J.D., Bauer, M. and Pankratz, M.J. (2002) Nutrient control of gene expression in *Drosophila*: microarray analysis of starvation and sugar-dependent response. *Embo J*, **21**, 6162-6173.

Zweytick, D., Athenstaedt, K. and Daum, G. (2000) Intracellular lipid particles of eukaryotic cells. *Biochim Biophys Acta*, **1469**, 101-120.

Danksagung

Die vorliegende Arbeit wurde am Max-Planck-Institut für biophysikalische Chemie unter der Anleitung von Prof. Dr. Herbert Jäckle angefertigt.

Mein ganz besonderer Dank gilt Prof. Dr. Herbert Jäckle für die uneingeschränkte Unterstützung und sein stetes Interesse an meiner Arbeit, sowie für die Möglichkeit weite Teile der Dissertation frei zu gestalten.

Dr. Ronald Kühnlein danke ich für die Bereitschaft mich an dem LSD-Protein Projekt und seiner Energie-Homöostase Gruppe teilhaben zu lassen, sowie für sein stetes Interesse und die Diskussionsbereitschaft.

Herrn Prof. Dr. Hans-Henning Arnold danke ich für die Bereitschaft die Dissertation an der Technischen Universität zu Braunschweig zu vertreten.

Meinen Kooperationspartnern Prof. Dr. Jürgen Wehland, Dr. Lothar Jänsch und Dr. Dirk Wehmhöhner danke ich für die Möglichkeit das „lipid droplet" Proteom untersuchen zu können. Hierbei war die exzellente technische Unterstützung von Jaqueline Majewski und Kirsten Minkhart eine große Hilfe. Desweiteren danke ich Dr. Dietmar Riedel für die elektronenmikroskopischen Aufnahmen der aufgereinigten „lipid droplets".

Bei den Mitgliedern der Energie-Homöostase Gruppe möchte ich mich für die sehr gute Integration bedanken. Besonderer Dank gilt Sonja Fellert für die Durchführung der TAG-assays und den „Schweinespeck". Bei allen Mitgliedern der Abteilung 170, insbesondere „Labor 1", möchte ich mich für all die Dinge bedanken, die den Alltag erleichtern. Dr. Alf Herzig danke ich für die Einführung in das Gateway-Klonierungssystem, nebst Bereitstellung der benötigten Vektoren.

Gordon Dowe danke ich für die kritische Durchsicht der Dissertation und für DNA-Sequenzierungen, Ursula Jahns-Meyer und Iris Plischke für Embryo-Injektionen.

Zu guter Letzt danke ich meiner Mutter für Ihre Unterstützung, ohne sie wäre vieles nicht möglich gewesen, und meiner Freundin Katharina Veit, die immer für mich da ist, für das Verständnis und die Geduld, die ich leider manchmal beanspruche.

Lebenslauf

Mathias Beller

10.01.1976	Geburt in Mutlangen (Baden-Württemberg); Eltern: Werner Beller und Lieselotte Beller, geborene Heidrich
1982-1986	Besuch der Grundschule in Mutlangen
1986-1995	Besuch des Parler-Gymnasiums in Schwäbisch Gmünd
1995	Abitur
1995-1996	Zivildienst im Gehörlosenheim St. Vinzenz in Schwäbisch Gmünd
1996-2000	Studium der Biologie an der Georg-August-Universität in Göttingen
1998	Vordiplom in Biologie in den Fächern Zoologie, Mikrobiologie, Anorganische Chemie und Physikalische Chemie
2000	Diplomprüfungen in den Fächern: Mikrobiologie, Immunologie und Physikalische Chemie
2000-2001	Anfertigung der Diplomarbeit am Max-Planck-Institut für biophysikalische Chemie unter der Anleitung von Prof. Dr. Herbert Jäckle: “Molekulargenetische Untersuchungen zur Funktion von Ral-interagierenden *Drosophila* Genen”.
2001	Diplom in Biologie
seit 2001	Anfertigung der Dissertation am Max-Planck-Institut für biophysikalische Chemie unter der Anleitung von Prof. Dr. Herbert Jäckle: “Identification and characterization of *Drosophila* lipid droplet-associated proteins”.

Tagungsbeiträge

Beller M., Blanke S., Brentrup D., Jänsch L., Wehland J. und Jäckle H.: Ima, a novel partner of dRalA interacts with Smox and RNA binding proteins. (Poster) 43rd annual *Drosophila* Research Conference, San Diego (2002).

Veröffentlichungen

Beller M.*, Blanke S.*,Brentrup D. und Jäckle H.: Identification and expression of Ima, a novel Ral-interacting *Drosophila* protein. Mech Dev. 19 (Suppl 1): 253-60 (2002). * geteilte Erstautorenschaft